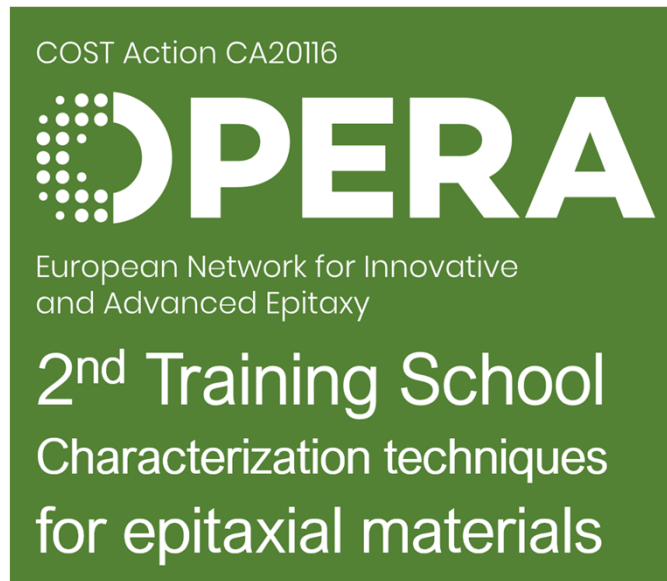

X-ray Metrology of Epitaxial Group-III-Nitrides for Device Fabrication

Lutz Kirste

Fraunhofer Institute for Applied Solid State Physics (IAF), Freiburg, Germany



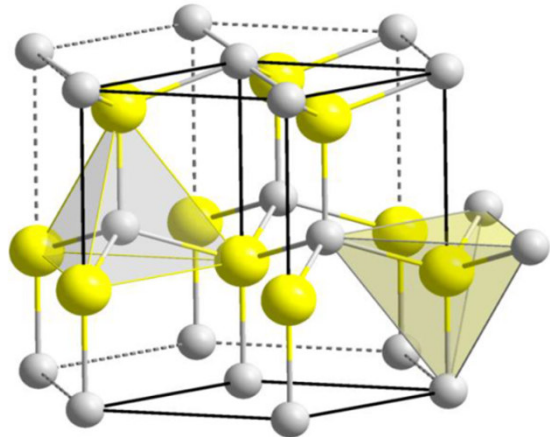
University of Aveiro, Aveiro, Portugal

13th-17th of June 2023

Outline

- Motivation
- Basics of X-ray Diffraction Method
- Instrumentation for High Resolution X-ray Diffraction
- Scanning in Reciprocal Space
- Stress and Strain in Epitaxial Thin Films
 - Fully strained Films
 - Partially Strained Films
 - Composition of Alloy Films
- Measurement of the Layer's Thickness
 - Single Layers and Layer Stacks
 - Superlattices
- Analysis of the Orientation of a Thin Film
- Mosaicity in Thin Films
- Synchrotron Bragg Diffraction Imaging for Substrate Analysis
- Recommended Readings

Motivation

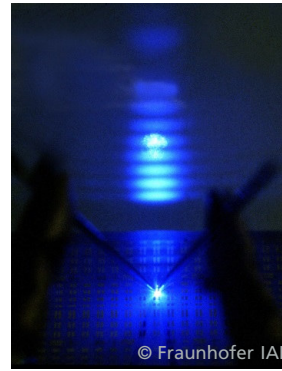


GaN (Wurtzite structure)
SG: P6₃mc

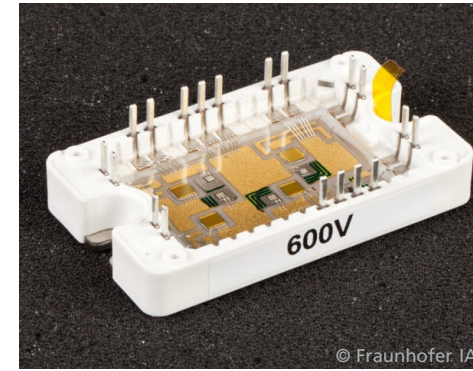
Properties	AlN	GaN	InN	Si	GaAs	4H-SiC
Bandgap (eV)	6.2	3.42	0.65	1.11	1.43	3.26
Relative Dielectric Constant	58.9	8.9	15.3	11.8	12.8	9.7
Breakdown Field (V / cm)	1.8e6	3.5e6	-	2.5e5	3.5e5	3.5e6
Electron Mobility (cm ² / V s)	300	1000	3200	1350	6000	800
Hole Mobility (cm ² / V s)	14	300	-	450	330	120
Thermal Conductivity (W / m K)	1.8	1.7	0.41	1.5	0.46	4.9



III-N-based white LED

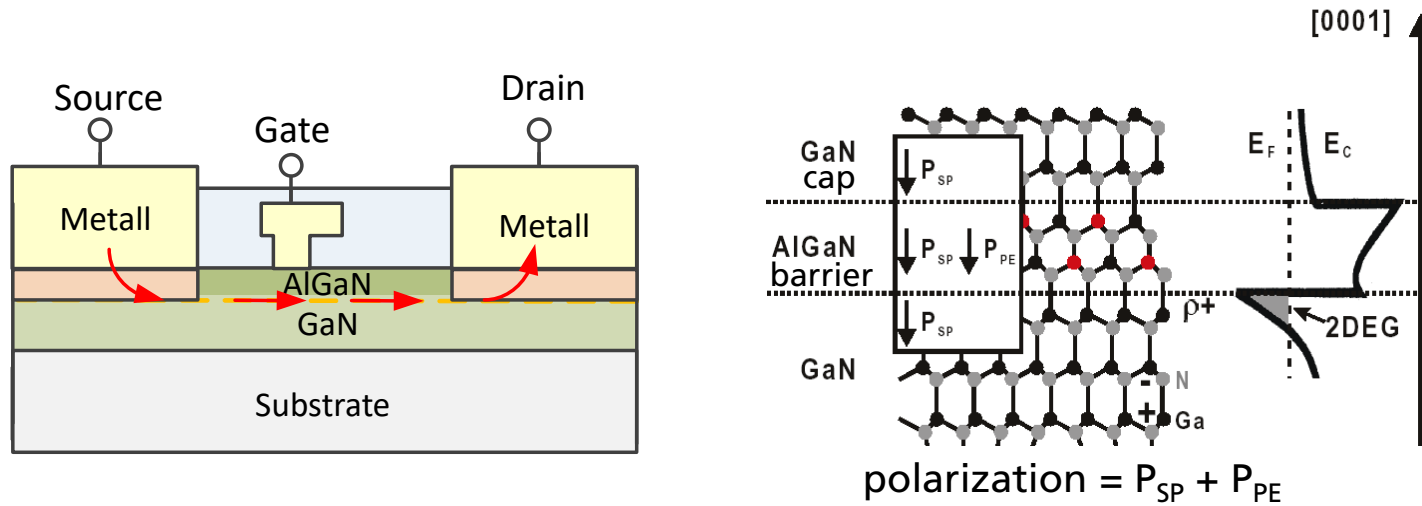


III-N-based laser diode



GaN-based power module

AlGaN / GaN High Electron Mobility Transistors (HEMTs) for High Power and High Frequency Electronics



PV power inverter



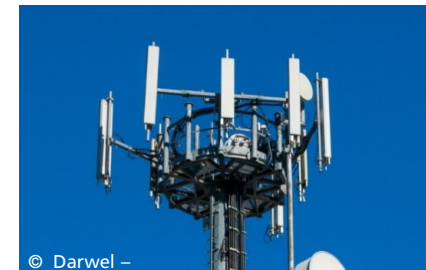
Voltage transformer



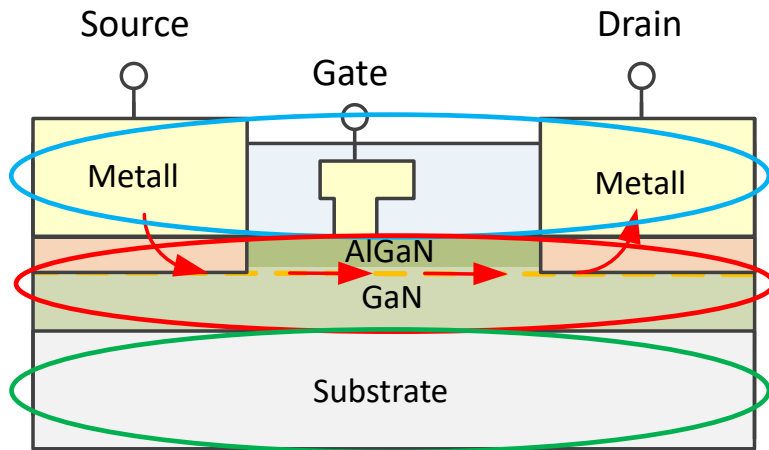
Radar systems



Base station for
mobile communication



Questions that can be answered using X-ray metrology for AlGaN / GaN high electron mobility transistors



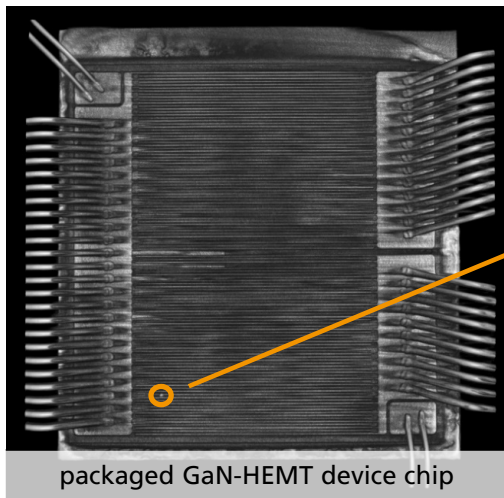
Metallization / Technology: Voids, short cuts, chip deformation, cracks

Layer stack: State of strain, composition, defect types and density, subsurface damage, roughness

Substrate: Defect types and density, subsurface damage

Demand for non-destructive, fast, contactless and accurate metrology → **X-ray methods**

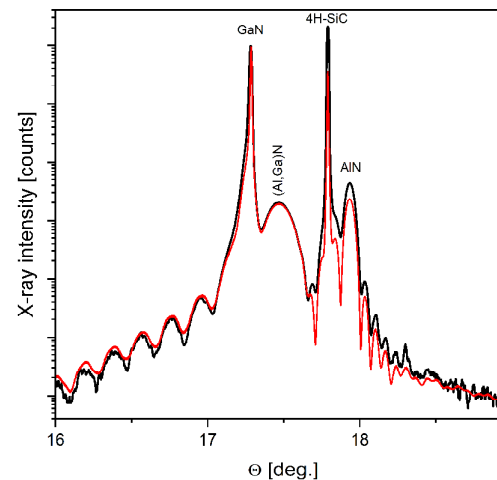
X-ray microscopy



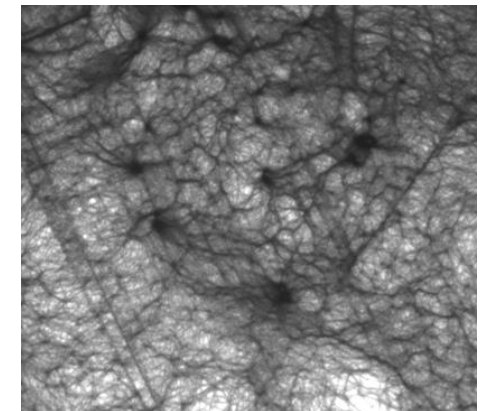
Solder spatter, as potential short cut, imaged through housing.

packaged GaN-HEMT device chip

X-ray diffraction

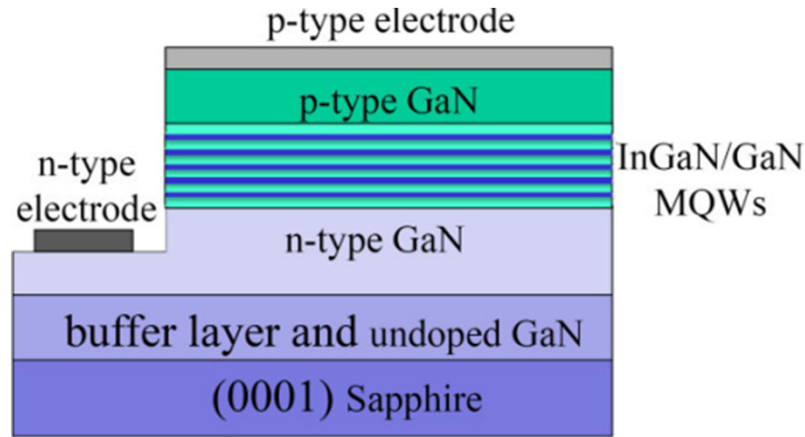


X-ray topography

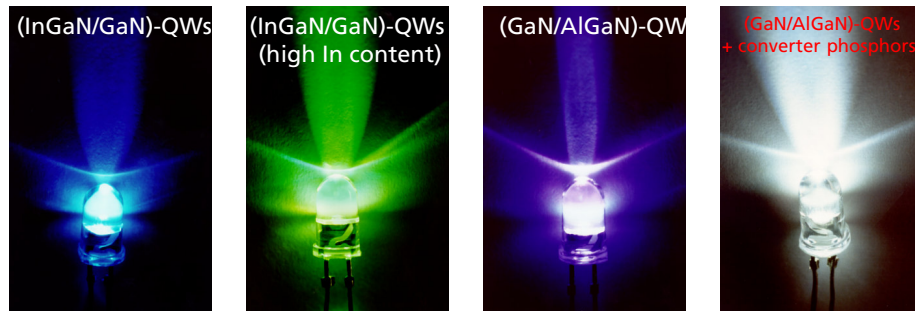
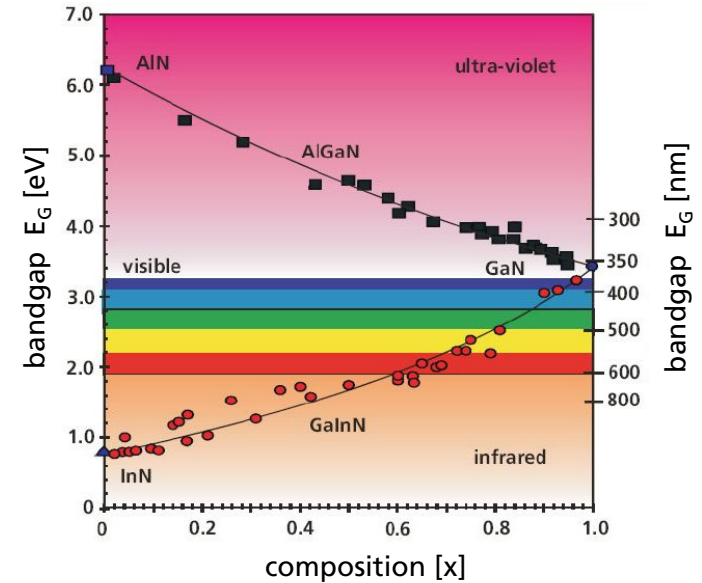


Super screw dislocations in SiC substrate

GaN Light emitting diode (LED)



Schematic structure of an (AlGaIn)N LED-Chip



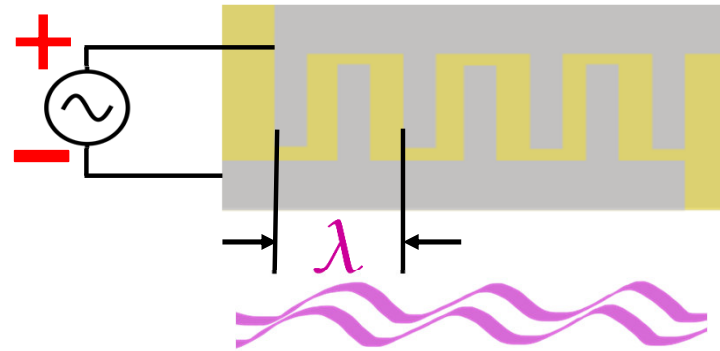
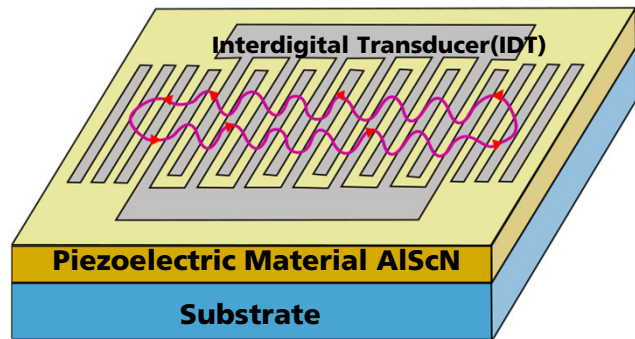
Blue, green, UV and white LED

Structural properties that determine the characteristics of a LED:

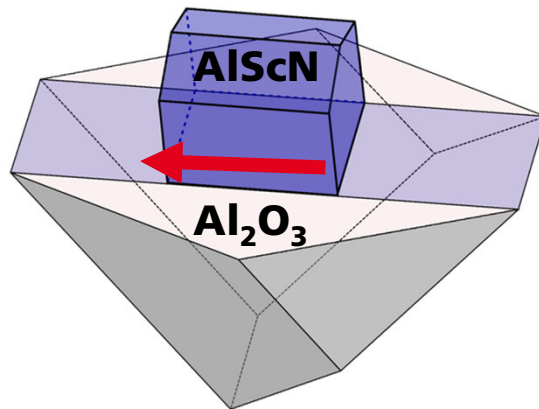
- quantum well composition
- quantum well thickness
- quantum well strain
- crystalline perfection

→ All of these issues can be addressed with XRD

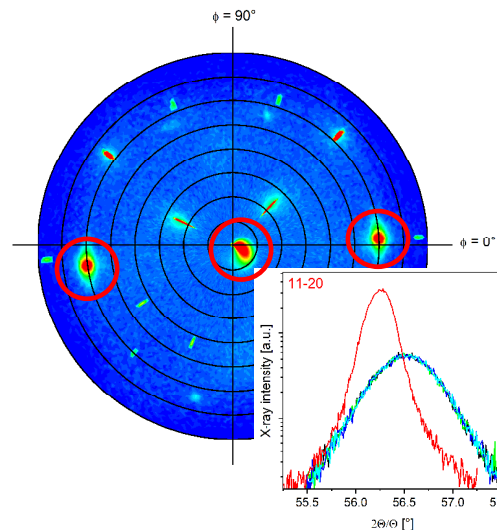
Surface Acoustic Wave (SAW) devices fabrication for 5G applications using AlN and AlScN



Surface waves propagating through piezoelectric material (AlScN)



Piezoelectric AlScN (11 $\bar{2}$ 0) deposited on Al₂O₃ (1 $\bar{1}$ 02) substrate



XRD texture and reflection profile analysis

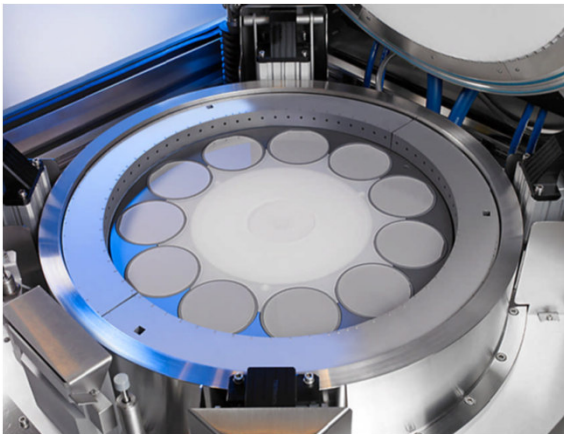
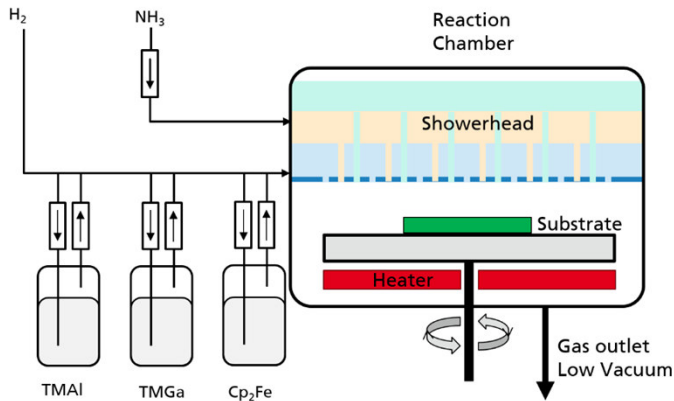
Structural properties that determine the characteristics of a SAW device:

- AlScN composition
- crystallographic phase
- epitaxial orientation
- layer thickness
- layer strain
- crystalline perfection

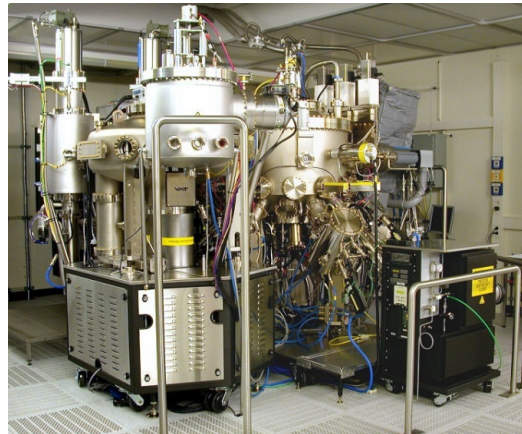
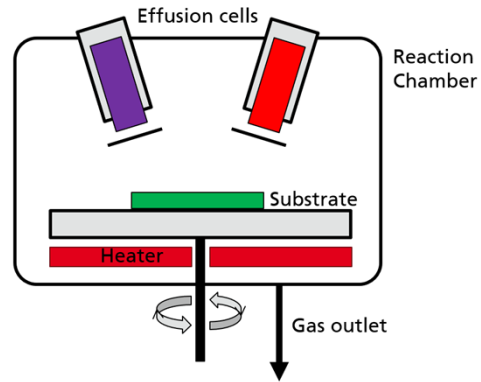
→ All of these issues can be addressed with XRD

Nitride layer growth

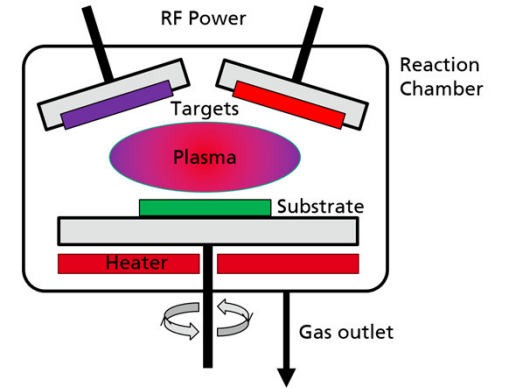
Metall-Organic Chemical Vapor Deposition (MOCVD)



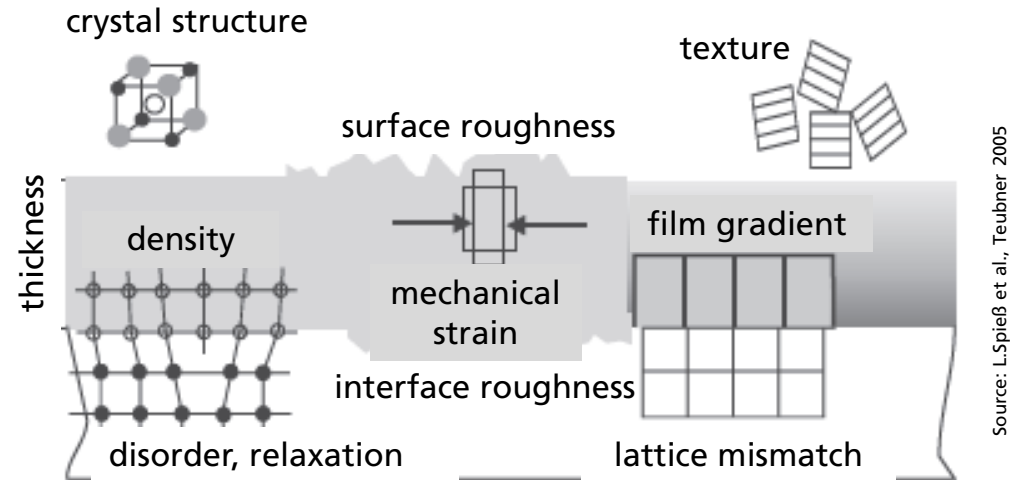
Molecular Beam Epitaxy (MBE)



Magnetron Sputtering Deposition



Structural properties of thin film material for thin film devices addressed by X-ray diffraction techniques



→ The structural properties of layered structures can be very different

Fields of application of X-ray diffractometry / reflectivity are manifold:

Polycrystalline samples / layers: phase analysis, texture, strain, size of crystallites, thickness, roughness, density,

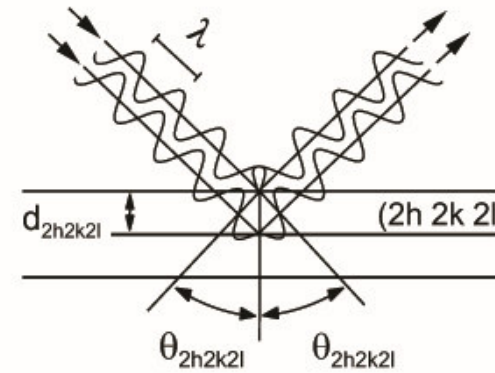
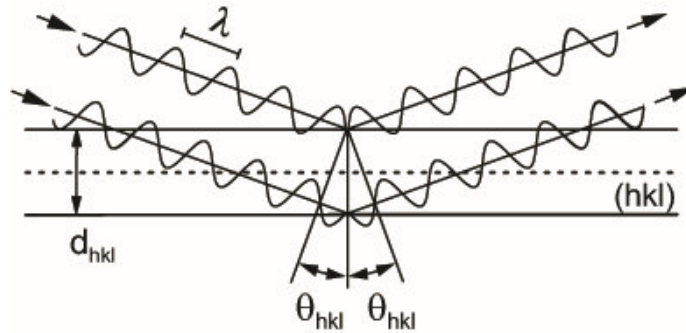
...

Single crystalline layers: layer thickness, strain, layer composition, superlattice periods, perfection, roughness, homogeneity, ...

Outline

- Motivation
- **Basics of X-ray Diffraction Method**
- Instrumentation for High Resolution X-ray Diffraction
- Scanning in Reciprocal Space
- Stress and Strain in Epitaxial Thin Films
 - Fully strained Films
 - Partially Strained Films
 - Composition of Alloy Films
- Measurement of the Layer's Thickness
 - Single Layers and Layer Stacks
 - Superlattices
- Analysis of the Orientation of a Thin Film
- Mosaicity in Thin Films
- Synchrotron Bragg Diffraction Imaging for Substrate Analysis
- Recommended Readings

Bragg's law depicted in real space



$$n\lambda = 2d_{hkl} \sin\theta_{hkl}$$

where: n = order of diffraction

λ = X-ray wavelength

d_{hkl} = distance between lattice planes

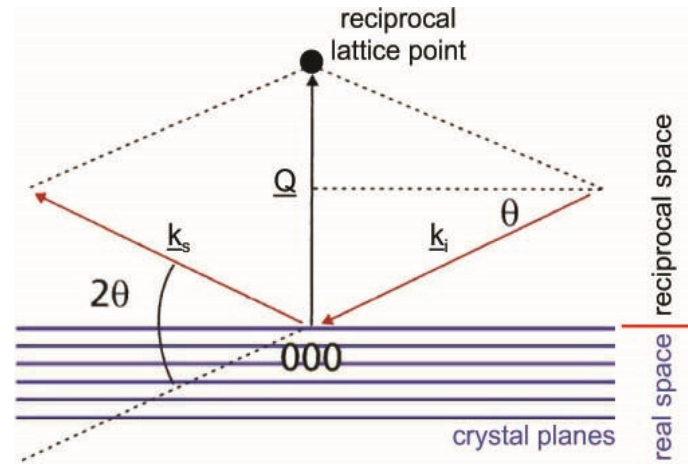
θ_{hkl} = Bragg angle

$$d_{2h2k2l} = d_{hkl} / 2$$

$$\sin\theta_{2h2k2l} = 2 \sin\theta_{hkl}$$

A monochromatic X-ray beam of wavelength λ is diffracted by a set of lattice planes (hkl) according to their spacing d_{hkl} . Different orders of X-ray diffraction can occur at various Bragg angles Θ_1, Θ_2 , etc., according to the integer n , which is defined by the difference between the propagation lengths of the X-ray waves. Examples for $n = 1$ and $n = 2$ are shown here.

Bragg's law depicted in reciprocal space



The experimental conditions are defined by following construction:

In the reciprocal space interpretation of Bragg's law the incident beam is represented by a wave vector k_i which has length $|k_i| = 1/\lambda$. The detected beam is represented by the vector k_s which also has the same length $|k_s| = 1/\lambda$. Together these vectors define the scattering vector Q , in which $Q = k_s - k_i$. The angle between k_i and k_s is 2Θ and so the length of the scattering vector $|Q| = 2\sin\Theta |k_i|$.

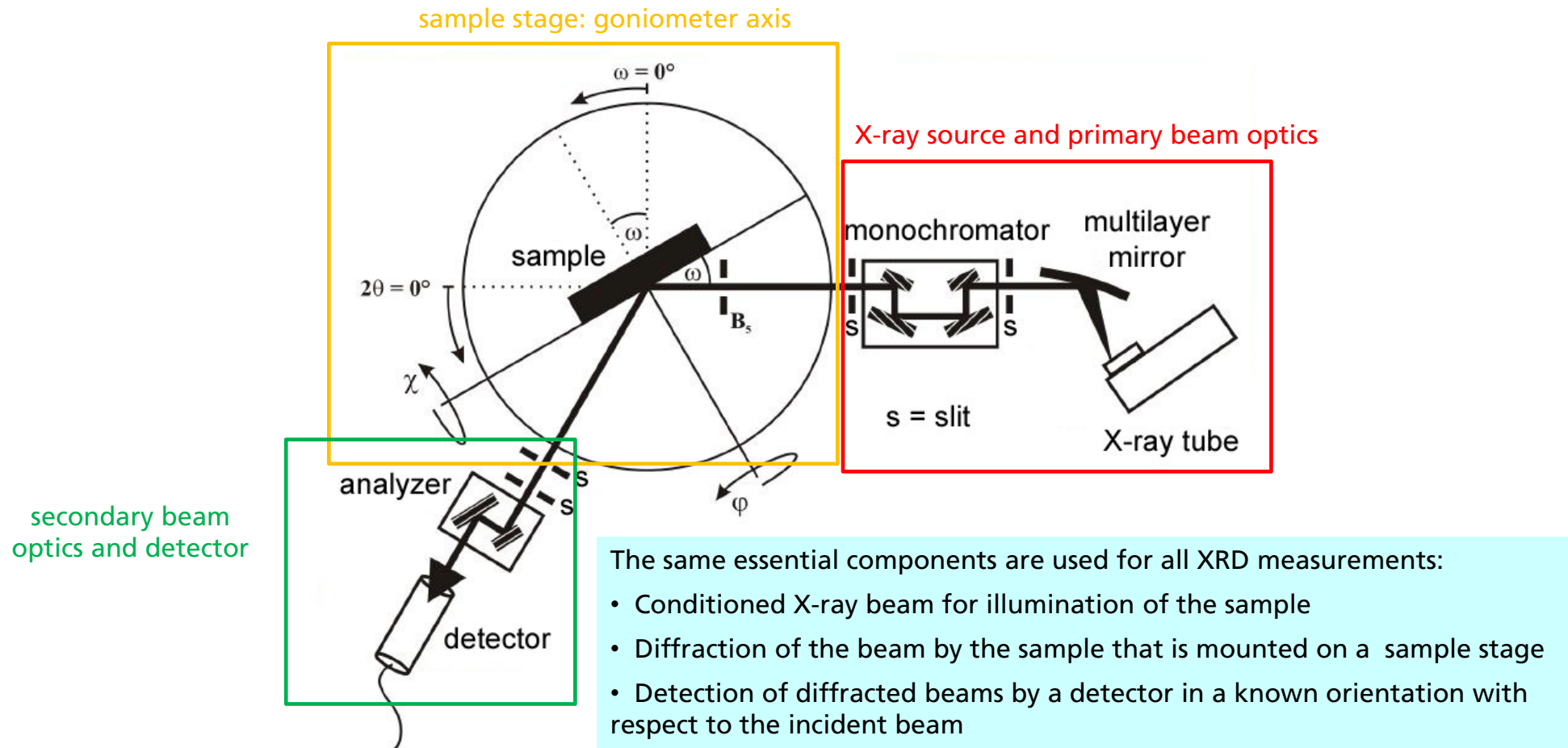
Bragg scattering from a set of planes (hkl) occurs when a crystal is introduced into the experiment such that the scattering vector Q is exactly equivalent to the reciprocal lattice vector d_{hkl}^* . The reciprocal lattice vector is normal to the planes hkl and has length $|d_{hkl}^*| = 1/d_{hkl}$. The Bragg condition is therefore also expressed by: $1/d = |Q|$

That, on substitution, rearranges to give: $\lambda = 2d \sin\Theta$

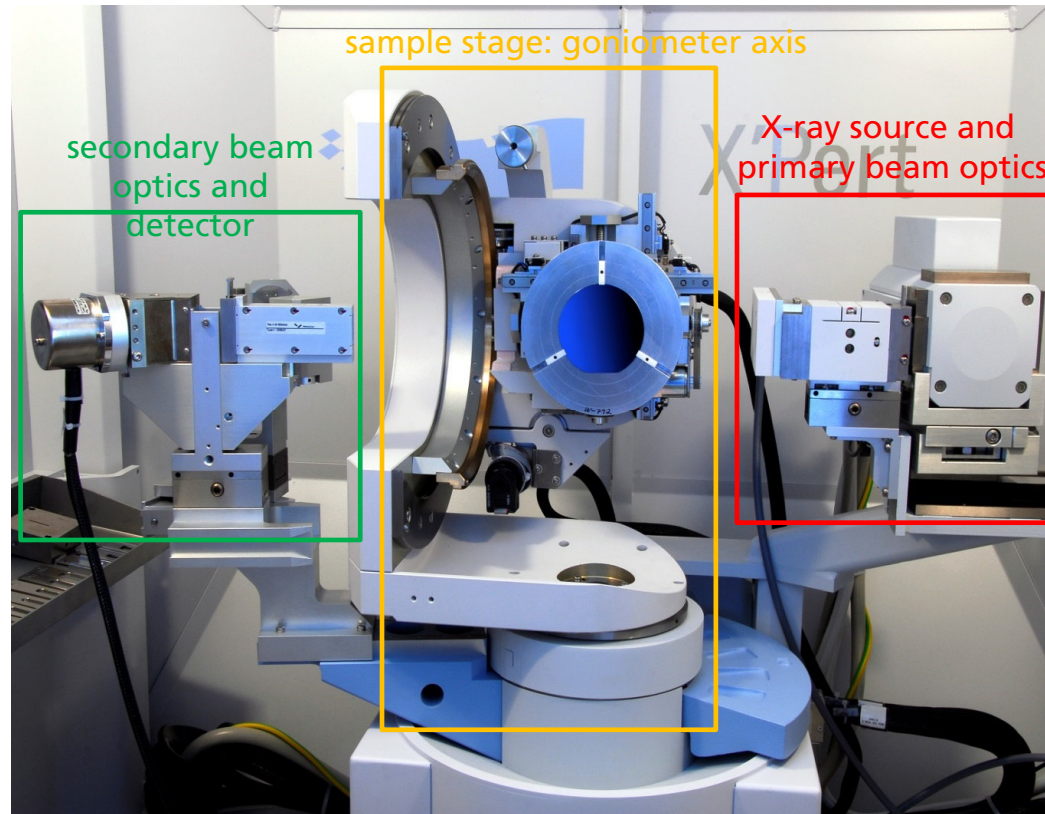
Outline

- Motivation
- Basics of X-ray Diffraction Method
- **Instrumentation for High Resolution X-ray Diffraction**
- Scanning in Reciprocal Space
- Stress and Strain in Epitaxial Thin Films
 - Fully strained Films
 - Partially Strained Films
 - Composition of Alloy Films
- Measurement of the Layer's Thickness
 - Single Layers and Layer Stacks
 - Superlattices
- Analysis of the Orientation of a Thin Film
- Mosaicity in Thin Films
- Synchrotron Bragg Diffraction Imaging for Substrate Analysis
- Recommended Readings

Instrumentation for High Resolution X-ray Diffraction



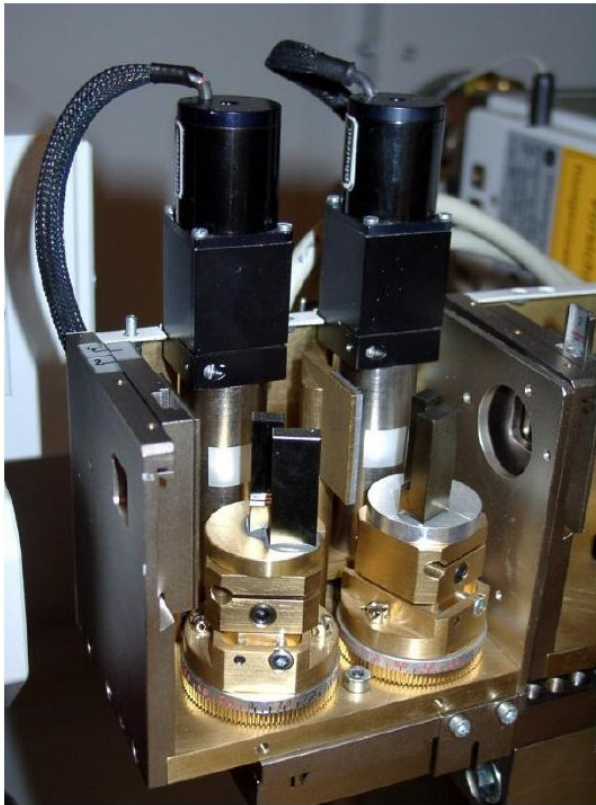
Instrumentation for High Resolution X-ray Diffraction



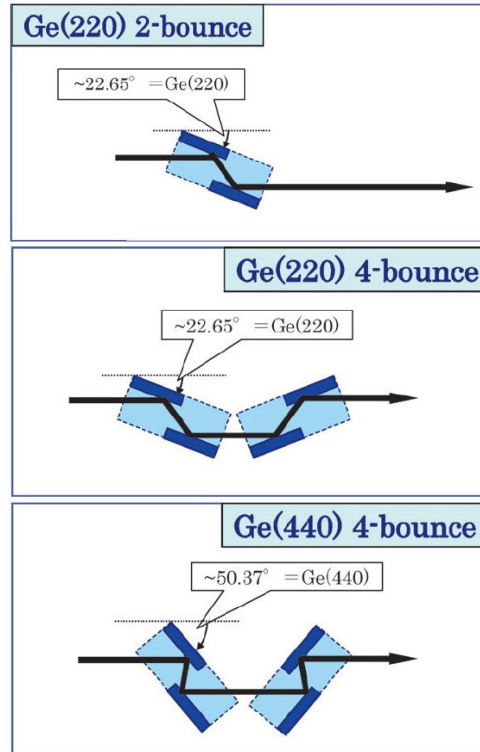
Malvern-Panalytical X'Pert Pro MRD system

Primary beam optics: monochromator

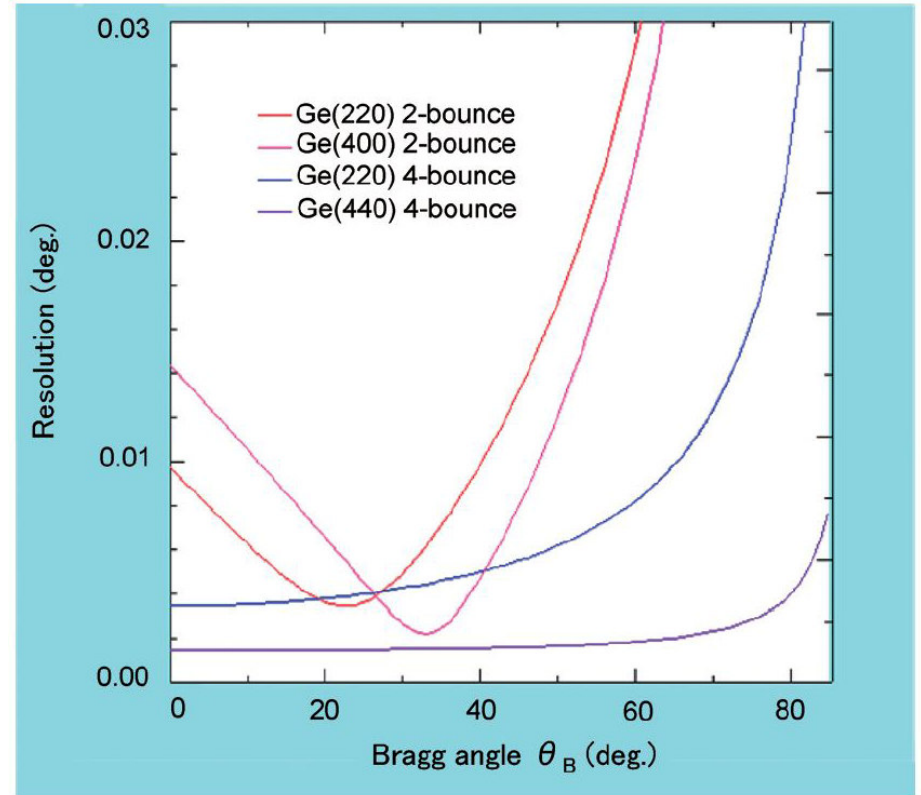
Resolution function for different types of monochromators



Bartels-DuMond Ge 220 four-crystal monochromator



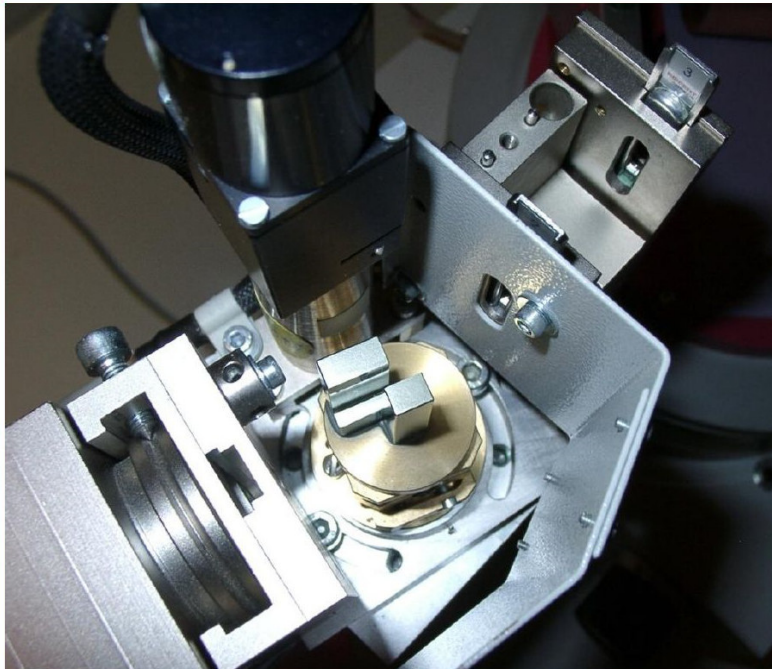
T. Konya, The Rigaku Journal 25(2), 2009



Monochromators and their resolution.

Secondary beam optics: analyzer

An analyzer is a “monochromator on the diffracted beam side” behind the sample and is placed before the detector.



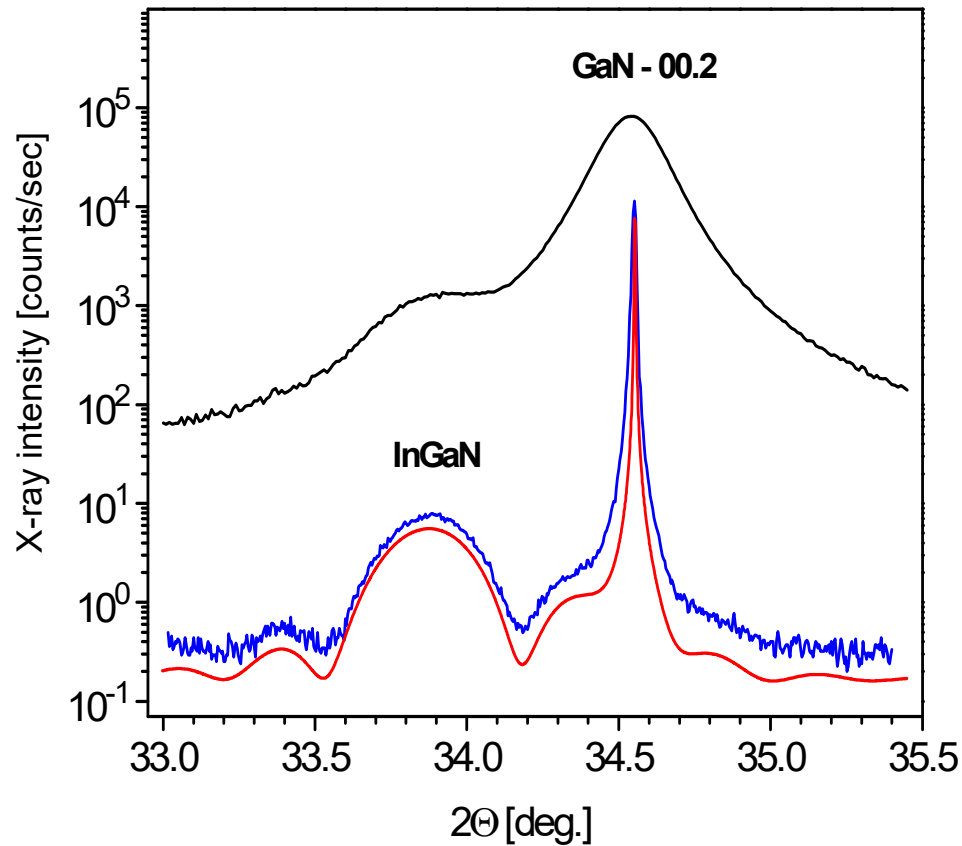
Channel cut Ge (110) analyzer (symmetrical cut) aligned for Ge 220 reflection.

Analyzers are used to increase the angular acceptance to achieve a better reflection or fringe resolution or better intensity dynamics.

For a Ge 220 analyzer the angular acceptance $\Delta 2\theta$ of the diffracted beam is reduced to $\approx 12''$.

Choice of the right optics for resolving diffraction peaks with lower structural perfection

Example: InGaN / GaN / Al₂O₃ (0001), dislocation density $\sim 10^9$ - 10^{10} cm⁻²



intended sample structure:

30 nm InGaN
2.7 μm GaN
500 μm sapphire (00.1)

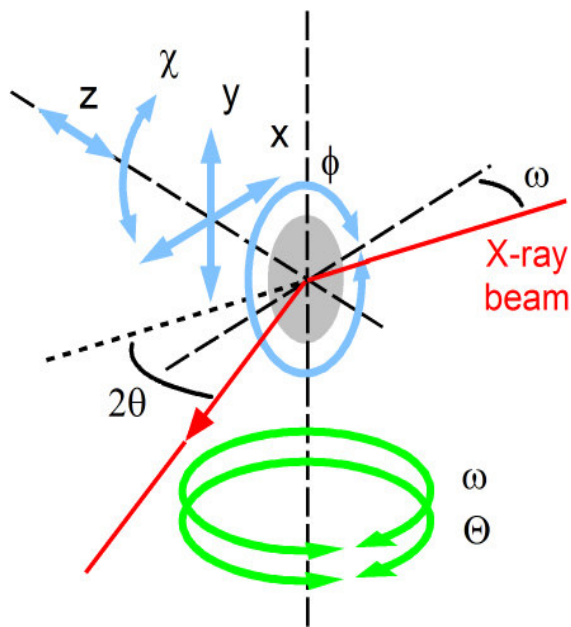
— open ended detector
— with analyzer
— simulation

X-ray results (InGaN-layer):

$$t = (28.0 \pm 0.6) \text{ nm}$$

$$\Delta d/d_{\text{perp.}} = (20 \pm 1) \times 10^{-3}$$

Sample stage



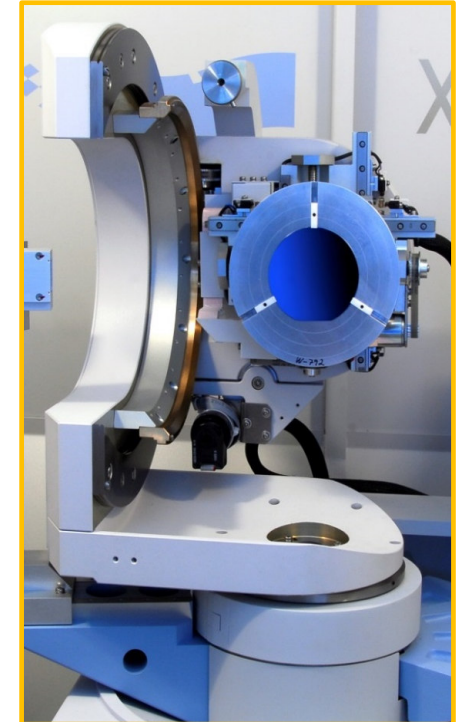
Scheme of a sample stage with goniometer

The sample stage may offer various alignment axes:

- Orthogonal **X, Y and Z axes** that drive the sample stage so that the wafer as a whole is positioned as required with respect to the incident beam
- **Phi (ϕ) axis** to align the crystal in the correct azimuth
- **Chi (χ) axis** for a fine adjustment to optimize a peak alignment
- The **goniometer axes** are the largest and most precise:

They regulate and control the incident beam angle **omega (ω)** with respect to the sample stage and the detector position, **2theta (2θ)** with respect to the incident beam direction.

For HRXRD systems the minimum step size for ω and 2θ is 0.0001° .



Panalytical X'Pert Pro MRD system

Outline

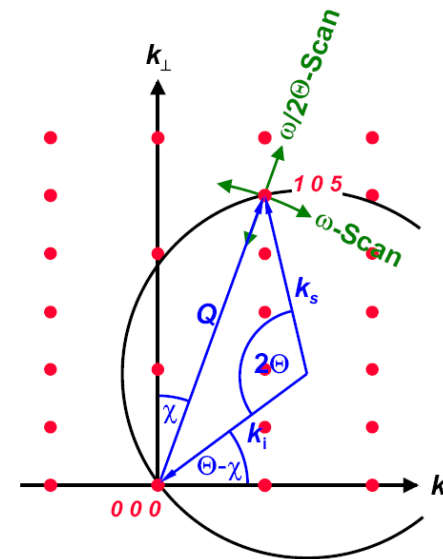
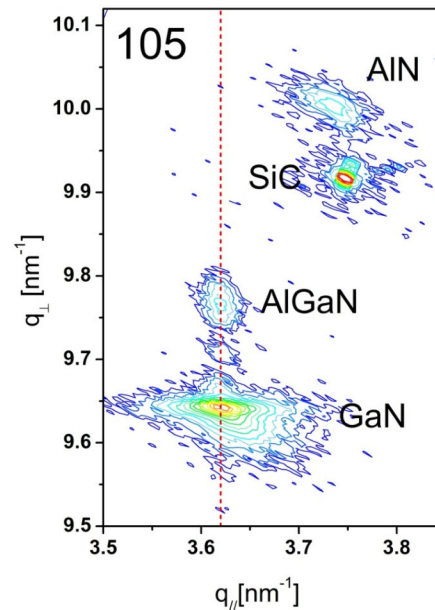
- Motivation
- Basics of X-ray Diffraction Method
- Instrumentation for High Resolution X-ray Diffraction
- **Scanning in Reciprocal Space**
- Stress and Strain in Epitaxial Thin Films
 - Fully strained Films
 - Partially Strained Films
 - Composition of Alloy Films
- Measurement of the Layer's Thickness
 - Single Layers and Layer Stacks
 - Superlattices
- Analysis of the Orientation of a Thin Film
- Mosaicity in Thin Films
- Synchrotron Bragg Diffraction Imaging for Substrate Analysis
- Recommended Readings

Scanning in reciprocal space

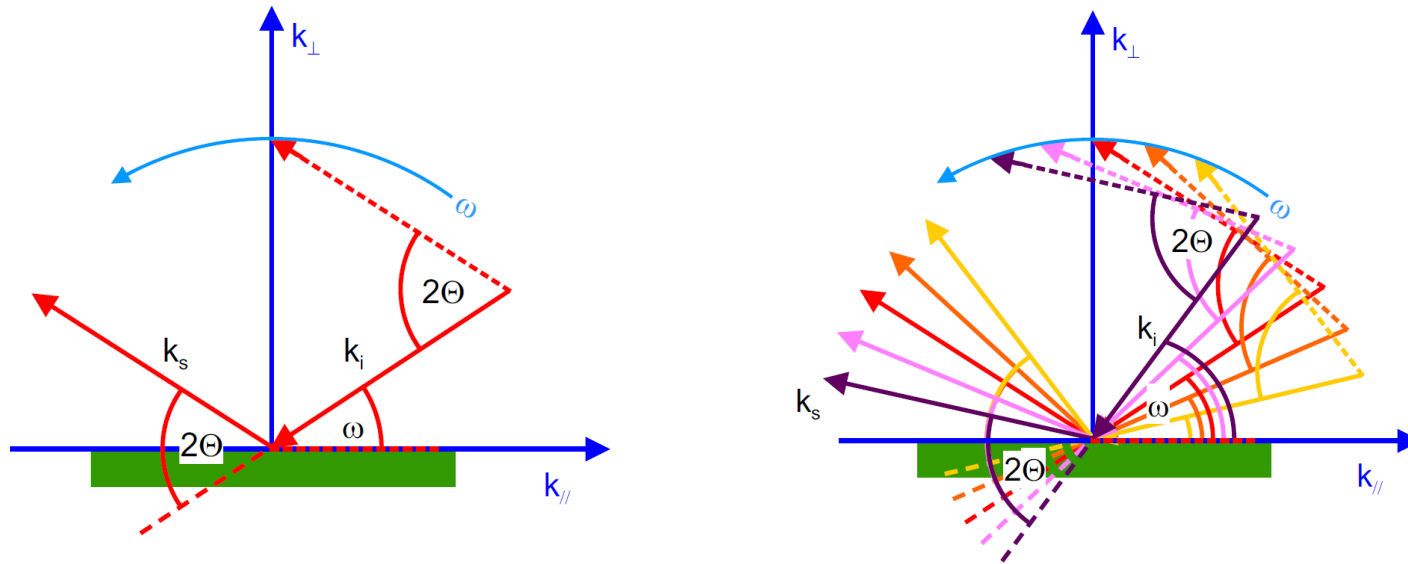
Why do we need different scan-types?

- A crystal is a three-dimensional body. Thus, the structural properties can be different in different directions (e.g. thickness, strain, perfection, ...).
- These structural differences are revealed by the position and shape of the reciprocal lattice points (RLPs) in the diffraction experiment.
- Depending on the crystal property to be measured, the scan direction in reciprocal space must be selected.

Reciprocal space map of an AlGaIn/GaN/AlN/SiC (0001) HEMT structure



The ω scan

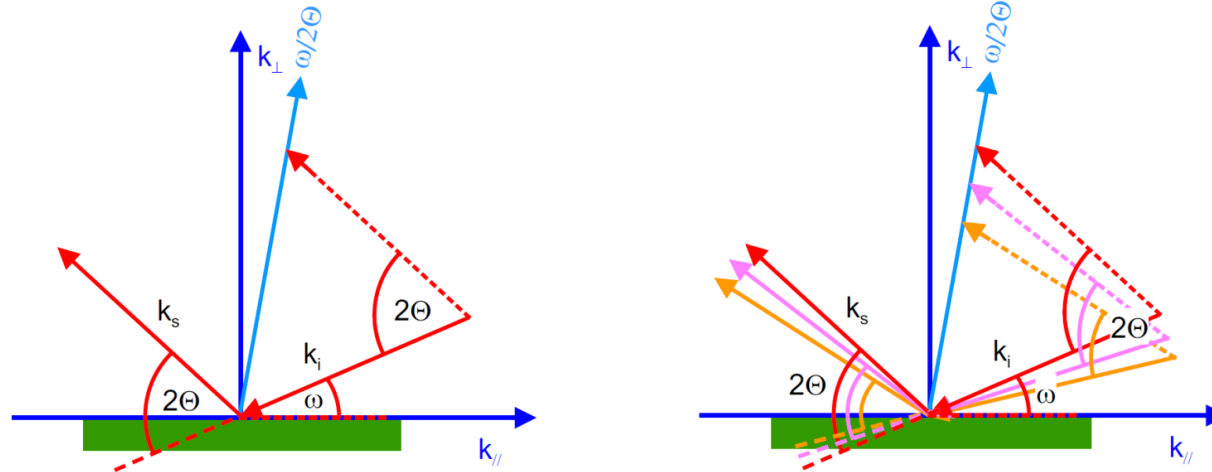


2Θ (= position of the detector angle) is fixed

ω scan:

If the sample is rotated by changing ω , while the detector angle 2Θ remains stationary, the Ewald sphere is rotated around 000 (= origin of the reciprocal space). During this motion the reciprocal space probe moves along a circle with the center 000 and radius of the scattering vector.

The $\omega/2\Theta$ scan, $2\Theta/\omega$ scan and $\Theta/2\Theta$ scan



$\omega/2\Theta$ scan:

The sample is rotated by ω and the detector is rotated by 2Θ with an angular ratio of 1:2. In reciprocal space, the reciprocal space probe moves outward from the origin 000. The length of the scattering vector changes, but its direction remains the same and depends on the offset between ω and Θ .

$2\Theta/\omega$ scan:

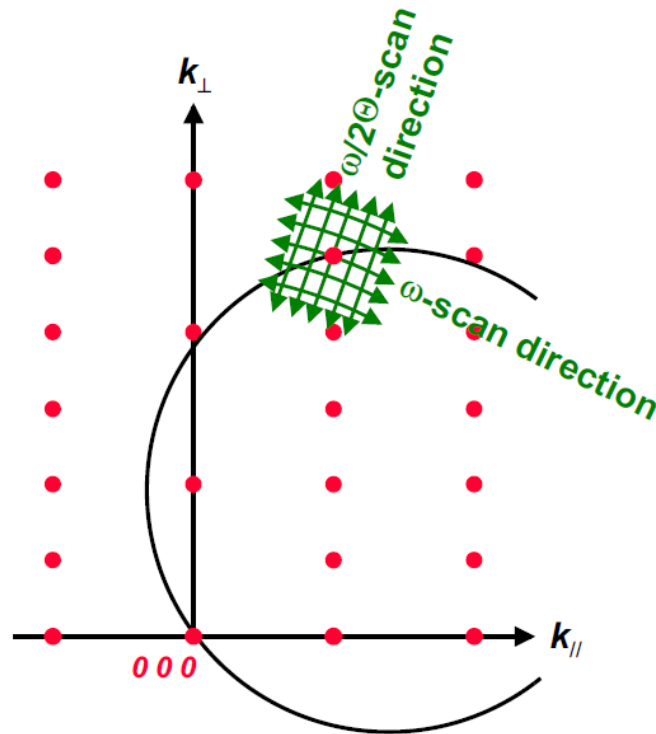
The same scan movements like for a $\omega/2\Theta$ scan but for $2\Theta/\omega$ scans, the scanned number is in units of 2Θ , whereas for $\omega/2\Theta$ scans, the scanned number is in units of ω .

$\Theta/2\Theta$ scan:

If there is no axis offset, i.e. $\omega = \Theta$. This is called a symmetrical $\Theta/2\Theta$ scan, which is a vertical scan movement in reciprocal space.

Reciprocal space maps (RSMs)

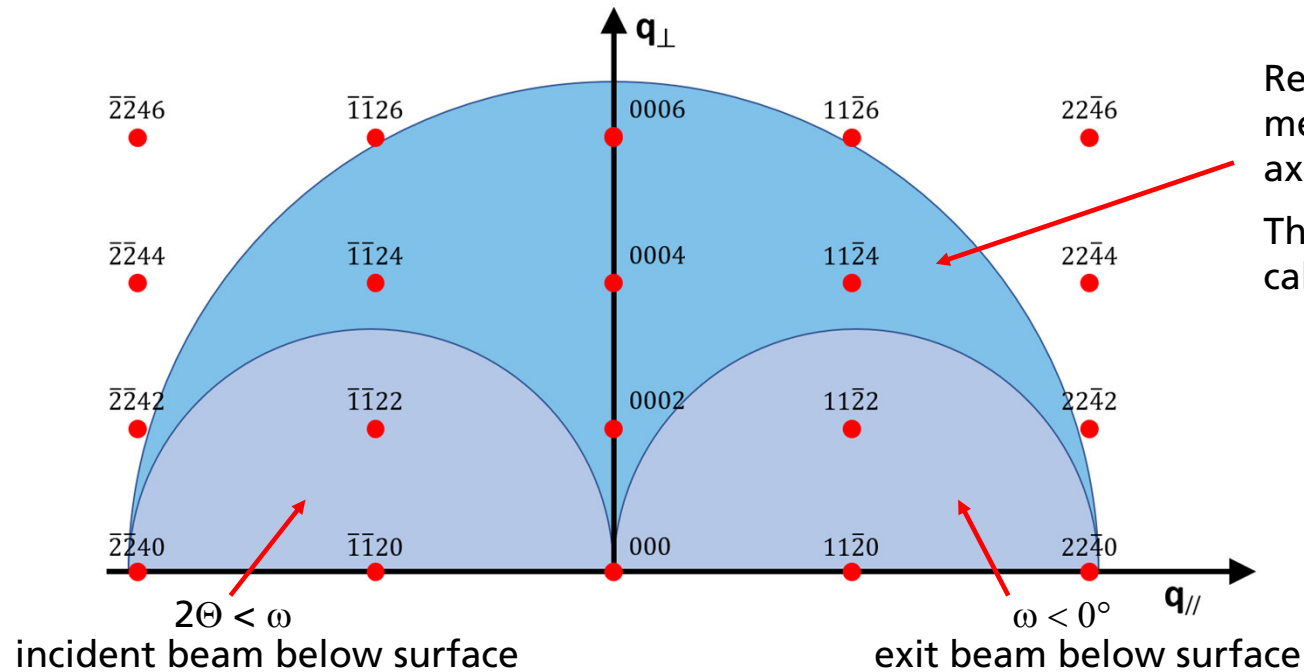
Combining $\omega/2\Theta$ scans with ω scans:



Much of the information about inter-plane spacing and defect-induced broadening can be captured in reciprocal space maps (RSM), which show a 2D slice through reciprocal space (the intensity shown in RSM is usually a projection of the 3D intensity of the diffraction spot(s) onto a 2D plane).

RSMs can be obtained by taking a series of $\omega/2\Theta$ scans at successive ω values (or vice versa) and presenting the results in the map form.

Reciprocal lattice of $\text{Al}_{0.5}\text{Ga}_{0.5}\text{N}$ (0001) in the $[11\bar{2}0]$ azimuth for $\text{CuK}\alpha_1$ radiation



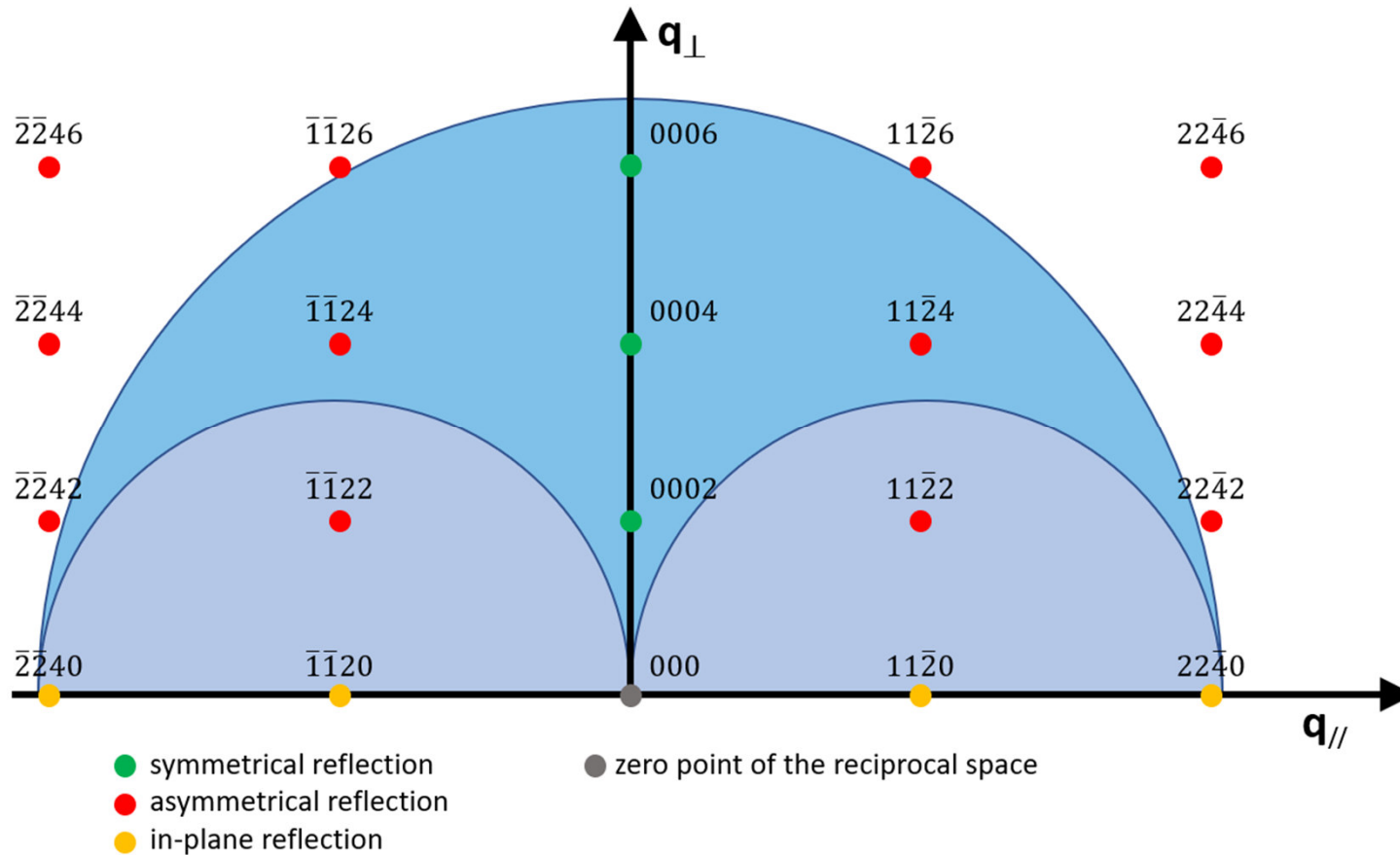
Reflections in this area can be measured by moving the 2θ -axis and ω -axis.

This measurement geometry is called "**coplanar geometry**".

Schematic representation of the accessible reciprocal lattice points (RELPs) for $\text{Al}_{0.5}\text{Ga}_{0.5}\text{N}$ (0001) in the $[11\bar{2}0]$ azimuth for $\text{CuK}\alpha_1$ radiation (wavelength $\lambda = 154.059$ pm). The limit for the accessibility of the RELPs in Bragg reflection is the maximum diffractometer angle $\sim 2\theta = 160^\circ$ (wavelength dependent!). In addition, regions of reciprocal space where the sample blocks a beam are shown in light blue (inaccessible if only 2θ and ω are used as scan axis).

(Note: By tilting the sample by the axis χ of the sample stage, the lighter blue areas getting accessible, too)

Reciprocal lattice of $\text{Al}_{0.5}\text{Ga}_{0.5}\text{N}$ (0001) in the $[11\bar{2}0]$ azimuth – types of reflections



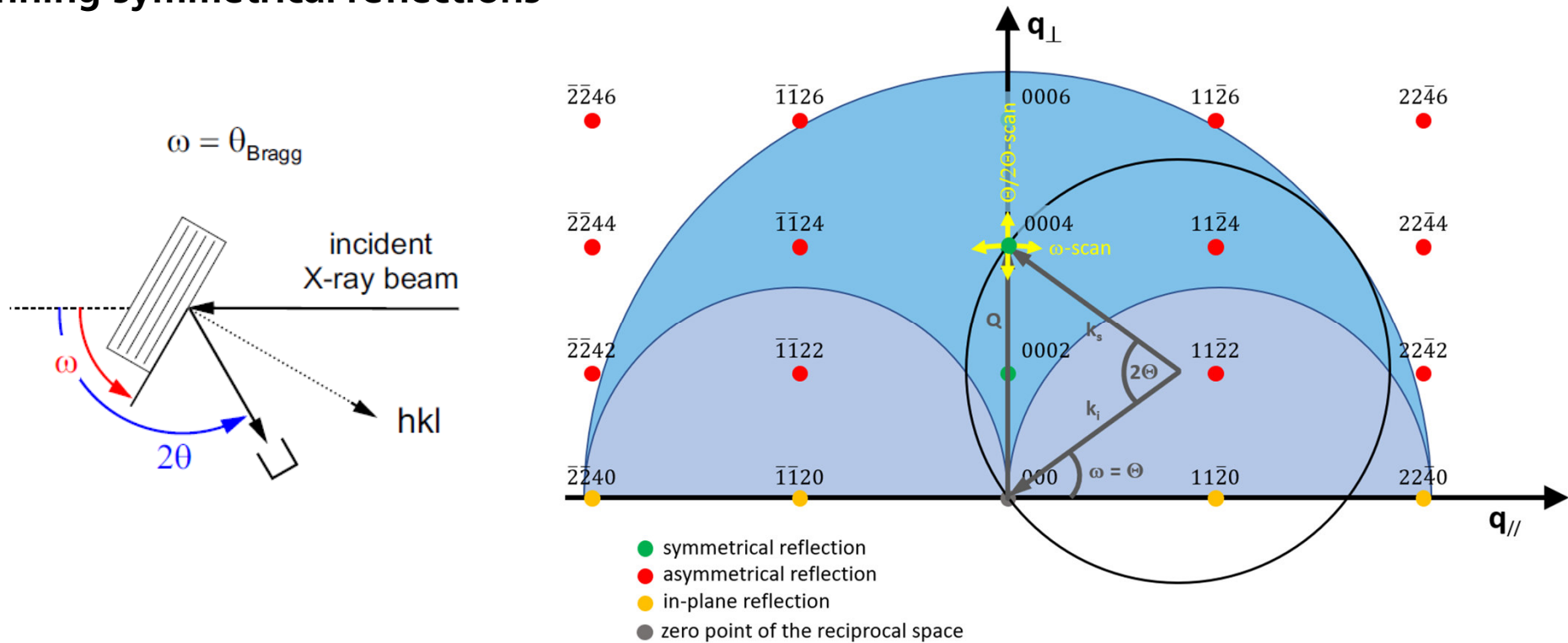
Definitions:

Bragg reflections from lattice planes running parallel to the surface are called **symmetrical reflections**.

If lattice planes are not parallel to the surface, the corresponding Bragg reflections are denoted as **asymmetric reflections**.

Bragg reflections from lattice planes that are perpendicular to the sample surface are referred to as **in-plane reflections**.

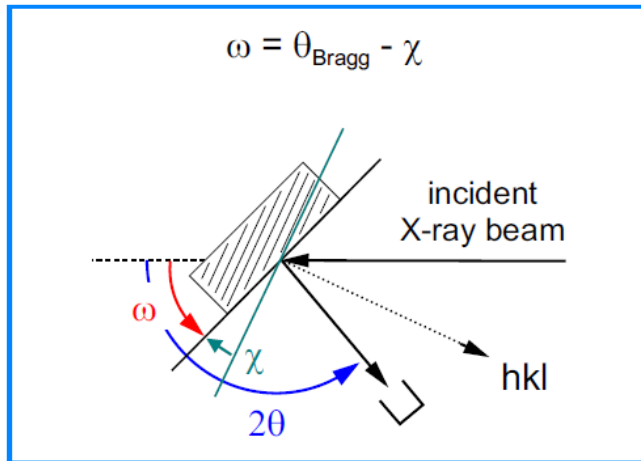
Scanning symmetrical reflections



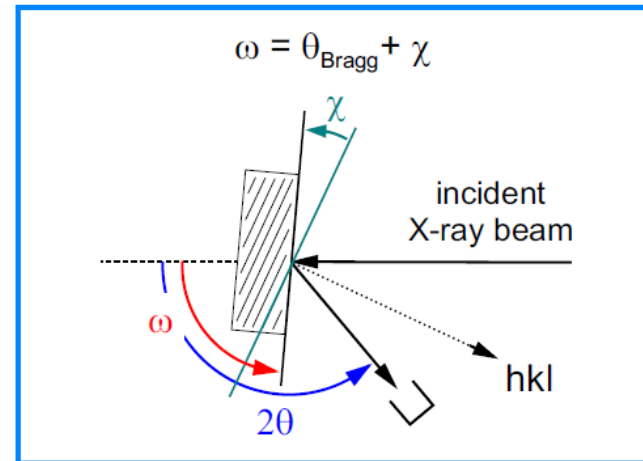
→ A special case of the $\omega/2\theta$ radial scan is the symmetric scan where $\omega = \Theta$ and the scan is perpendicular to the sample surface. Bragg diffraction occurs when there are crystal planes parallel to the surface and when $\Theta = \Theta_{\text{Bragg}}$. This is called the $\Theta/2\Theta$ scan.

Scanning asymmetrical reflections

For scanning in the **coplanar geometry** there are two possibilities for scanning asymmetrical reflections:



1) Scattering geometry with a **shallow angle of incidence** and a **steep angle of exit** (reflection: **h k l⁻**)



2) Scattering geometry with a **steep angle of incidence** and a **shallow angle of exit** (reflection: **h k l⁺**)

For scattering condition there is an offset $\omega \neq \Theta$

For the shallow incidence geometry $\omega = \Theta_{\text{Bragg}} - \chi$

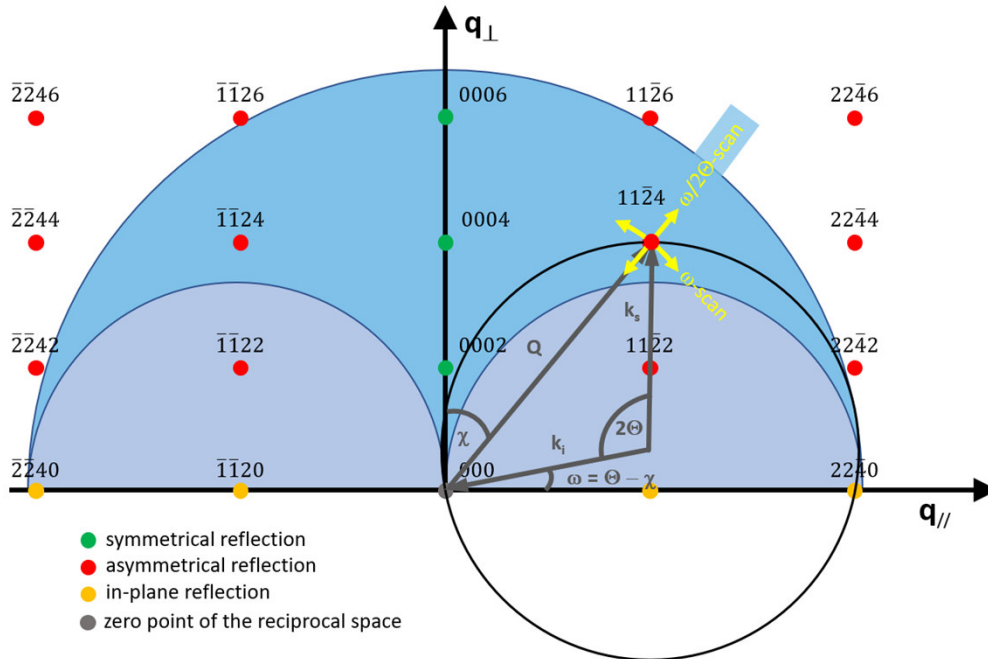
For the steep incidence geometry $\omega = \Theta_{\text{Bragg}} + \chi$

(χ = angle of inclination relative to the normal of the surface)

Scanning asymmetrical reflections

$\text{Al}_{0.5}\text{Ga}_{0.5}\text{N}$ (0001) in the $[1\bar{1}20]$ azimuth, $\text{CuK}\alpha_1$ -radiation, reflection $11\bar{2}4$

(shallow angle of incidence and steep angle of exit)



$\text{Al}_{0.5}\text{Ga}_{0.5}\text{N}$: $11\bar{2}4$ reflection

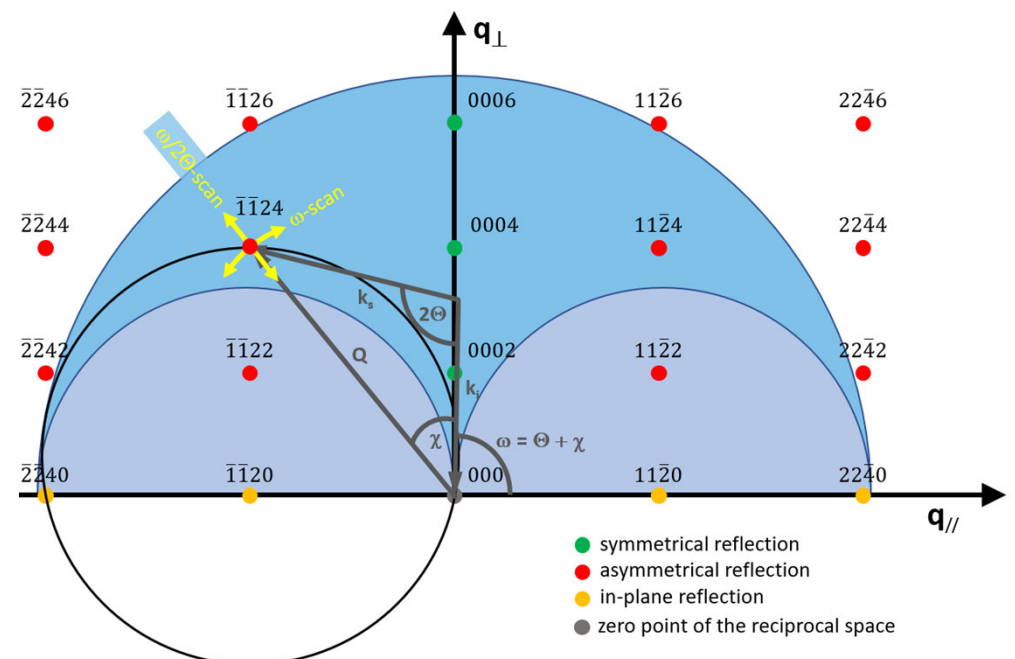
$$2\Theta = 102.2896^\circ$$

$$\chi = 38.8925^\circ \text{ (= offset)}$$

$$\omega = \Theta - \chi = 12.2523$$

$\text{Al}_{0.5}\text{Ga}_{0.5}\text{N}$ (0001) in the $[1\bar{1}20]$ azimuth, $\text{CuK}\alpha_1$ -radiation, reflection $\bar{1}124$

(steep angle of incidence and shallow angle of exit)



$\text{Al}_{0.5}\text{Ga}_{0.5}\text{N}$: $\bar{1}124$ reflection

$$2\Theta = 102.2896^\circ$$

$$\chi = 38.8925^\circ \text{ (= offset)}$$

$$\omega = \Theta - \chi = 90.0373$$

Scan units

Scans can be performed or displayed in angular units or diffraction space units (which is a reciprocal length). The diffraction space coordinates, q_x and q_z (or q_{\perp} and q_{\parallel} , k_{\perp} and k_{\parallel}), are expressed with reference to the angular positions as follows:

$$q_x = R(\cos \omega - \cos(2\Theta - \omega))$$

$$q_z = R(\sin \omega - \sin(2\Theta - \omega))$$

where $R = |k_s| = |k_i|$

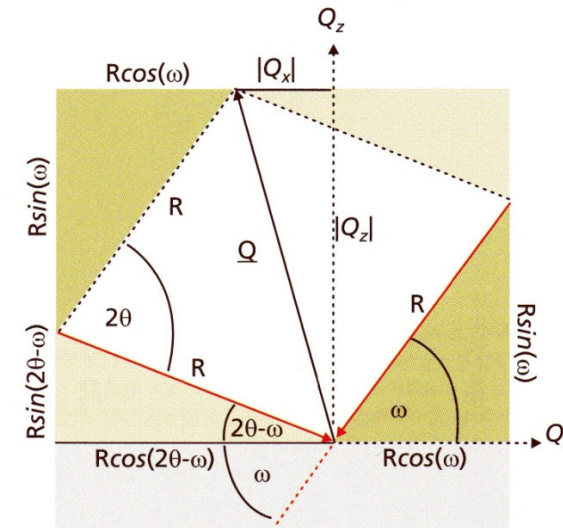
In principle R can take on many values, for example commonly used values are:

$$1/\lambda, 2\pi/\lambda, 1, 1/2$$

The length of the diffraction vector $|Q|$ is given by:

$$|Q| = \sqrt{(q_x^2 + q_z^2)} = 2R \sin(\Theta)$$

If there is Bragg diffraction and $R = 1/\lambda$, then $d_{hkl} = 1/|Q|$.



Schematic diagram to illustrate the relationship between the diffraction vector and the angles of incidence and detection

Kidd, XRD of GaN and related compounds

Outline

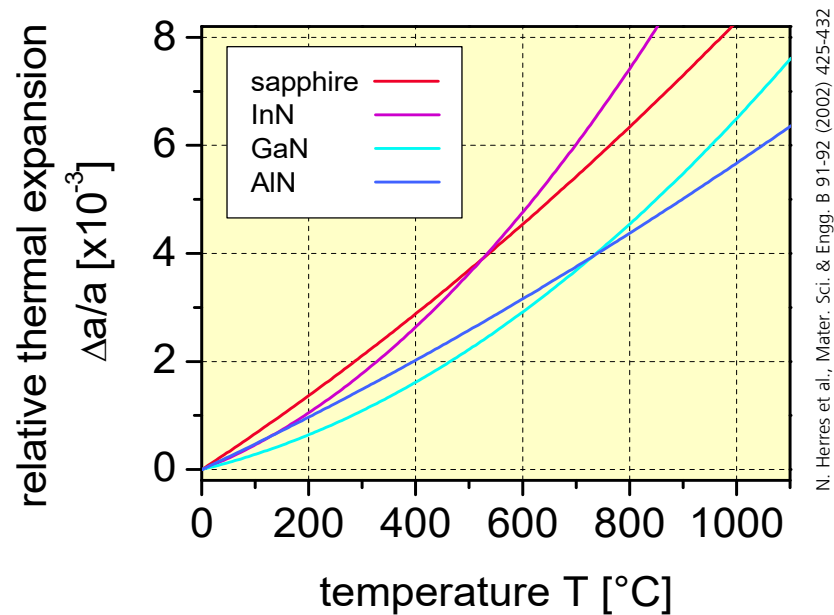
- Motivation
- Basics of X-ray Diffraction Method
- Instrumentation for High Resolution X-ray Diffraction
- Scanning in Reciprocal Space
- **Stress and Strain in Epitaxial Thin Films**
 - Fully strained Films
 - Partially Strained Films
 - Composition of Alloy Films
- Measurement of the Layer's Thickness
 - Single Layers and Layer Stacks
 - Superlattices
- Analysis of the Orientation of a Thin Film
- Mosaicity in Thin Films
- Synchrotron Bragg Diffraction Imaging for Substrate Analysis
- Recommended Readings

Reasons for mechanical stress in thin films (1)

- substitutional or interstitial impurities, segregations, growth processes, phase transformations
- mismatch of the coefficient of thermal expansion of film and substrate

→ **intrinsic strains**

→ **thermal strains**



Relative thermal expansion of the a -lattice parameter of InN, GaN, AlN and sapphire (often used as a substrate material)

Reasons for mechanical stress in thin films (2)

Thermal mismatch:

When a film on a substrate is subjected to a temperature change (e.g. cooling down from deposition temperature), differential thermal expansion will result in thermal stresses in film and substrate.

Thermal mismatch strain:

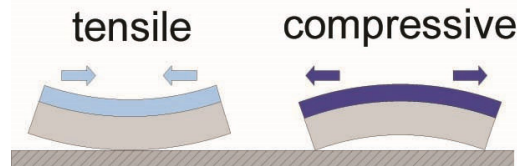
$$\varepsilon_{F,mismatch} = (\alpha_{T,F} - \alpha_{T,S})\Delta T$$

With linear thermal expansion coefficient

$$\alpha_T = \frac{d\varepsilon}{dT}, \quad T = \text{temperature (Kelvins}^{-1}\text{)}$$

For $\alpha_{T,F} > \alpha_{T,S} \Rightarrow$ tensile strain.

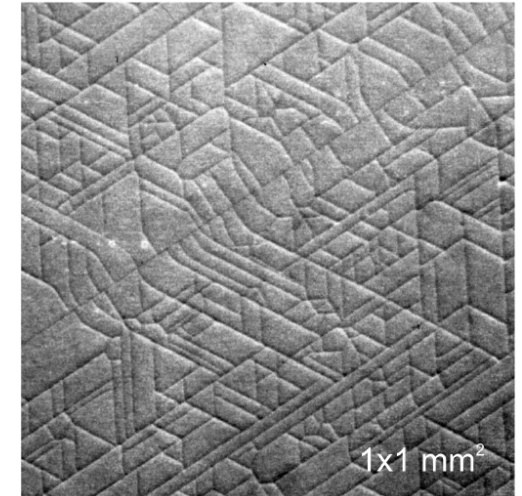
For $\alpha_{T,F} < \alpha_{T,S} \Rightarrow$ compressive strain.



In-plane biaxial stress:

$$\sigma_{F,mismatch} = \left(\frac{E}{1-\nu} \right) \cdot \varepsilon_{F,mismatch}$$

$E = \text{Young's modulus}$
 $\nu = \text{Poisson number}$



1.3 μm GaN on Si with cracks:
When cooling down silicon shrinks less than GaN which leads to tensile strain and cracking

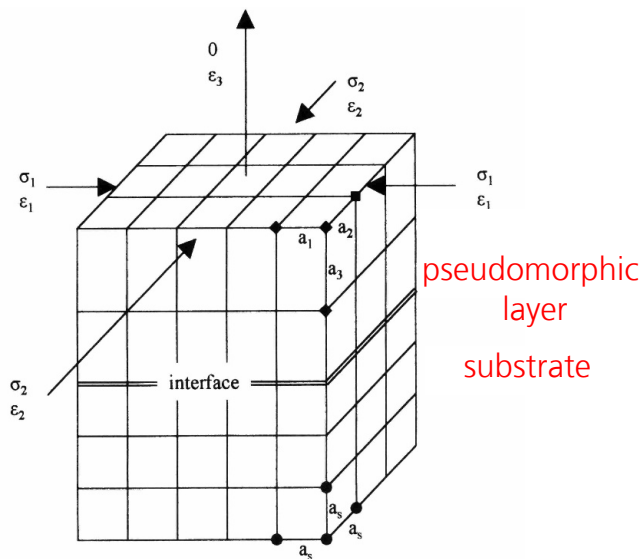
A. Krost, Univ. Magdeburg

Reasons for mechanical stress in thin films (3)

- pseudomorphic fit in epitaxial heterostructures
- local stress from partial relaxation due to large **lattice mismatch**, handling, and other nonuniform influences

- **epitaxial strains**
- **relaxation (plastic deformations)**

Pseudomorphic fit

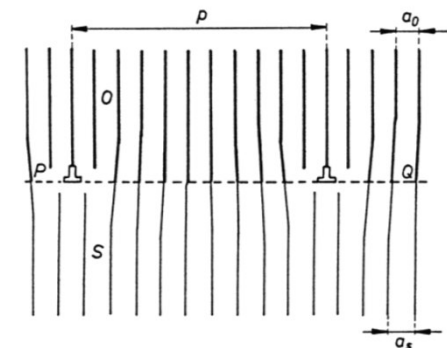
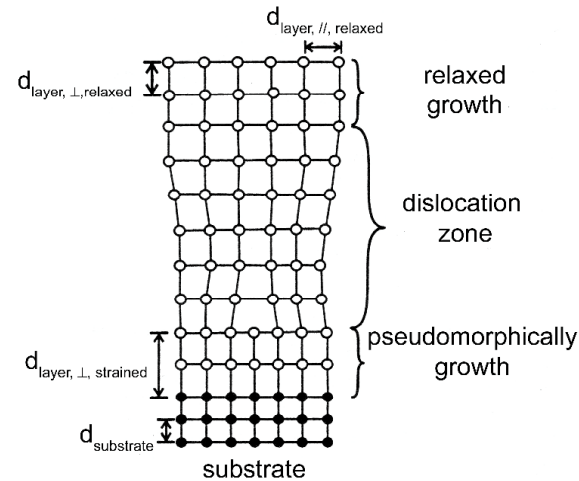


A. Kelly et al. "Crystallography and Crystal Defects" (Wiley, 2000)
 M. Ohring "Materials Science of Thin Films" (Academic Press, 2002)

Lattice mismatch

Situation: Same crystal structure, but different chemical composition of layer and substrate material:

With increasing layer thickness, the epitaxial layer is increasingly strained until misfit dislocations appear which lead to the relaxation of the layer (*exceeding the critical layer thickness*).



A pure misfit dislocation geometry of edge type at interface PQ of crystals O (overgrowth) and S (substrate), with lattice spacings a_o and a_s , respectively

J. Xu, Dissertation, Univ. Aachen, 1999
 M.A. Herman & H. Sitter, Molecular Beam Epitaxy, Springer, 1996

Stress – strain relation for single crystalline epitaxial films

Relation between stress and strain (Hooke's Law)

$$\sigma_{ij} = C_{ijkl} \varepsilon_{kl}$$

- In case of epitaxial films on a substrate crystal, uniaxial unit cell deformation, i.e. biaxial strain, usually occurs.
- The biaxial strain is largely due to the mismatch between film and substrate thermal expansion coefficients, as well as lattice parameter deviations.

Solving this matrix equation for certain "epitaxial cases":

Example: (Al,Ga)N layer grown on a GaN (0001) substrate:

→ Uniaxial deformation of the hexagonal unit cell along [0001] axis

Stress conditions: $\sigma_{xx} = \sigma_{yy}$ and $\sigma_{zz} = 0$

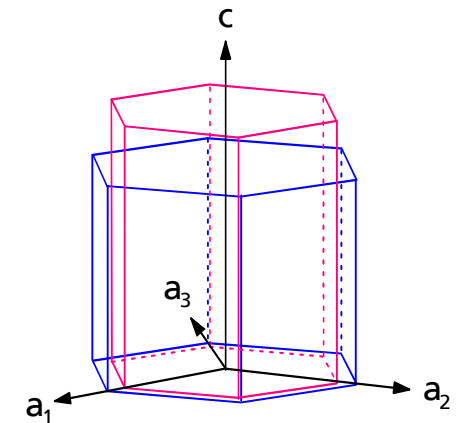
Resulting strains: $\varepsilon_{xx} = \varepsilon_{yy} =$

Stress-strain relationship:

$$\sigma_{xx} =$$

$$\begin{pmatrix} - (C_{33} / 2C_{13}) \\ (C_{11} + C_{12} - 2 C_{13}^2 / C_{33}) \end{pmatrix} \begin{pmatrix} \varepsilon_{zz} \\ \varepsilon_{xx} \end{pmatrix}$$

Film stress from material parameters and film strain



Stress determination via HRXRD strain measurements for single crystalline films (1)

This biaxial strain is a type of homogeneous strain and is defined by the relaxed reference lattice parameters \mathbf{c}_0 and \mathbf{a}_0 :

$$\varepsilon_c = \frac{\mathbf{c}_{\text{meas}} - \mathbf{c}_0}{\mathbf{c}_0} \quad (\text{S1})$$

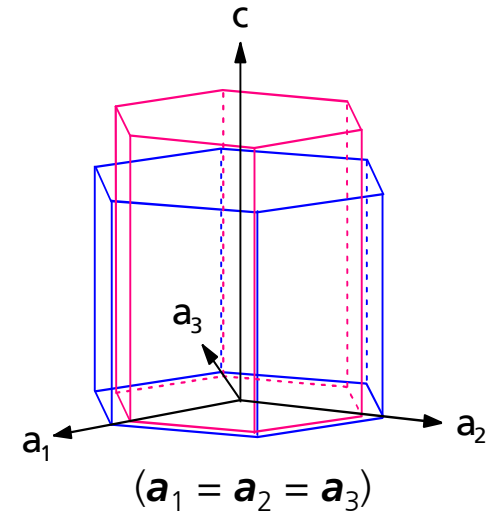
and

$$\varepsilon_a = \frac{\mathbf{a}_{\text{meas}} - \mathbf{a}_0}{\mathbf{a}_0} \quad (\text{S2})$$

For a simple hexagonal biaxial strain, the out-of-plane strain is related to in-plane strain by the strain factor D :

$$\begin{aligned} \frac{\mathbf{c}_{\text{meas}} - \mathbf{c}_0}{\mathbf{c}_0} &= -D \frac{\mathbf{a}_{\text{meas}} - \mathbf{a}_0}{\mathbf{a}_0} = \frac{2C_{13}}{C_{33}} \frac{\mathbf{a}_{\text{meas}} - \mathbf{a}_0}{\mathbf{a}_0} \\ &= \frac{2\nu}{1 - \nu} \frac{\mathbf{a}_{\text{meas}} - \mathbf{a}_0}{\mathbf{a}_0} \end{aligned} \quad (\text{S3})$$

Here, \mathbf{c}_{meas} and \mathbf{a}_{meas} are the measured strained lattice parameters, \mathbf{c}_0 and \mathbf{a}_0 are the relaxed parameters, C_{13} and C_{33} are the components of the elastic stiffness tensor, and ν is Poisson's ratio.



Stress determination via HRXRD strain measurements for single crystalline films (2)

The uniaxial Poisson's ratio ν is used to find the "unstrained" lattice parameters of strained alloy films and to relate the in-plane and out-of-plane lattice parameters in strained films (equation ((S3)), as well as in calculations used to find the composition of alloy films.

The uniaxial Poisson's ratio along [0001] direction for a hexagonal system is related to the elastic constants by:

$$\frac{2\nu}{1-\nu} = \frac{2C_{13}}{C_{33}} = -D \quad \text{with:} \quad \nu = \frac{(C_{13}/C_{33})}{1 + (C_{13}/C_{33})} \quad (S4)$$

Calculation of the unstrained lattice parameter:

The strained unit cells can be mathematically unstrained using the following equation:

$$c_0 = \frac{(c_{\text{meas}} + a_{\text{meas}} D^{hkl} E^{hkl})}{(1 + D^{hkl})} \quad \text{with} \quad E^{hkl} = \frac{c_0}{a_0} \quad (S5)$$

E^{hkl} is a normalization factor. For hexagonal (0001) orientation:

$$E^{0001} = \frac{c_0}{a_0} \quad (S6) \quad (\text{e.g. GaN } E^{0001} = 1.626)$$

Calculation of the composition for an alloy layer from the relaxed lattice parameter

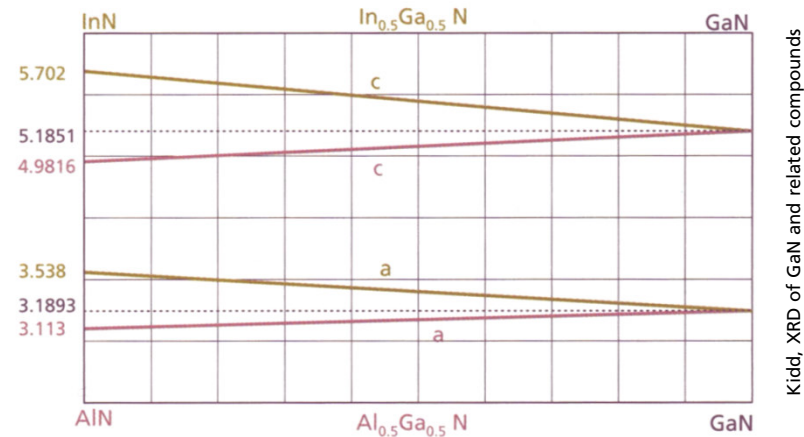
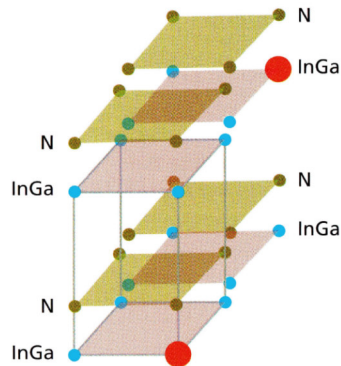
Example: hexagonal nitride solid solution (alloy) layers like AlGaN, InGaN, AlInN

If it is assumed that the material is not strained, then the composition is the only factor that affects the lattice parameters, and only one lattice parameter needs to be measured. Vegard's rule is applicable, which states that the lattice parameters of an alloy vary linearly between the end-members.

For example, for InGaN:

$$c_0^{\text{InGaN}}(x) = c_0^{\text{GaN}}(1-x) - c_0^{\text{InN}}(x) \quad (S7)$$

In a solid solution the solute atoms are randomly sited in metal positions and have the overall effect of expanding or contracting the lattice parameter in proportion to their concentration.



This means: the relaxed lattice parameters are always needed to determine the composition!

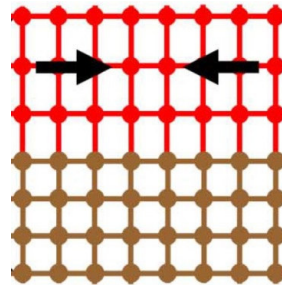
Degree of relaxation

For partially relaxed layers, the degree of in-plane relaxation, or in-plane relaxation percentage $R\%$, can be calculated by:

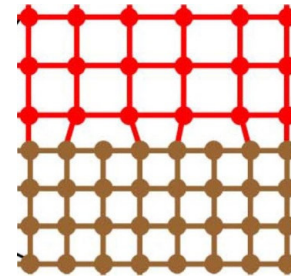
$$R(\%) = \frac{a_{layer}^{measured} - a_{substrate}^{measured}}{a_{layer}^0 - a_{substrate}^0} \quad (S8)$$

For $R = 0\%$ the layer is fully strained and for $R = 100$ the layer is completely relaxed.

fully strained



partially relaxed



Pseudomorphically (or fully) strained layers to a substrate

When the film is fully strained in the in-plane direction, the out-of-plane difference in the unit cell parameters will increase.

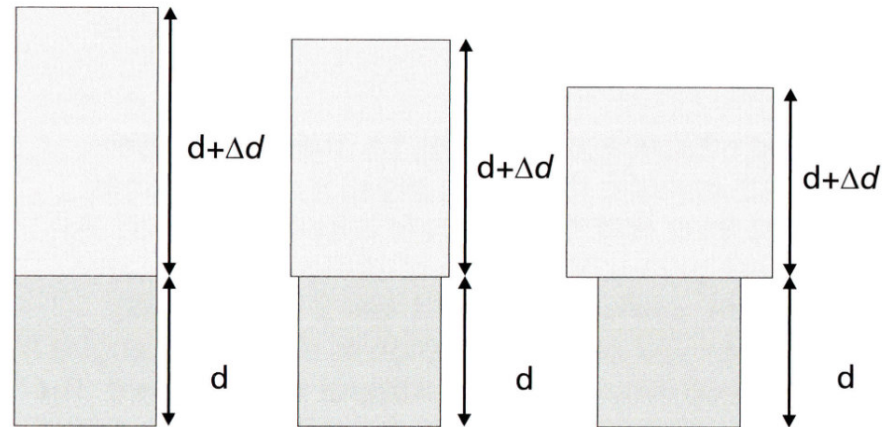


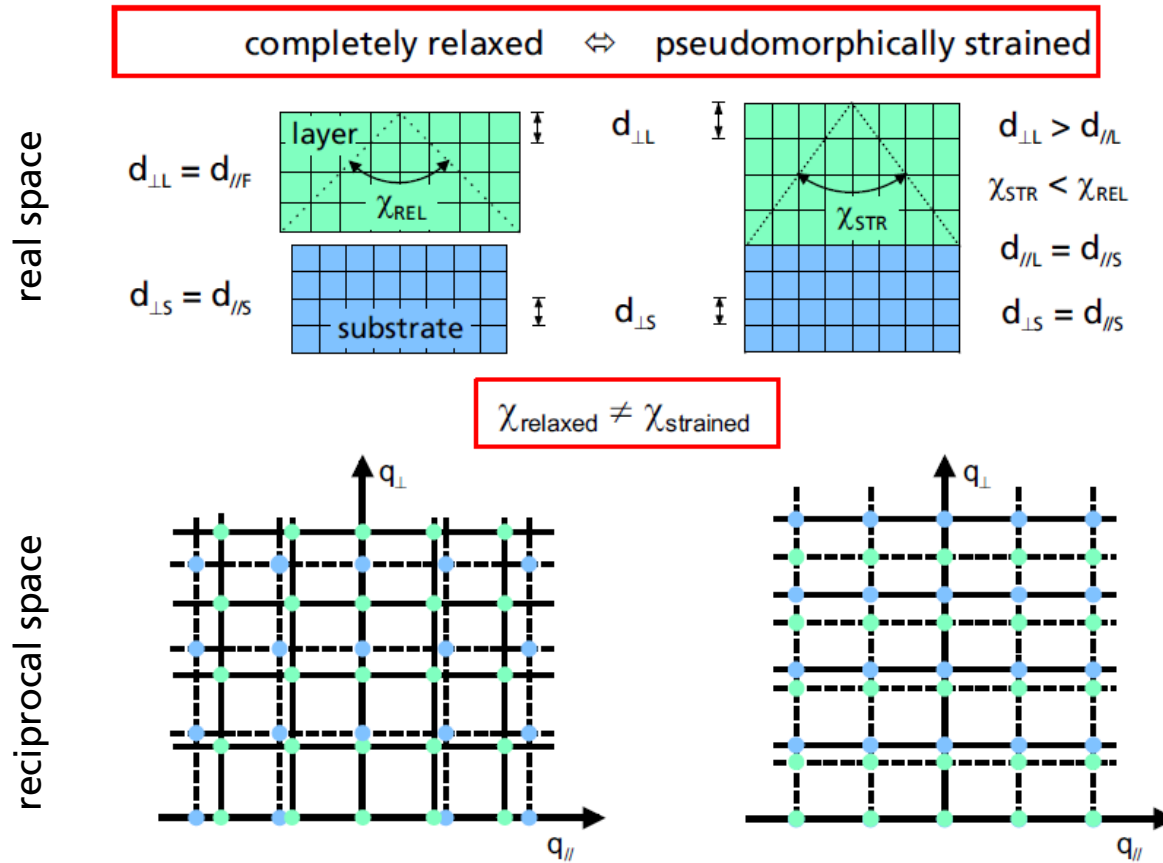
Illustration of how a layer d-spacing can be represented as an incremental addition to a comparable Substrate d-spacing. (left) Fully strained, (middle) partially relaxed, (right) fully relaxed.

However, when the film is fully strained to match the substrate, a simple correction is applied to equation S7 to restore the out-of-plane parameter to its relaxed value.

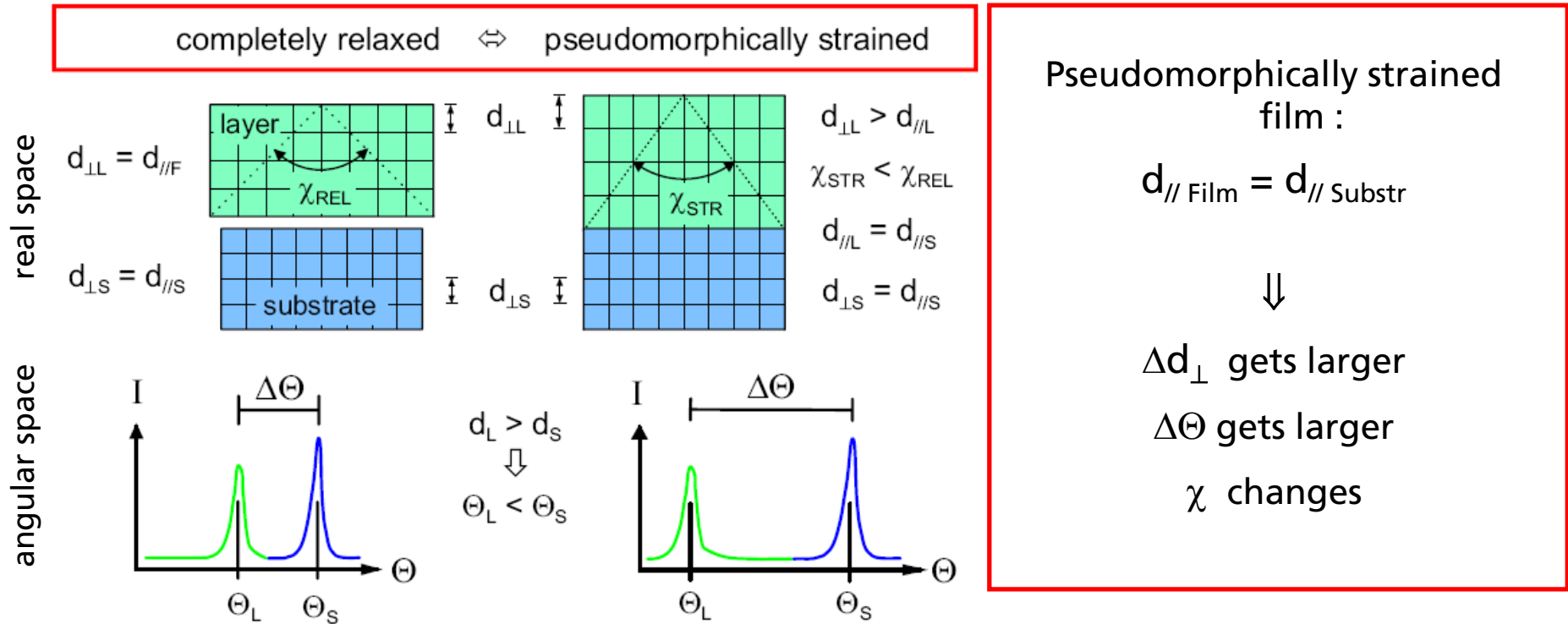
For example, for InGaN:

$$c_0^{\text{InGaN}}(x) = \frac{(1 - \nu)}{(1 + \nu)} \frac{(c_{\text{meas}}^{\text{InGaN}} - c_0^{\text{GaN}})}{(c_0^{\text{InN}} - c_0^{\text{GaN}})} \quad (\text{S9})$$

Measuring an X-ray strain of a pseudomorphically strained layer relative to a substrate (1)



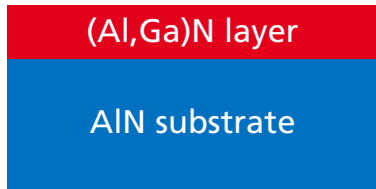
Measuring an X-ray strain of a pseudomorphically strained film relative to a substrate (2)



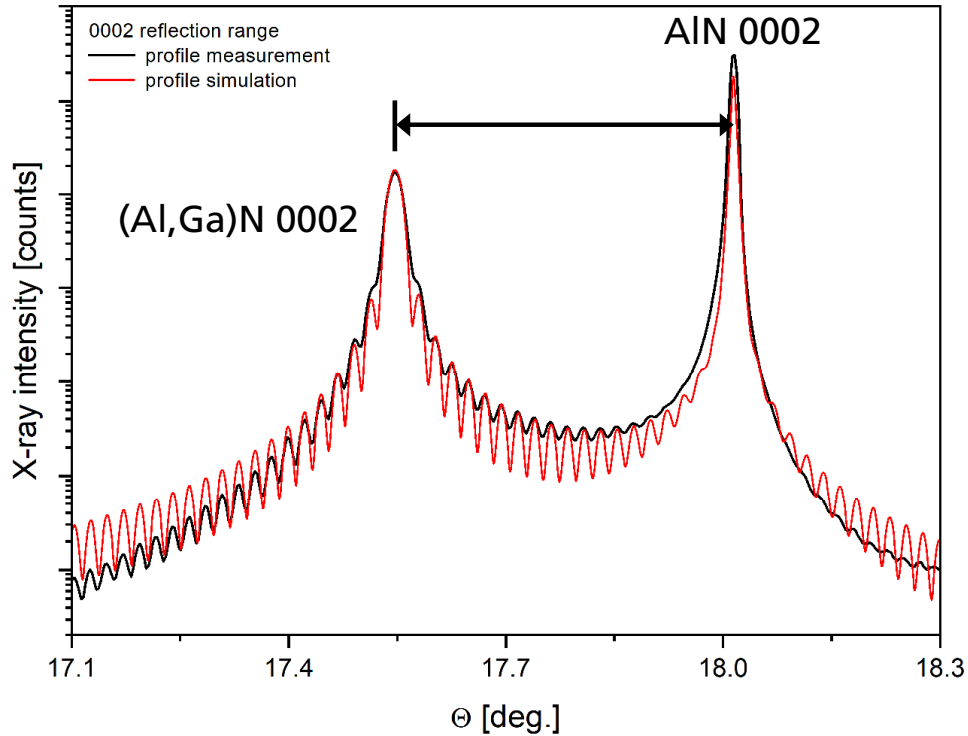
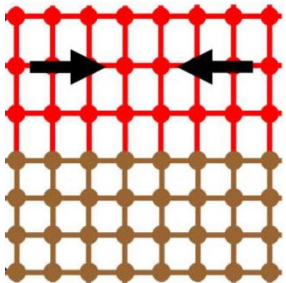
Measuring an X-ray strain of a pseudomorphically strained film relative to a substrate (3)

Example: (Al,Ga)N layer on AlN (0001)

What is the strain and the composition of the layer?



fully strained



From the position of the layer peak relative to the substrate peak:

(Al,Ga)N layer:

$$(\Delta c / c) = 25.9 \times 10^{-3}$$

Strained (Al,Ga)N *c*-lattice parameter:
511.02 pm

Using the relaxed lattice parameter *c* of the (Al,Ga)N layer (using Eq. S9) we can calculate the composition:

$$c(\text{Al,Ga})\text{N, relaxed} = x c \text{ AlN} + (1-x) c \text{ GaN}$$

$$\rightarrow \text{Al} = 52.5\%$$

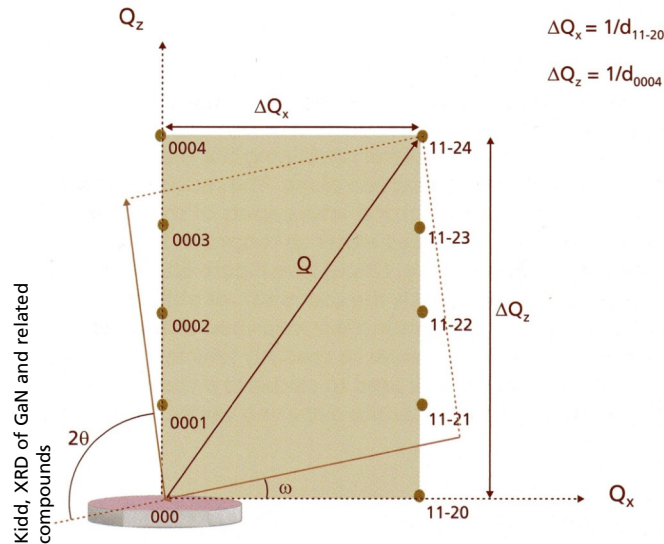
Measuring an X-ray strain of partially relaxed layers (1)

Situation: No pseudomorphic growth of the layer with respect to the substrate

→ The layer peaks have to be measured independently of substrate peaks

Procedure: Measurement and calculation of d-spacings with reference to 000

- 2Θ and ω zero positions of the goniometer have to be precisely aligned.
- Reciprocal space maps are measured to collect Bragg scattering from a number of reciprocal lattice spots and 2Θ and ω coordinates for these spots can then be obtained.
- If the layers are not tilted one RSM of an asymmetrical reflection is principle sufficient to measure the strained lattice parameters (extremely unlikely case).



The d-spacings can be calculated by the equations for d_x and d_z :

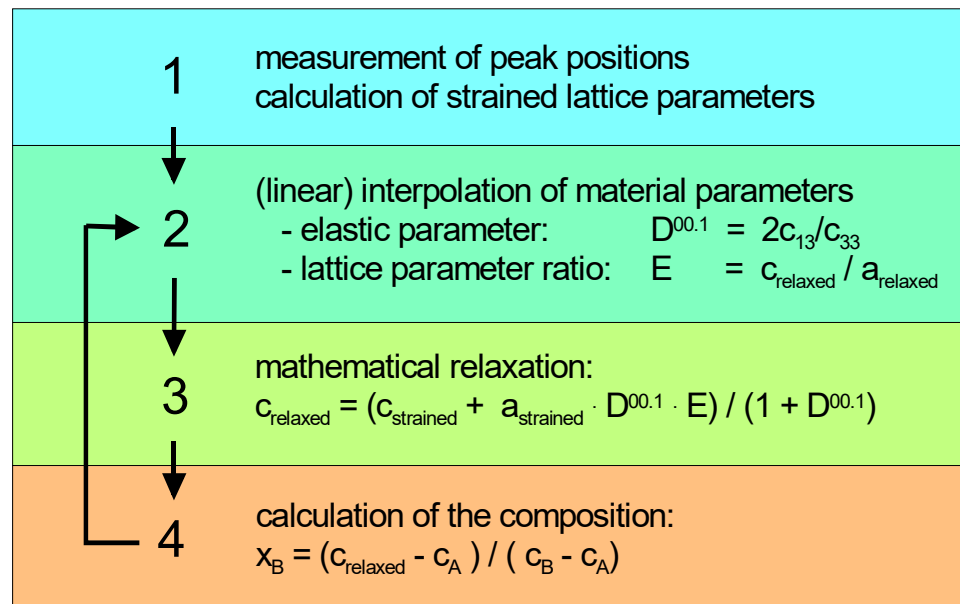
$$d_x = \frac{1}{Q_x} = \frac{\lambda}{\cos \omega - \cos(2\Theta - \omega)}$$

$$d_z = \frac{1}{Q_z} = \frac{\lambda}{\sin \omega - \sin(2\Theta - \omega)}$$

(left: Obtaining d_x and d_z of GaN from measurement of a single reciprocal lattice spot when there is no layer tilt.)

Calculation of the composition for a solid solution layer from the relaxed lattice parameter

- If the composition of a solid solution layer, x , is unknown, then the expressions for $\varepsilon_{//}$ and ε_{\perp} can not be solved individually, because the bulk values d_0 (etc.) are not known.
- To solve for x , the strain equations are combined with Vegard's law and a recursion procedure has to be performed. There are many routes through to a final solution. The complexity of the mathematics can become high and obviously depends upon the crystal structure of the layer and its orientation.

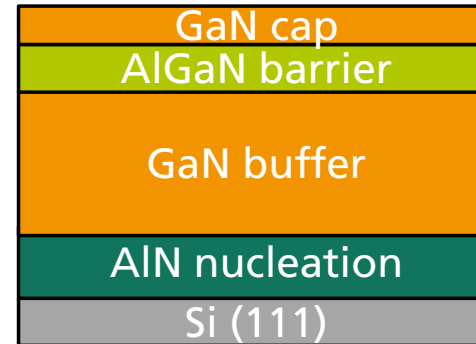
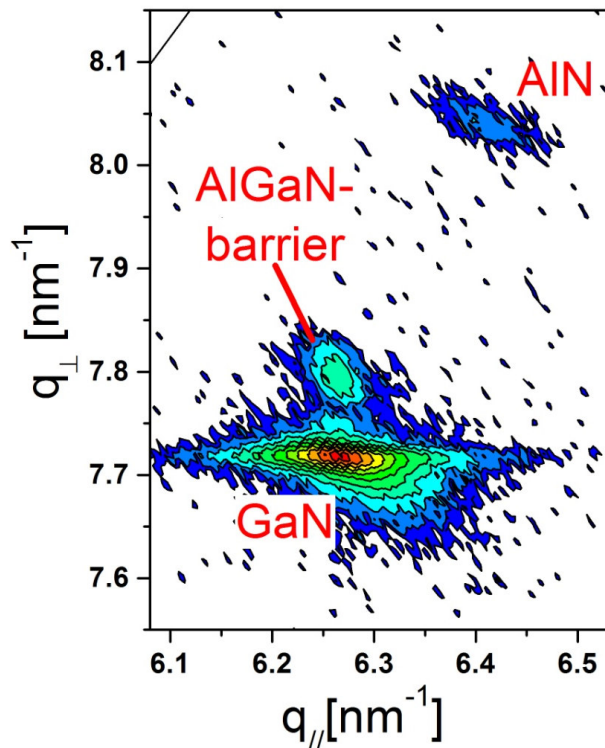


Procedure for composition determination with hexagonal nitrides after Herres et al. (2002)

Example: AlGaN / GaN HEMT structure on Si (111) substrate

Motivation: The electronic properties of AlGaN / GaN HEMTs depend (among other things) on the composition of the AlGaN barrier and strain management is important to prevent cracking.

HRXRD reciprocal space mapping of the (Al,Ga)N $11\bar{2}4$ reflection range



Scheme of the structure

strained lattice parameters

GaN $a = (319.26 \pm 0.02) \text{ pm}$
 $c = (518.31 \pm 0.01) \text{ pm}$
 (Al,Ga)N $a = (319.26 \pm 0.02) \text{ pm}$
 $c = (513.01 \pm 0.02) \text{ pm}$
 => Al: 20.4%

GaN: tensile strain
 AlGaN: tensile strain
 buffer

relaxed lattice parameters

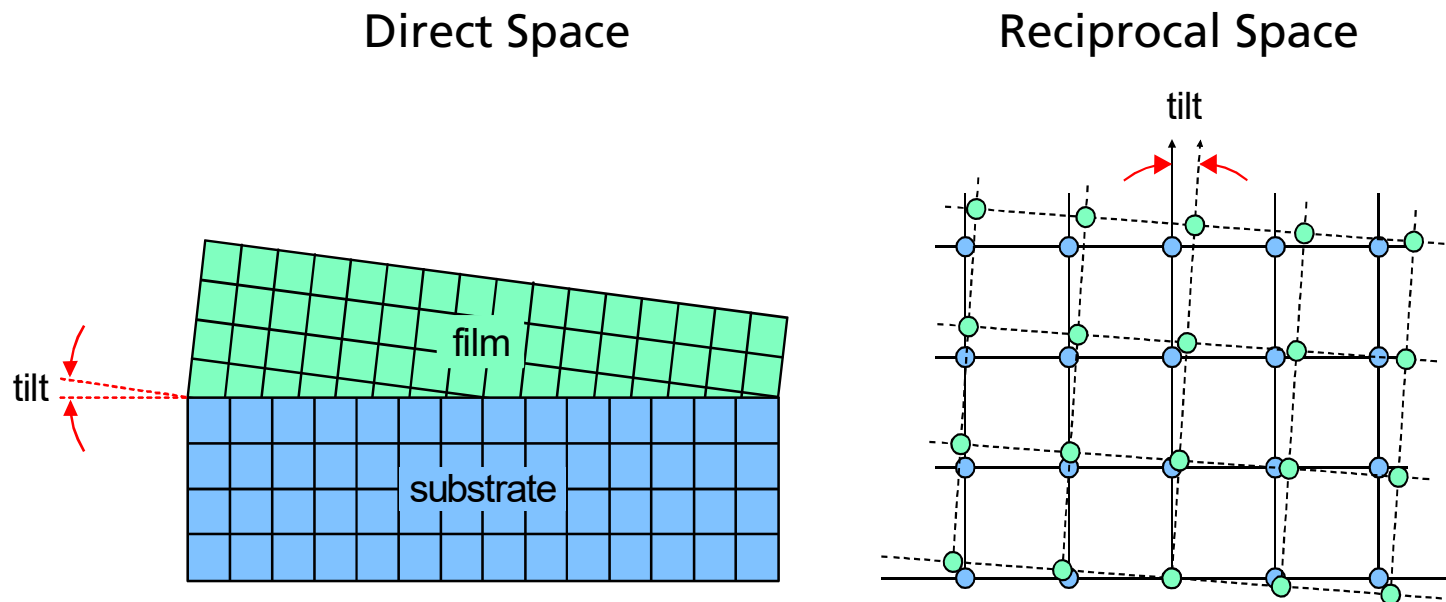
$a = (318.91 \pm 0.02) \text{ pm}$
 $c = (518.55 \pm 0.01) \text{ pm}$
 $a = (317.37 \pm 0.02) \text{ pm}$
 $c = (514.39 \pm 0.02) \text{ pm}$

$(a_{\text{strained}} > a_{\text{relaxed}})$

$(a_{\text{strained}} > a_{\text{relaxed}})$, and AlGaN fully strained to GaN

Tilt of the film relative to the substrate due to misfit / defects at the interface

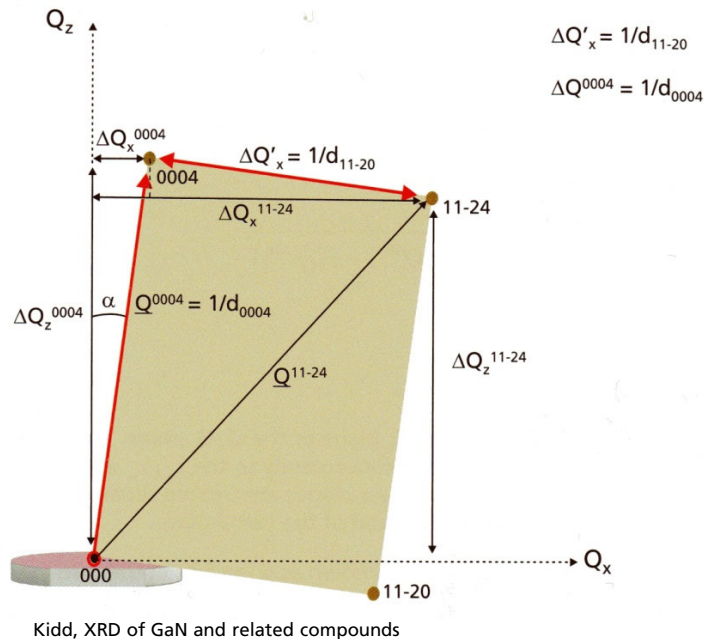
Relaxation of layers with large lattice mismatch or/and due to substrate offcut is often accompanied by the tilt of the layer relative to the substrate.



Influence of the layer tilt on the position of the reciprocal lattice points

Calculation of d-spacings from two measurements to account for small tilt

- Crystallographic tilt is common in semiconductor epitaxial layers with high lattice mismatch and so most measurements of d-spacing incorporate a tilt correction.
- For small tilts at least measurements from two reflections have to be combined.
- Measurements correspond to either the $Q_x - Q_z$ plane or the $Q_y - Q_z$ plane.



Calculation of the d-spacings of e.g. a tilted GaN layer can be obtained by the combination of two RSM measurements by:

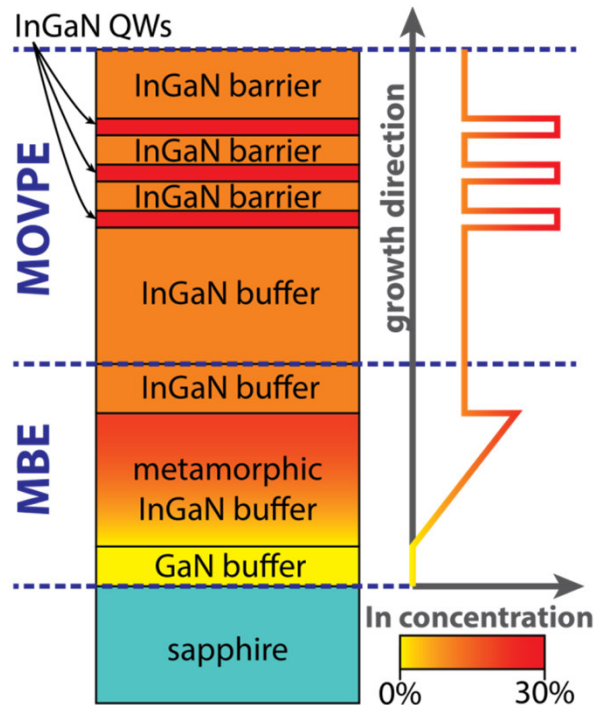
$$\frac{1}{d_{11\bar{2}0}} = Q_x = \sqrt{(\Delta Q_z^{0004} - \Delta Q_z^{11\bar{2}4})^2 + (\Delta Q_x^{11\bar{2}4} - \Delta Q_x^{0004})^2}$$

$$\frac{1}{d_{0004}} = |Q^{0004}|$$

(left: Q_x and Q_z can be obtained from measurements of two GaN reciprocal lattice spots where there is a layer tilt.)

Example: InGaN graded buffer layers for green LEDs on a sapphire substrate showing layer tilt (1)

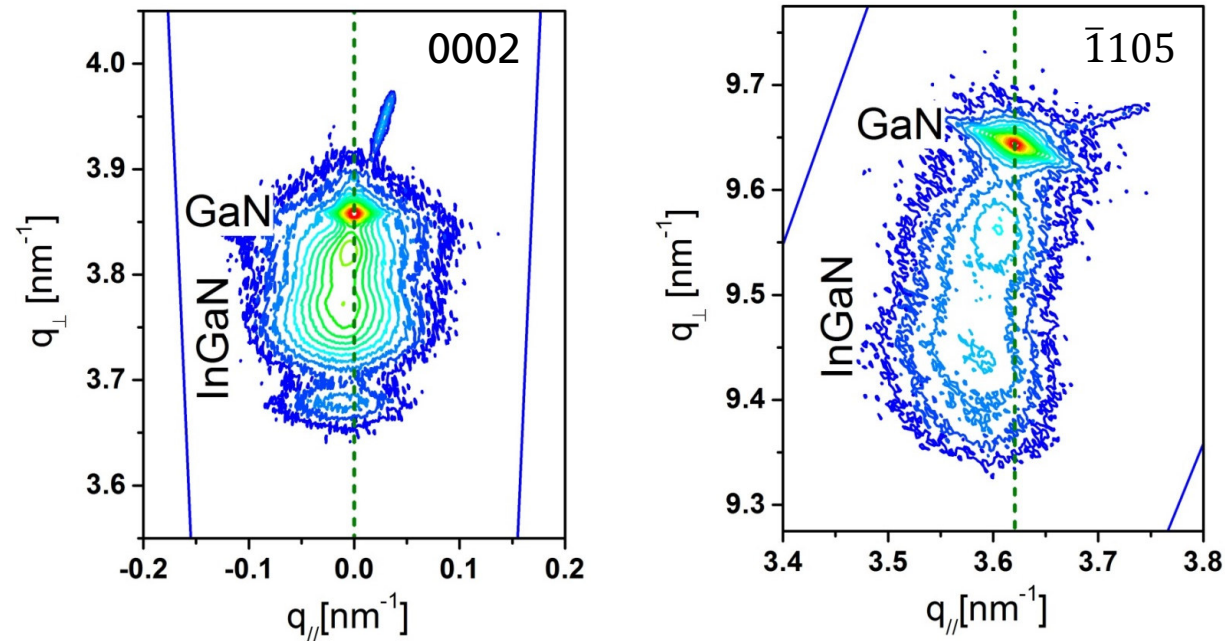
Motivation: Metamorphic (i.e. linear composition graded) GaInN buffer layers with an increased in-plane lattice parameter grown by plasma-assisted molecular beam epitaxy (PAMBE) for using as templates for MOVPE grown GaInN/GaN quantum wells (QWs), emitting in the green to red spectral region.



Green InGaN / GaN LED

Example: InGaN graded buffer layers for green LEDs on a sapphire substrate showing layer tilt (2)

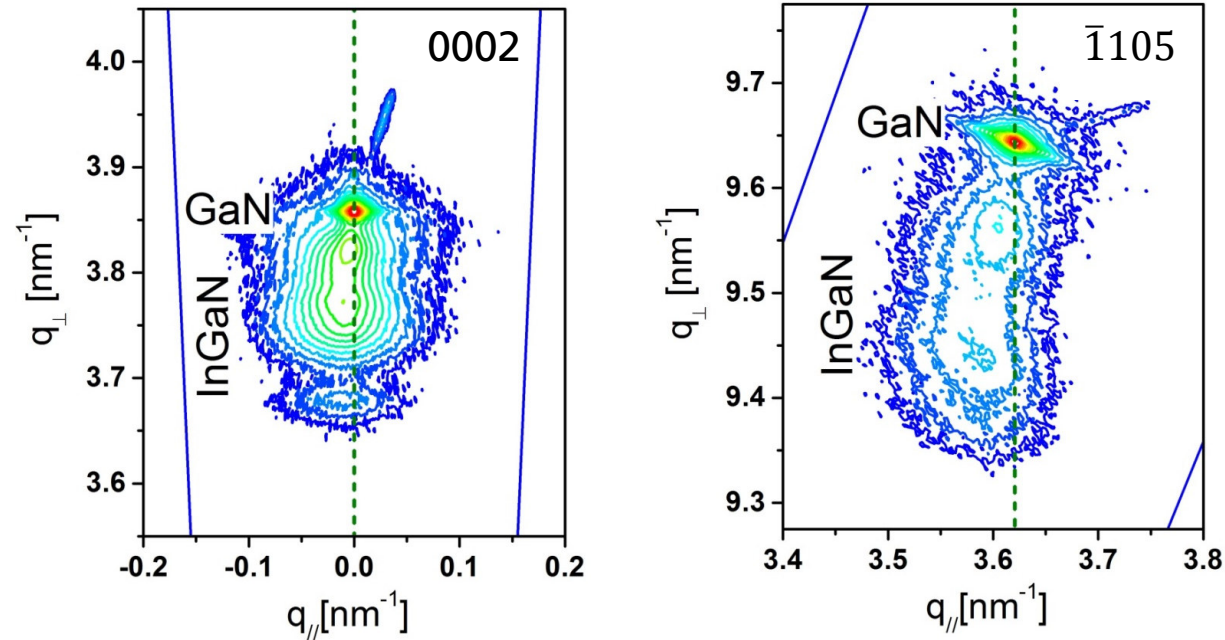
HRXRD reciprocal space mapping



- The interpretation alone for the RSM of the asymmetric $\bar{1}105$ reflection indicates only a relaxation of the InGaN graded buffer.
- But the symmetric 0002 reflection shows clearly that the InGaN graded buffer was tilted during growth.

Example: InGaN graded buffer layers for green LEDs on a sapphire substrate showing layer tilt (3)

HRXRD reciprocal space mapping



strained lattice parameters

GaN $a = (319.08 \pm 0.02) \text{ pm}$
 $c = (518.44 \pm 0.01) \text{ pm}$
(In,Ga)N $a = (319.66 \pm 0.10) \text{ pm}$
 $c = (530.83 \pm 0.10) \text{ pm}$

relaxed lattice parameter

$a = (318.91 \pm 0.02) \text{ pm}$
 $c = (518.55 \pm 0.01) \text{ pm}$
 $a = (324.55 \pm 0.10) \text{ pm}$
 $c = (526.98 \pm 0.10) \text{ pm}$

(compressive strain)

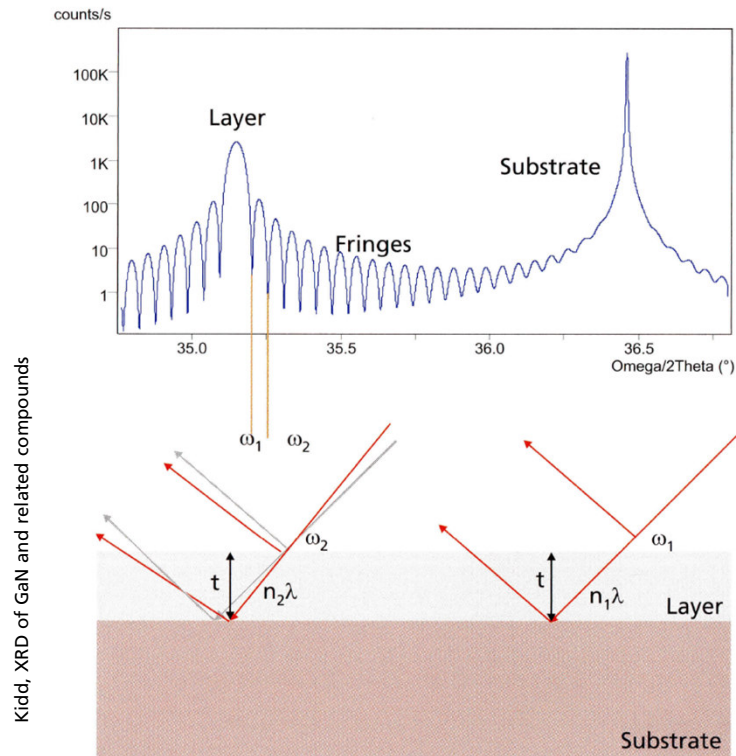
=> In: 16.3%

Outline

- Motivation
- Basics of X-ray Diffraction Method
- Instrumentation for High Resolution X-ray Diffraction
- Scanning in Reciprocal Space
- Stress and Strain in Epitaxial Thin Films
 - Fully strained Films
 - Partially Strained Films
 - Composition of Alloy Films
- **Measurement of the Layer's Thickness**
 - Single Layers and Layer Stacks
 - Superlattices
- Analysis of the Orientation of a Thin Film
- Mosaicity in Thin Films
- Synchrotron Bragg Diffraction Imaging for Substrate Analysis
- Recommended Readings

Measurement of the layer's thickness from fringes

In epitaxial thin films with very flat surfaces and interfaces and in which the film thicknesses are not subject to random fluctuations, the contributions of scattering from interfaces is strongly reinforced and can often be observed as fringes in the diffraction pattern. These fringes can be used to estimate the layer's thickness.

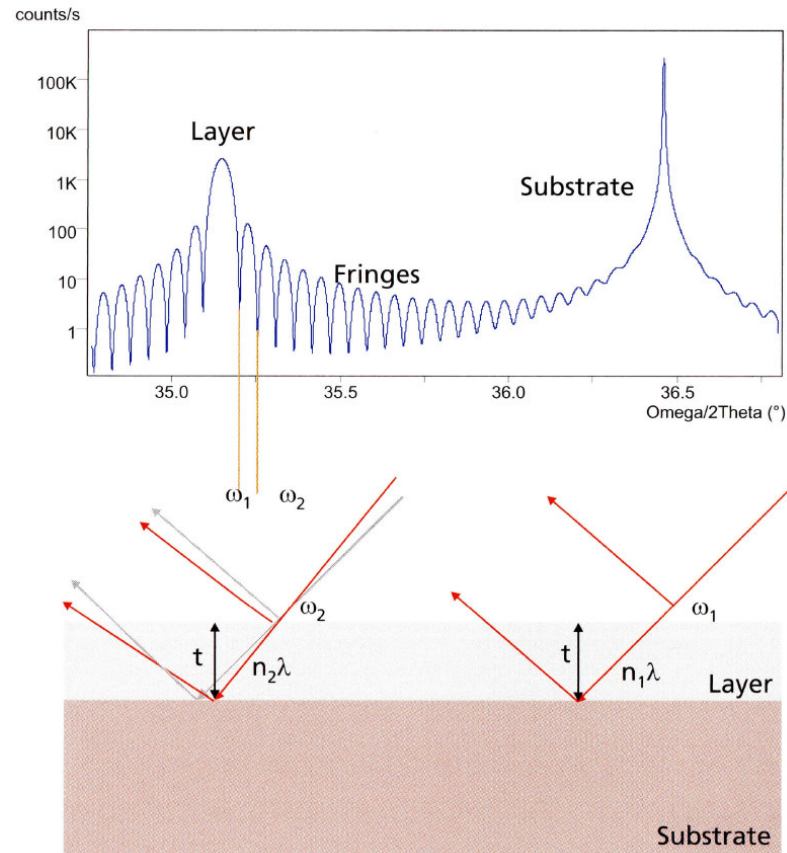


Thickness fringes in the diffraction patterns from highly perfect layers arise from dynamical diffraction effects.

The path difference between waves diffracting at the top surface of the film and those diffracting at the lower surface is a function of the angle of incidence and the film thickness, constructive and destructive interference effects are seen as a fringe modulation close to the main Bragg peak.

Simple calculations can be performed using the angular separation of fringes to obtain approximate values for layer thickness.

Thickness fringes of symmetrical reflections*



From two fringes, numbered n_1 and n_2 , that arise in the vicinity of Bragg peaks from **planes parallel to the surface**,

$2t \sin \omega_1 = n_1 \lambda$ and $2t \sin \omega_2 = n_2 \lambda$, the thickness t can be calculated:

$$t = \frac{(n_1 - n_2) \lambda}{2(\sin \omega_1 - \sin \omega_2)}$$

Where ω_1 and ω_2 correspond to the angular positions of the peaks n_1 and n_2 and $\Delta\omega = (\omega_1 - \omega_2)$. Note, that if n_1 and n_2 are neighboring fringes then:

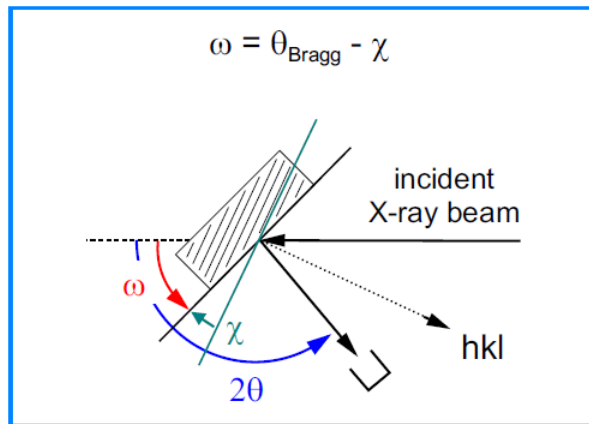
$$|(n_1 - n_2)| = 1$$

=>

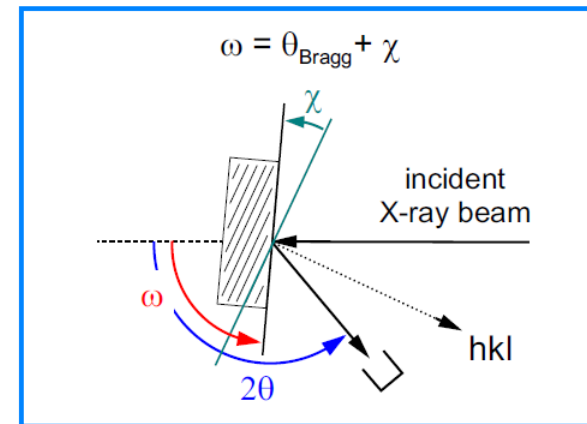
$$t = \left| \frac{\lambda}{2 \Delta\omega \cos \Theta_{\text{Bragg}}} \right|$$

Thickness fringes of asymmetrical reflections

Remember: For scanning in the **coplanar geometry** there are two possibilities for scanning asymmetrical reflections



1) Scattering geometry with a **shallow angle of incidence** and a **steep angle of exit** (reflection: $h k l$)



2) Scattering geometry with a **steep angle of incidence** and a **shallow angle of exit** (reflection: $h k l$)

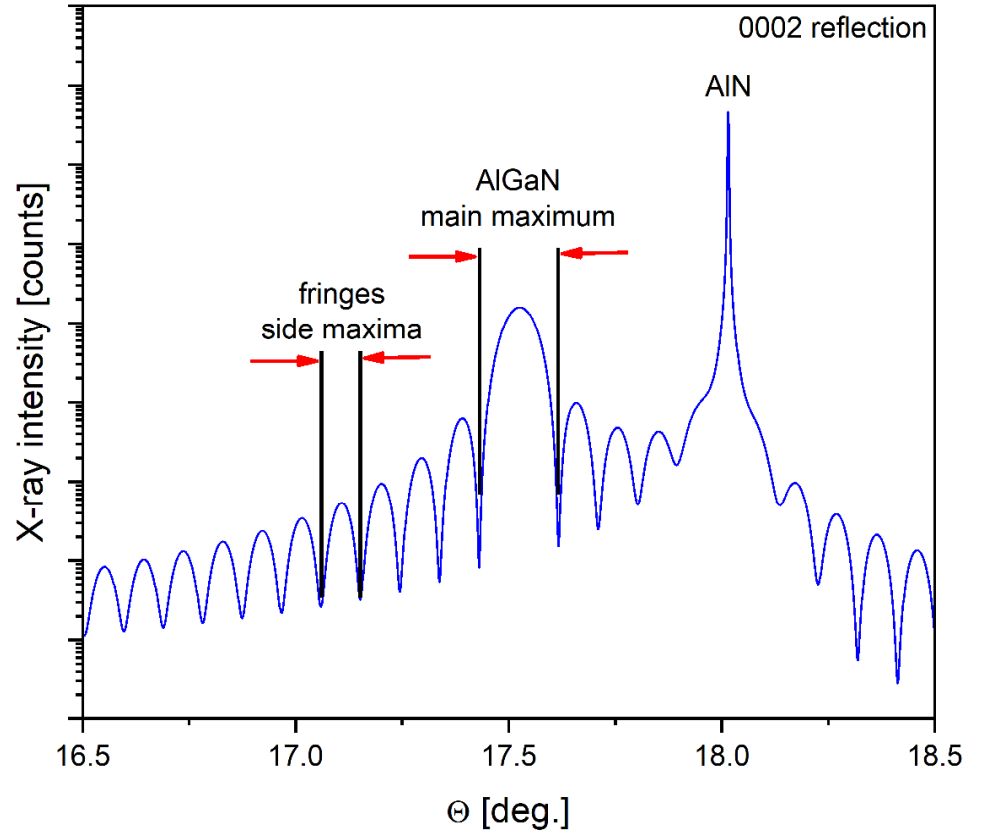
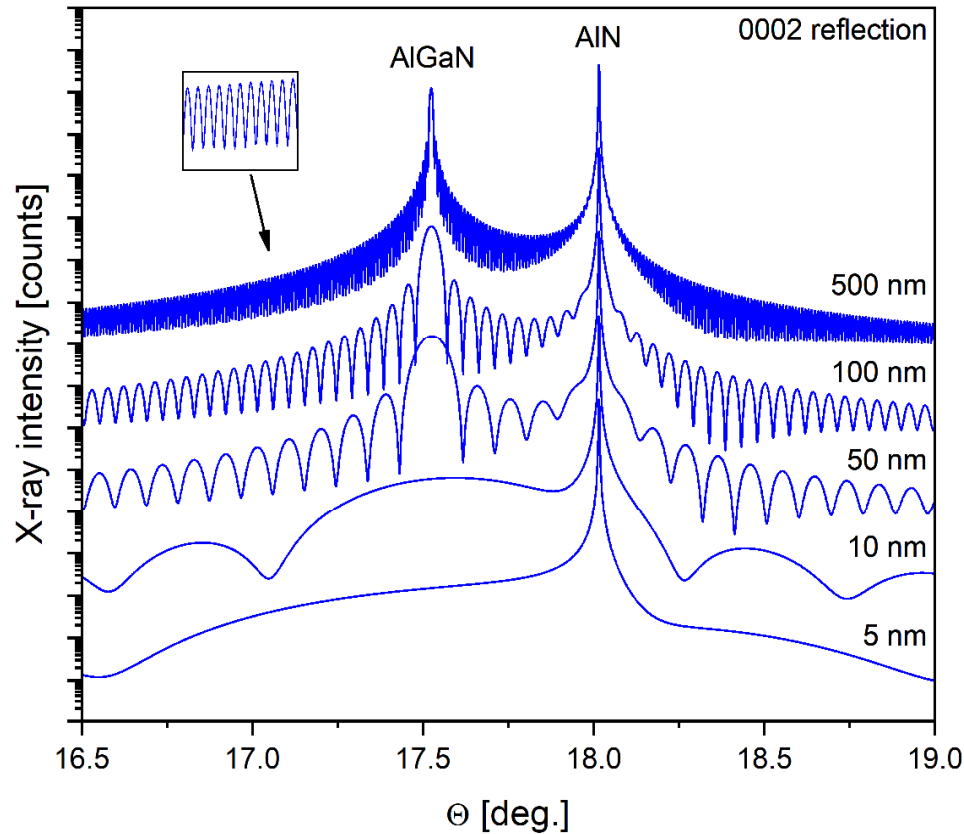
For reflections from planes that are **not parallel to the interface** the following equation can be used:

$$T = \frac{\lambda \sin(\Theta_{\text{Bragg}} \pm \chi)}{2\Delta\omega \sin \Theta_{\text{Bragg}}}$$

χ is the angle between the Bragg planes and the sample surface. Depending on the geometry, steep or shallow angle of incidence, it can be positive or negative.

Width of the fringes: main maximum and side maxima

Example: AlGaN on AlN (0001) substrate (calculated)



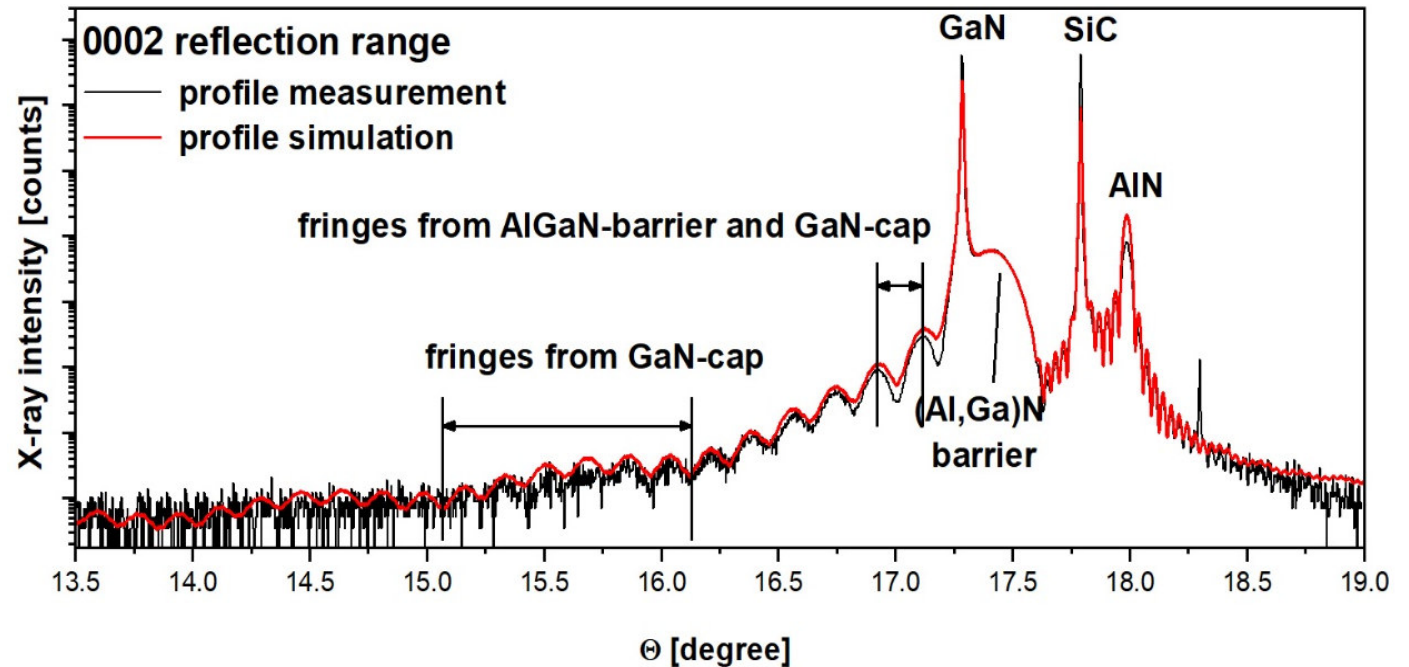
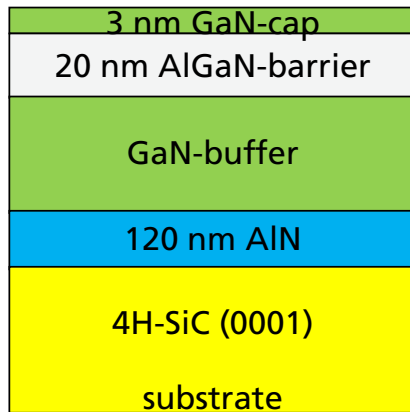
With increasing thickness the main maximum becomes narrower and the number of thickness fringes increases

The main peak has twice the width of the fringe maxima.

Layer thickness determination for multilayer structures (1)

Example: AlGaN / GaN HEMT structure on a SiC (0001) substrate

AlGaN / GaN HEMT structure

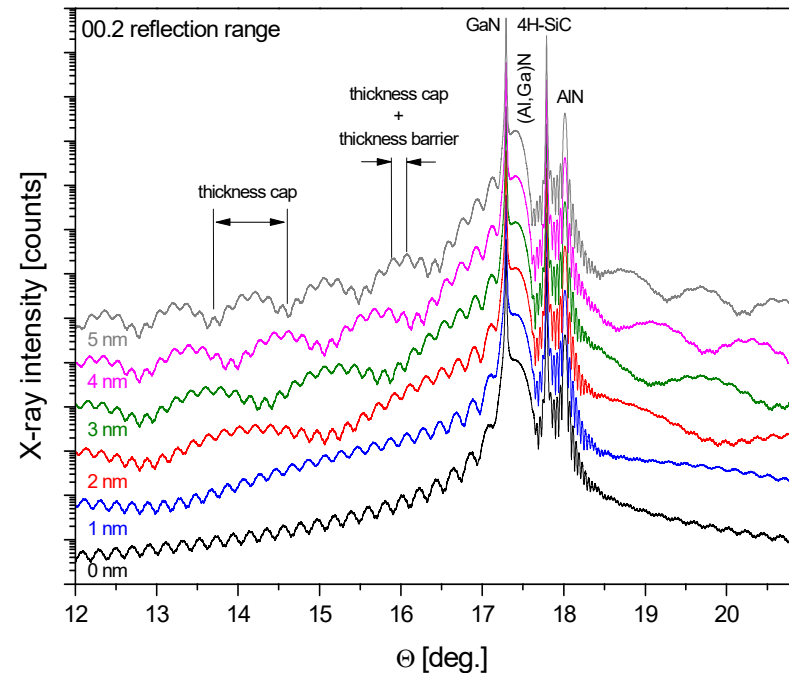
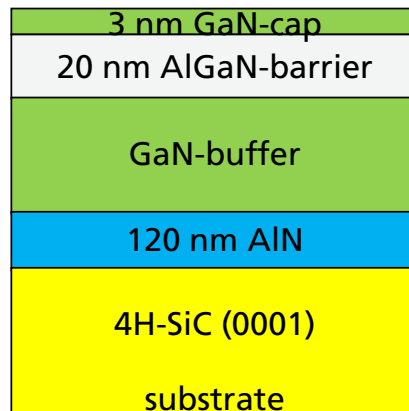


- We can see different thickness fringes: AlN starting layer, AlGaN barrier-layer and GaN cap-layer
- The GaN buffer does not show thickness fringes, because it is too thick ($\sim 2\mu\text{m}$)
- Note: if the density of two (or more) layers is very similar, the thicknesses can also add up. Here, for example, GaN cap and AlGaN barrier.

Layer thickness determination for multilayer structures (2)

Example: AlGaN / GaN HEMT structure on a SiC (0001) substrate

AlGaN / GaN HEMT structure

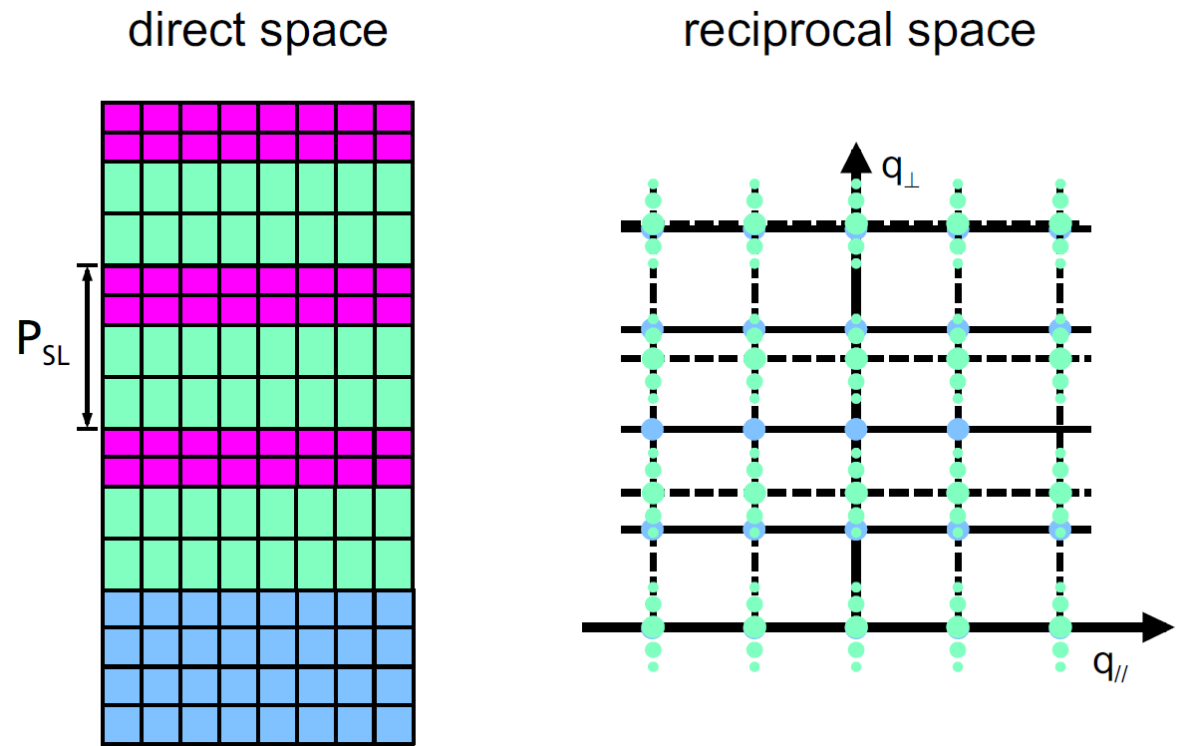


- We can see different thickness fringes: AlN starting layer, AlGaN barrier-layer and GaN cap-layer
- The GaN buffer does not show thickness fringes, because it is too thick ($\sim 2\mu\text{m}$)
- Note: if the density of two (or more) layers is very similar, the thicknesses can also add up. Here, for example, GaN cap and AlGaN barrier.

Superlattices in direct and reciprocal space

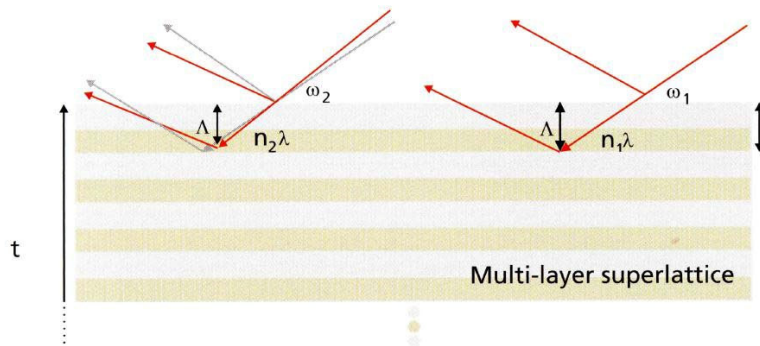
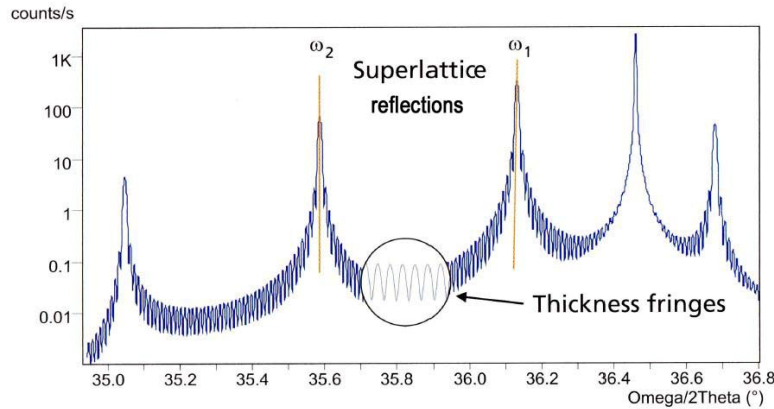
A periodic repetition of a certain layer sequence leads to an artificial crystal lattice (superlattice) with a unit cell equal to the superlattice period. X-ray diffraction pattern of such periodic structures consist of series of satellite peaks accompanying the main zero-order diffraction peak along the direction of chemical modulation.

Typical examples of such superlattices are the active regions (quantum wells) of LEDs or laser diodes.



Superlattices grown along [001] direction showing satellite reciprocal lattice points (green) accompanying the main hkl sites (blue).

Superlattice period of symmetrical reflections



The changing path differences between the waves diffracting at the upper and lower surface of a repetition period give rise to satellite reflections.

Analogous to measuring the thickness of single layers, the period P_{SL} of a superlattice is determined as follows:

From two satellites, numbered n_1 and n_2 , that arise in the vicinity of Bragg peaks from **planes parallel to the surface**, the period P_{SL} can be calculated:

$$P_{SL} = \frac{(n_1 - n_2)\lambda}{2(\sin \omega_1 - \sin \omega_2)}$$

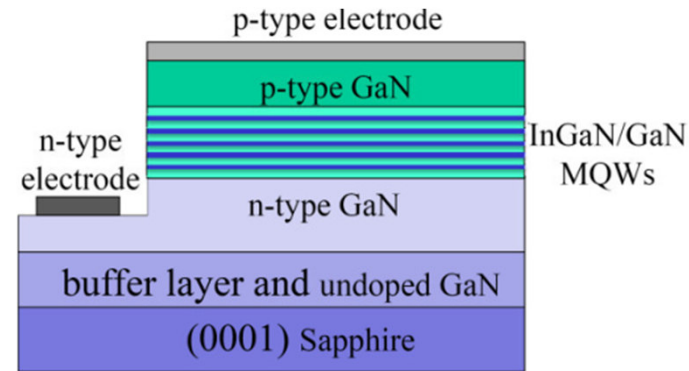
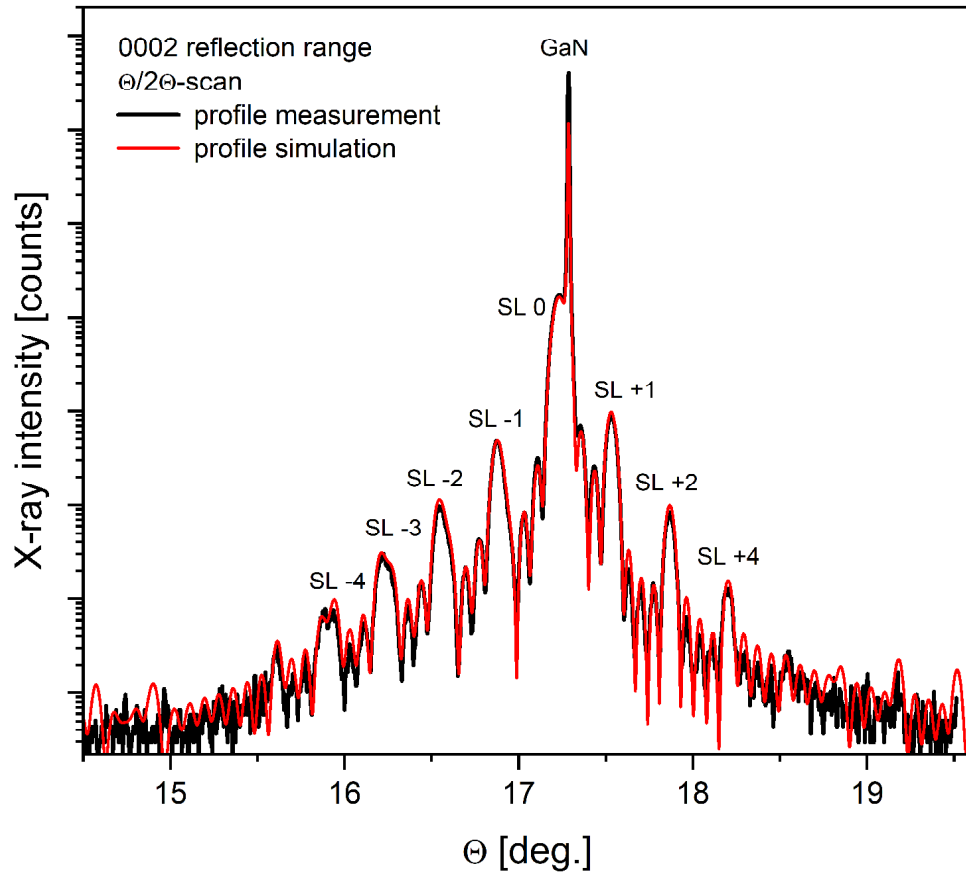
If n_1 and n_2 are neighboring satellites then:

$$P_{SL} = \left| \frac{\lambda}{2\Delta\omega \cos \Theta_{Bragg}} \right|$$

The determination of the superlattice period P_{SL} from asymmetric reflections is analogous to the determination of layer thickness.

Kidd, XRD of GaN and related compounds

(In,Ga)N/GaN superlattices on GaN/Al₂O₃ for LED and LASER structures



Period Superlattice (P_{SL}):

from the spacings of the superlattice peaks (SL)

here: $P_{SL} = (14.2 \pm 0.1)$ nm

(with GaN = 11.4 nm and InGaN = 2.8 nm, In = 12.7%)

Strain superlattice:

from the position of the "zero order" superlattice peak (SL-0).

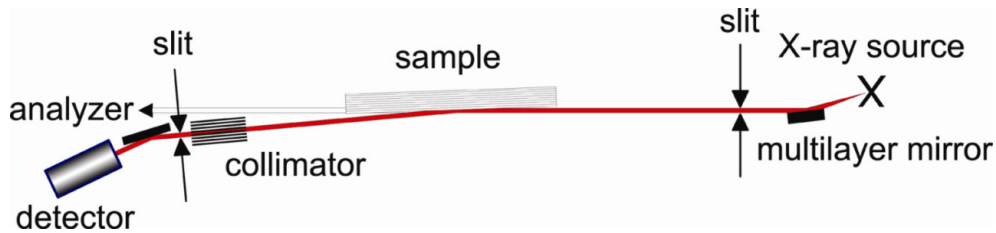
Here: $\{(d_{SL-0} - d_{GaN}) / d_{GaN}\}_L: (+3.3 \pm 0.1) \times 10^{-3}$

X-Ray Reflectivity for Thin Film Analysis (1)

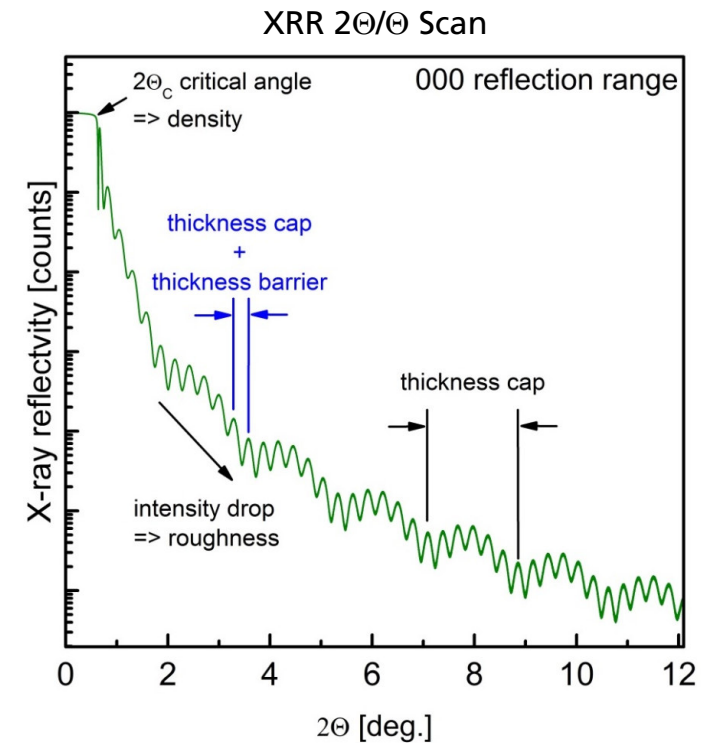
X-ray reflectivity (or X-ray reflection) is another surface-sensitive and non-destructive X-ray analysis technique.

XRR can be used to:

- study a single-crystalline, polycrystalline or amorphous material,
- determine the layer structure of a single- or multilayer film,
- measure film thickness from 0.1 nm to ~1000 nm,
- determine the density of material,
- evaluate surface and interface roughness.

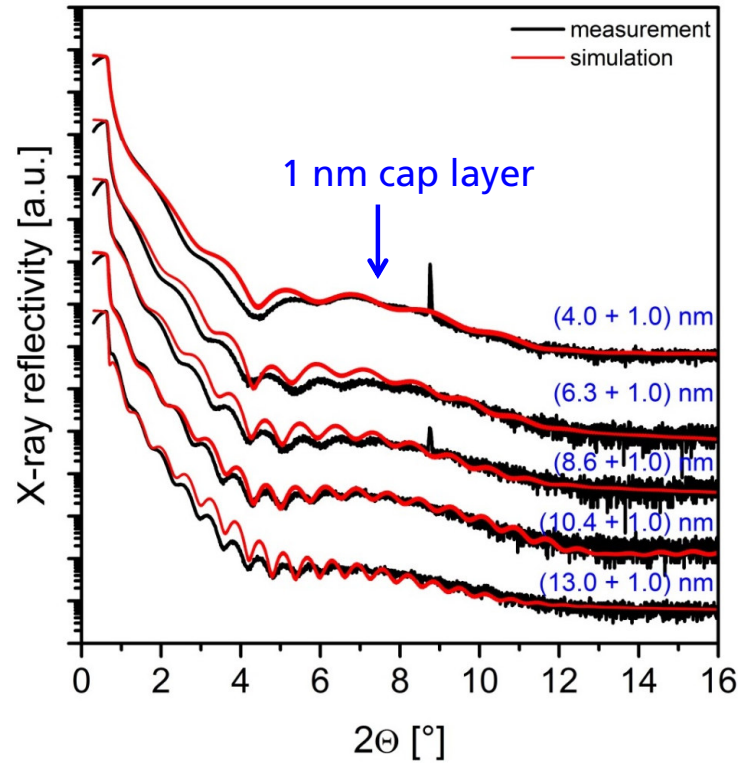
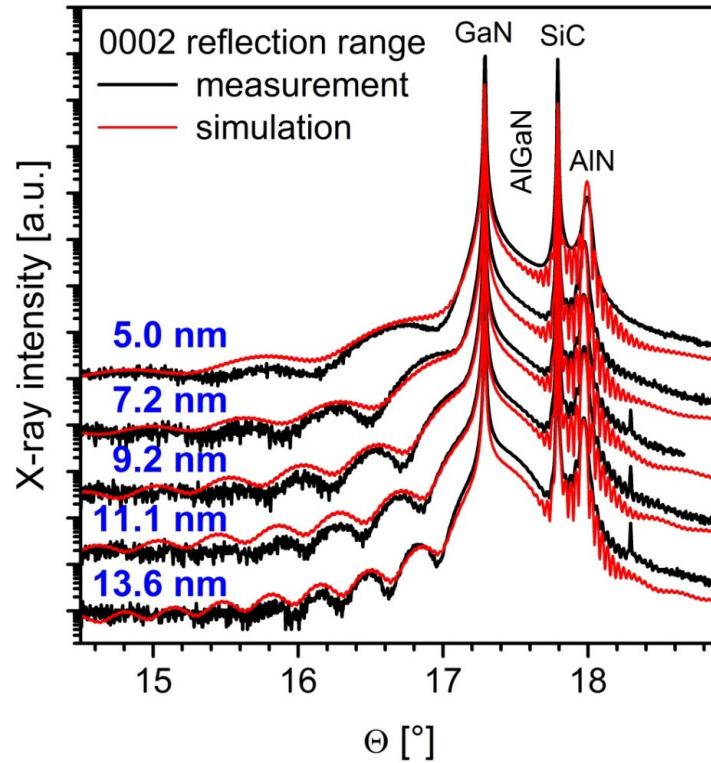


XRR set-up: multilayer mirror (CuK $\alpha_{1,2}$ -radiation)
0.1 mm slit + flat pyrolytic graphite analyzer



X-Ray Reflectivity for Thin Film Analysis (2)

GaN / AlGaN / GaN / AlN / SiC (0001) HEMT structures with different barrier- and thin cap-thicknesses:

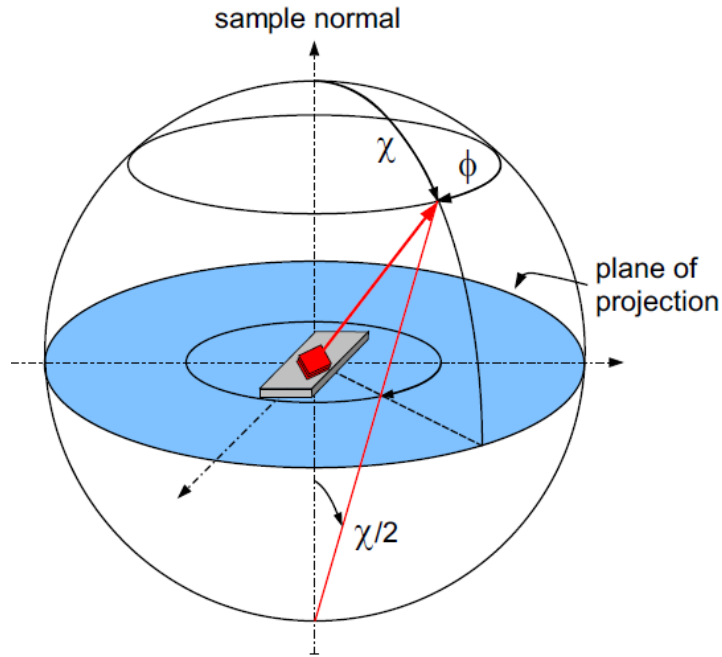


→ With the combination of HRXRD and XRR the thickness of the barrier and cap layer can be separated.

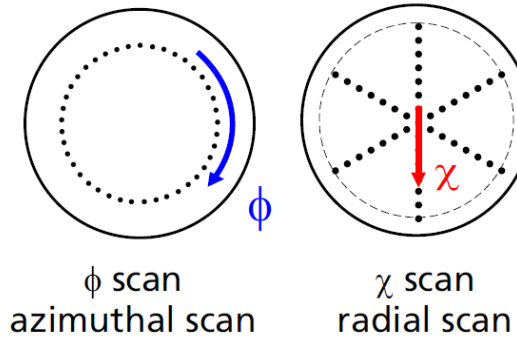
Outline

- Motivation
- Basics of X-ray Diffraction Method
- Instrumentation for High Resolution X-ray Diffraction
- Scanning in Reciprocal Space
- Stress and Strain in Epitaxial Thin Films
 - Fully strained Films
 - Partially Strained Films
 - Composition of Alloy Films
- Measurement of the Layer's Thickness
 - Single Layers and Layer Stacks
 - Superlattices
- **Analysis of the Orientation of a Thin Film**
- Mosaicity in Thin Films
- Synchrotron Bragg Diffraction Imaging for Substrate Analysis
- Recommended Readings

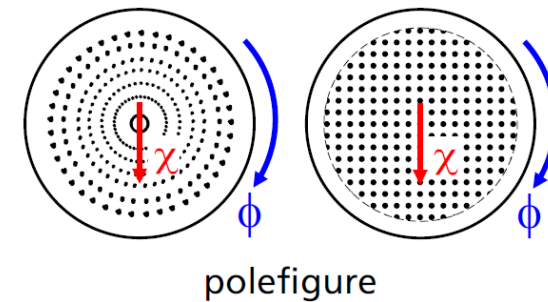
Determination of thin film orientation and epitaxial relationship to the substrate by XRD



The orientation of lattice planes (hkl) of a crystal / thin film are specified by two angles (χ , ϕ). These angles can be measured nondestructively with an X-ray diffractometer.



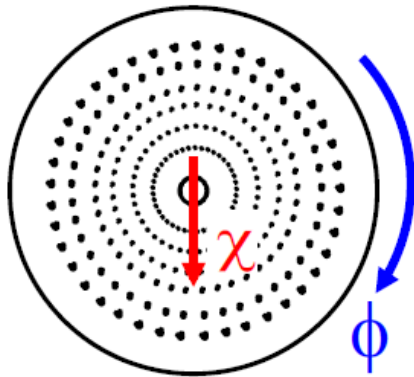
A pole figure measurement is a combination of an azimuthal ϕ scans and a polar χ scan.



Different strategies for pole figures measurements are possible.

Measurement, depiction and interpretation of pole figure measurements

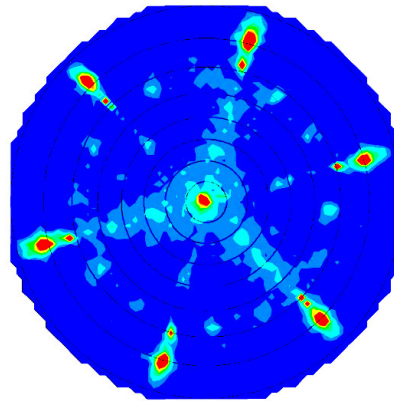
Step 1: measurement



χ, ϕ scan axis
 $2\Theta, \omega = \text{constant}$

A Bragg reflection with high intensity should be selected for the measurement.

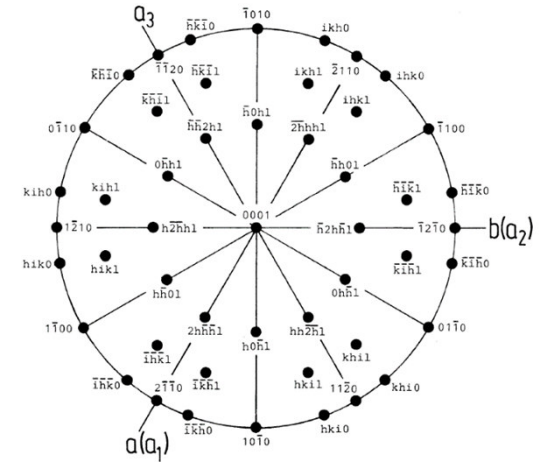
Step 2: depiction



stereographic projection

(A stereographic projection is a type of display similar to a globe map.)

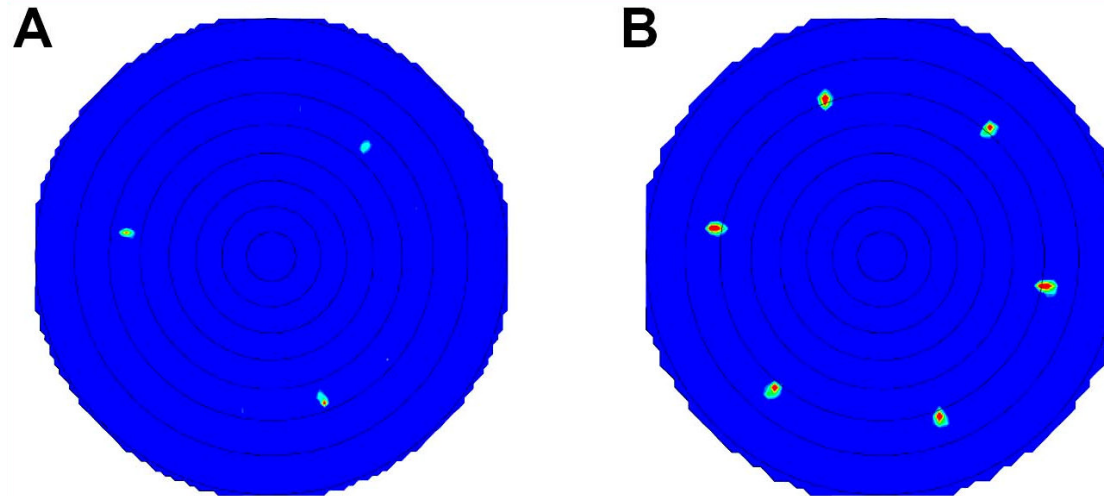
Step 3: interpretation



- orientation
- symmetry
- epitaxial relation

Epitaxial orientation measurements of crystal films

Example: MBE AlN / Si (111), nucleation temperature: 850°C



Si-200 ($\chi = 54.7^\circ$)
 $2\Theta = 69.1^\circ$

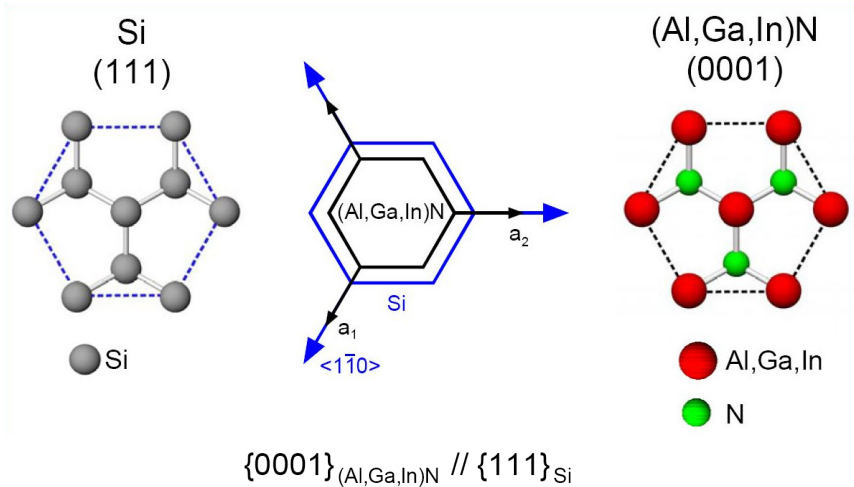
AlN-10.1 ($\chi = 62^\circ$)
 $2\Theta = 37.9^\circ$

$$\{0001\}_{(\text{Al,Ga,In})\text{N}} // \{111\}_{\text{Si}}$$

$$\langle 10\bar{1}0 \rangle_{(\text{Al,Ga,In})\text{N}} // \langle 11\bar{2} \rangle_{\text{Si}} , \langle 11\bar{2}0 \rangle_{(\text{Al,Ga,In})\text{N}} // \langle 1\bar{1}0 \rangle_{\text{Si}}$$

Epitaxial orientation measurements of crystal films

AlN / Si (111), lattice mismatch = -18.9%

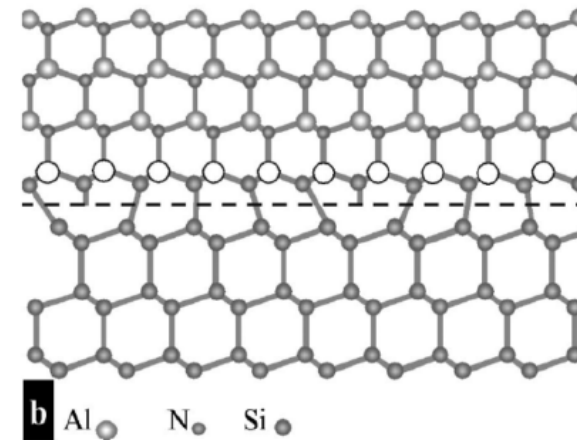
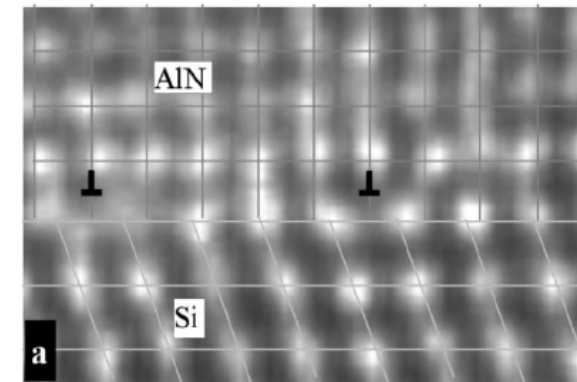


$$\langle 10\bar{1}0 \rangle_{(Al,Ga,In)N} // \langle 11\bar{2} \rangle_{Si} , \langle 11\bar{2}0 \rangle_{(Al,Ga,In)N} // \langle 1\bar{1}0 \rangle_{Si}$$

Formation of a coincidence interface layer between AlN (0001) and Si (111):

$$5 \times a_{AlN} : 4 \times d_{110,Si}$$

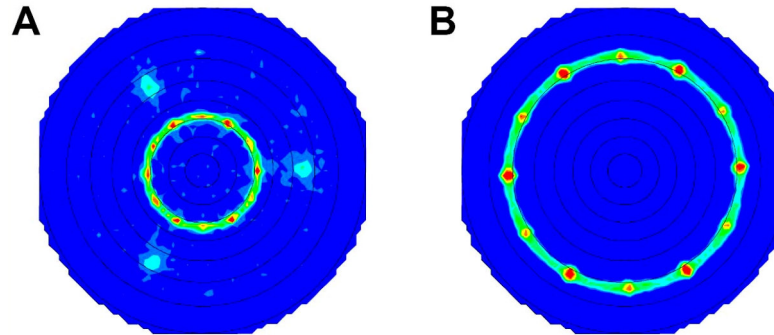
In the AlN coincidence lattice one misfit dislocation per unit cell is generated. For this coincidence interface the mismatch is only -1.3%.



R. Liu et.al. APL **83**, 860, 2003

Epitaxial orientation measurements of crystal films

Example: MBE AlN / Si (111), nucleation temperature: 1115°C

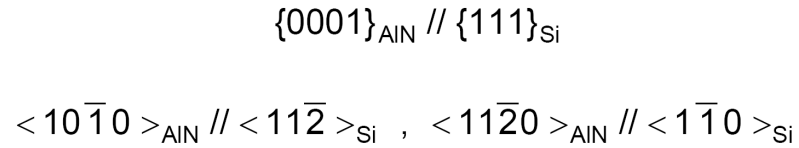


A
AlN-10.3 ($\chi = 32^\circ$)
Si-200 ($\chi = 54.7^\circ$)
 $2\theta = 66.0^\circ$

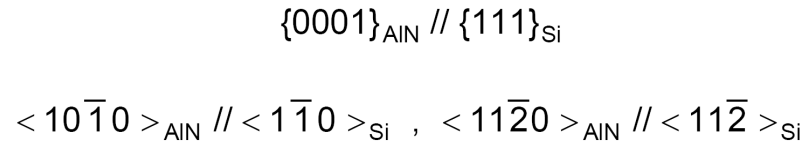
B
AlN-10.1 ($\chi = 62^\circ$)
 $2\theta = 37.9^\circ$

=> three different types of AlN orientations

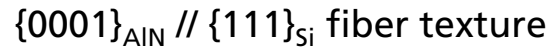
Fraction 1



Fraction 2



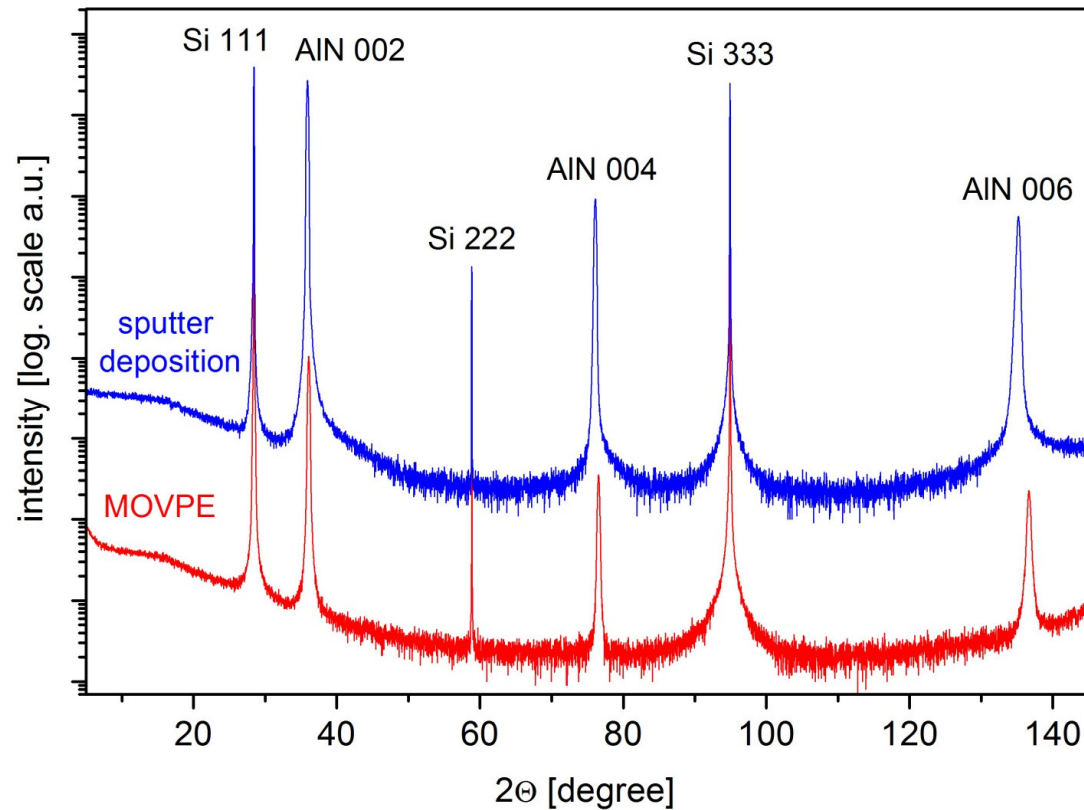
Fraction 3



Epitaxial orientation measurements of crystal films

Example: **MOVPE AlN / Si (111)** vs. **sputtered AlN / Si (111)**

XRD $2\theta/\theta$ scans



Only the 00L-reflections are visible for both AlN layers.

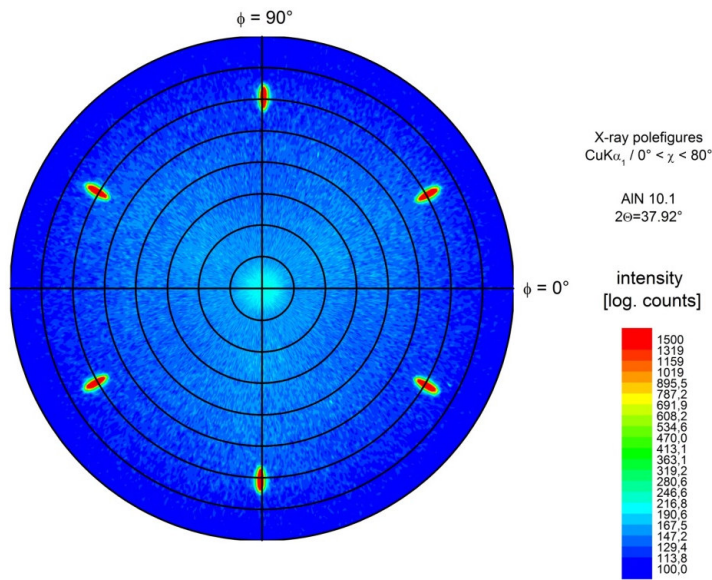
Is there an essential structural difference between the two layers?

Epitaxial orientation measurements of crystal films

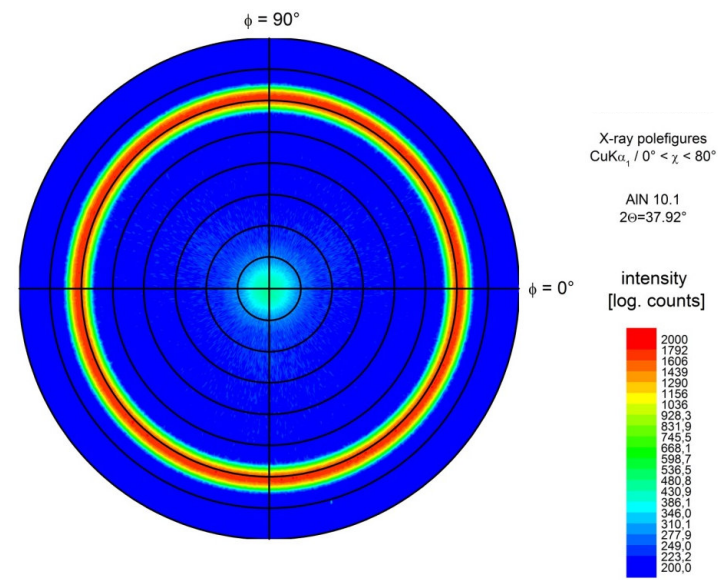
Example: MOVPE AlN / Si (111) vs. sputtered AlN / Si (111)

MOVPE AlN / Si (111)

Sputtered AlN / Si (111)



single crystalline

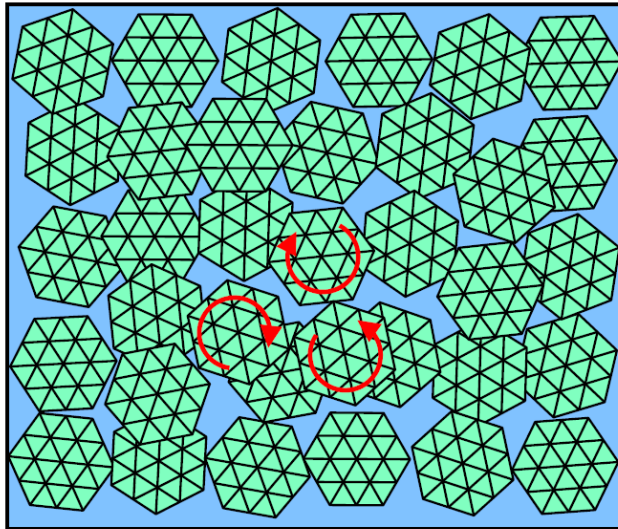


c-axis orientated,
but random in-plane orientation
=> **fiber texture**

Epitaxial orientation measurements of crystal films

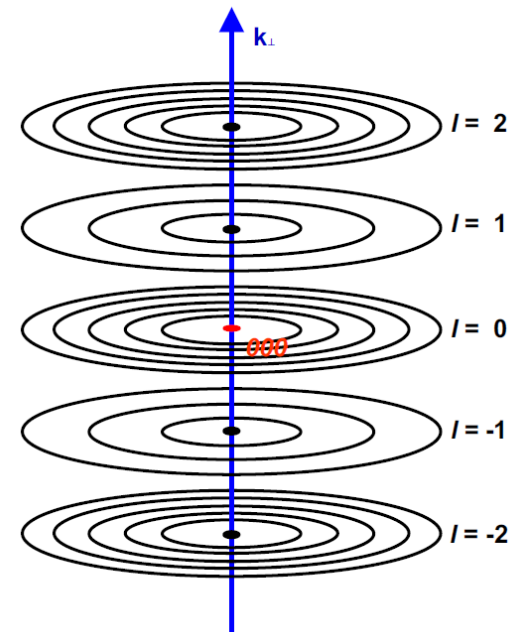
Fiber texture

Direct space



The grains are oriented on the c -axis, but have a random orientation in the plane.

Reciprocal space

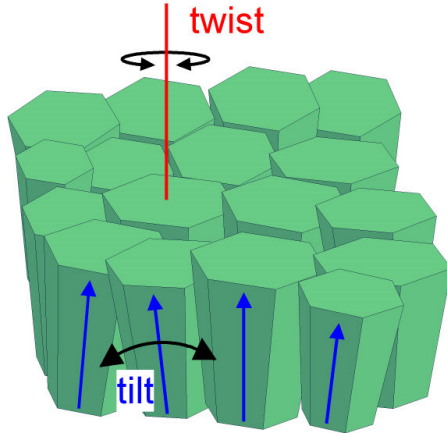


The term "texture" is used for the distribution of the orientation of the crystallites / crystal grains of a polycrystal sample if the orientation of the crystallites / crystal grains is not random in all directions.

Outline

- Motivation
- Basics of X-ray Diffraction Method
- Instrumentation for High Resolution X-ray Diffraction
- Scanning in Reciprocal Space
- Stress and Strain in Epitaxial Thin Films
 - Fully strained Films
 - Partially Strained Films
 - Composition of Alloy Films
- Measurement of the Layer's Thickness
 - Single Layers and Layer Stacks
 - Superlattices
- Analysis of the Orientation of a Thin Film
- **Mosaicity in Thin Films**
- Synchrotron Bragg Diffraction Imaging for Substrate Analysis
- Recommended Readings

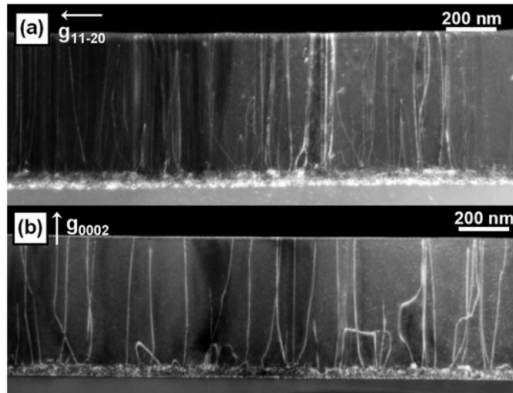
Mosaicity in thin films



Mosaicity is characterized by:

- **finite grain sizes** (10 ... 1000 nm)
sometimes with anisotropic grain shapes
- **intergranular strains** (tensile/compressive)
induced by thermal strains, precipitates ...

- **"tilt" = inter-grain rotation**
- **"twist" = inter-grain rotation**



M. Moram et al., J. Appl. Phys. **106**, 073513, (2009)

FIG. 9. Weak-beam dark-field cross-sectional TEM images of Sample (f) (500 nm coalesced GaN); (a) $g=11-20$ (showing both a -type and $(a+c)$ -type TDs), (b) $g=0002$ [showing only c -type and $(a+c)$ -type TDs].

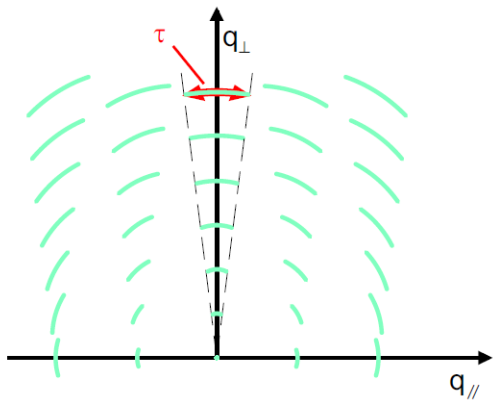
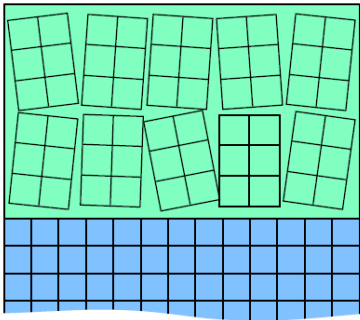
The amount of lattice tilt and twist can be related to dislocation densities.

Mosaicity usually leads to broadening of diffraction peaks which is reflection dependent.

Instrumental effects which broaden diffraction peaks have to be suppressed or accounted for.

Broadening of diffraction peaks (1)

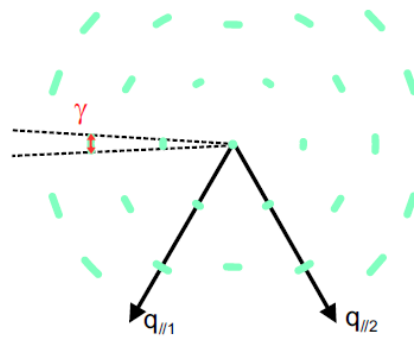
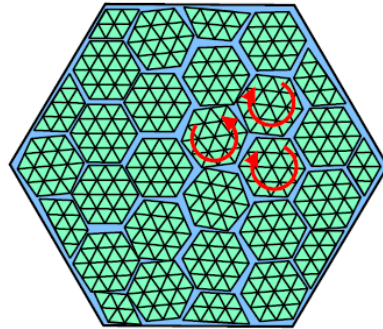
Tilt



$$\Delta q_\tau = \tau q_{hkl}$$

$$= \Delta \omega_\tau (2/\lambda) \sin \Theta$$

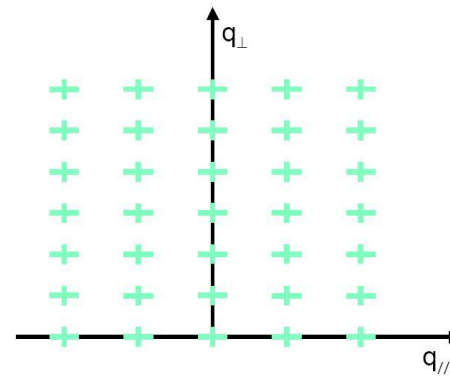
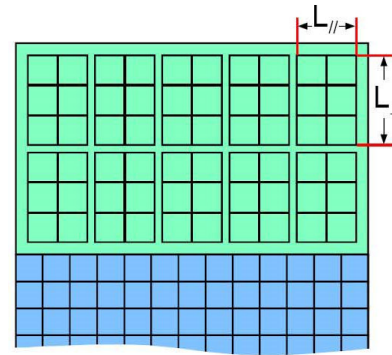
Twist



$$\Delta q_\gamma = \gamma q_{hkl}$$

$$= \Delta \omega_\gamma (2/\lambda) \sin \Theta$$

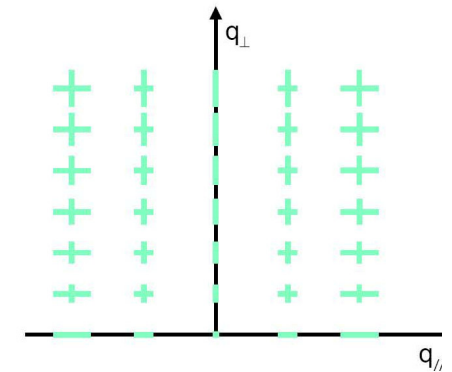
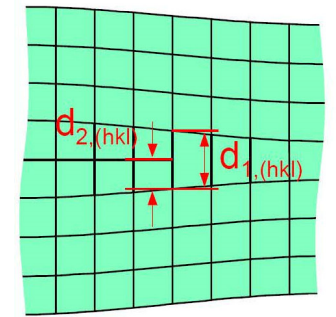
Crystal size
(correlation length)



$$\Delta q_{CS, //} = 1 / \langle L_{//} \rangle = \Delta \omega_{CS, hk0} (2/\lambda) \sin \Theta$$

$$\Delta q_{CS, \perp} = 1 / \langle L_{\perp} \rangle = \Delta \omega_{CS, 00l} (2/\lambda) \cos \Theta$$

Inhomogeneous strain
(micro strain)

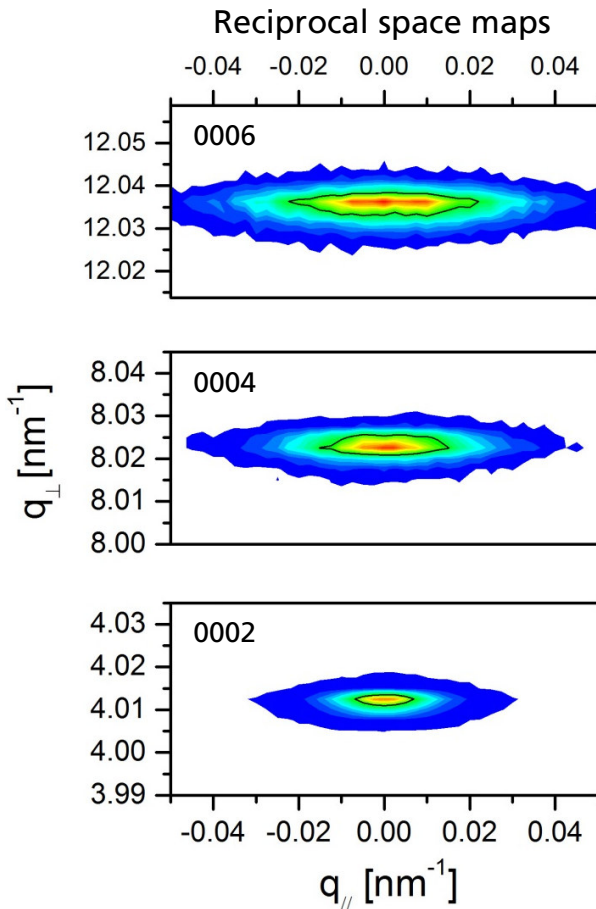


$$\Delta q_{ST, \perp} = \langle \epsilon_{\perp} \rangle q_{\perp} / 2$$

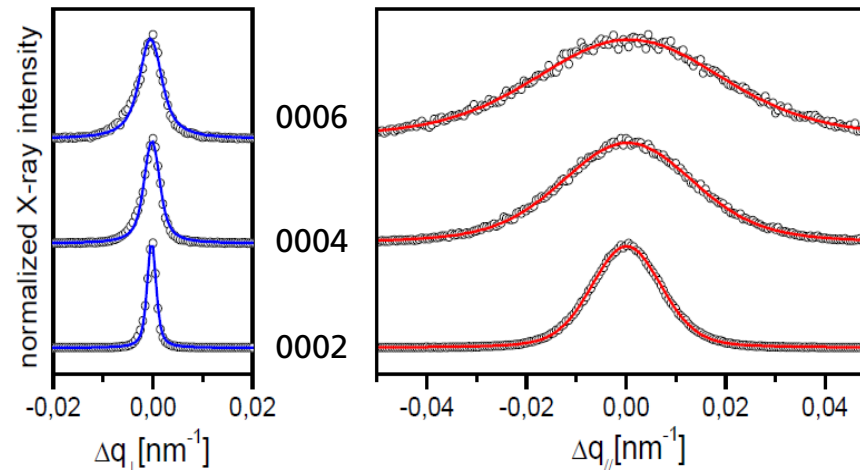
$$= \Delta \omega_{ST, 00l} (1/2\lambda) \cos \Theta$$

Broadening of diffraction peaks (2)

Example: 1570 nm AlN / Al₂O₃ (0001)



Reciprocal space scans for extraction of reflection broadening



reflection hkil	Δq_{\perp} [nm ⁻¹]	Δq_{\parallel} [nm ⁻¹]
0002	0.0020	0.0165
0004	0.0037	0.0308
0006	0.0054	0.0447

Broadening of reflections:

- depends on reflection
- depends on direction in reciprocal space
- depends on the type of defect (e.g. grain size, tilt, twist, inhomogeneous strain)

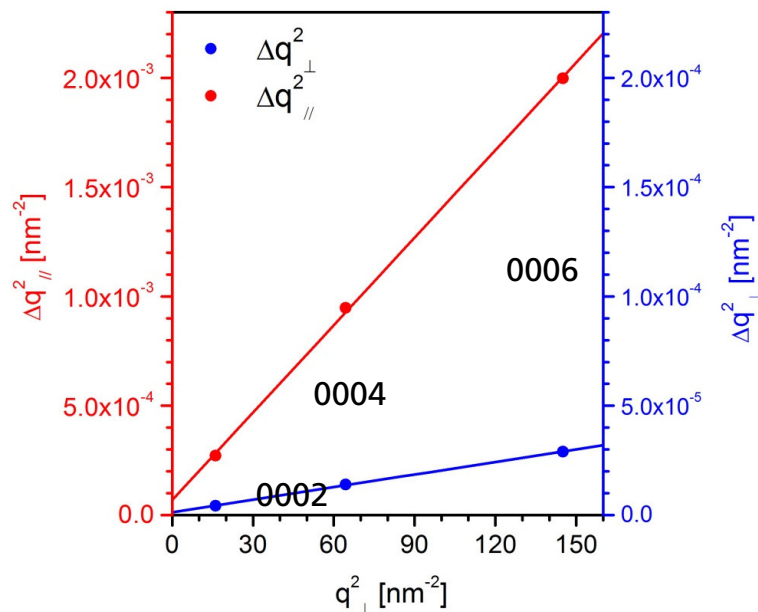
Broadening of diffraction (3)

Peak broadening analysis using a Williamson–Hall procedure:

Determination of the mosaic tilt, correlation length and inhomogenous strain

Example: 1570 nm AlN / Al₂O₃ (0001)

Performing a Williamson-Hall Analysis:



What does this graph show? Plot of the square of the reflection broadening against the square of the position in reciprocal space.

Vertical correlation length $\langle L_{\perp} \rangle$ from the intercept b_{\perp} with the ordinate:

$$(\langle L_{\perp} \rangle)^2 = 1 / b_{\perp}$$

Lattice distortions $\langle \varepsilon_{\perp} \rangle$ from the slope m_{\perp} :

$$(\langle \varepsilon_{\perp} \rangle)^2 = 4 m_{\perp}$$

Lateral correlation length $\langle L_{\parallel} \rangle$ from the intercept b_{\parallel} with the ordinate:

$$(1 / \langle L_{\parallel} \rangle)^2 = 1 / b_{\parallel}$$

Mosaic tilt τ from the slope m_{\parallel} :

$$(\tau)^2 = m_{\parallel}$$

Results for AlN / Al₂O₃ (0001):

L_{\perp} [nm]	879
$\langle \varepsilon_{\perp} \rangle$ [$\times 10^{-3}$]	0.87
L_{\parallel} [nm]	121
τ [°]	0.21

Outline

- Motivation
- Basics of X-ray Diffraction Method
- Instrumentation for High Resolution X-ray Diffraction
- Scanning in Reciprocal Space
- Stress and Strain in Epitaxial Thin Films
 - Fully strained Films
 - Partially Strained Films
 - Composition of Alloy Films
- Measurement of the Layer's Thickness
 - Single Layers and Layer Stacks
 - Superlattices
- Analysis of the Orientation of a Thin Film
- Mosaicity in Thin Films
- **Synchrotron Bragg Diffraction Imaging for Substrate Analysis**
- Recommended Readings

Motivation: substrates for GaN-based nitride power electronics and opto-electronics

Al_2O_3



V.V. Timofeev et al. /, Journal of Crystal Growth 445 (2016) 47–5248

SiC



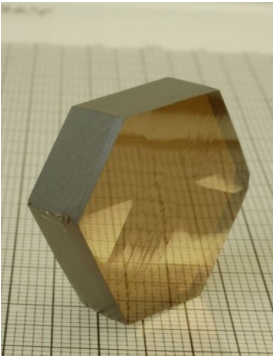
https://en.wikipedia.org/wiki/Silicon_carbide

Si



WaferPro, Santa Clara, CA, USA

GaN

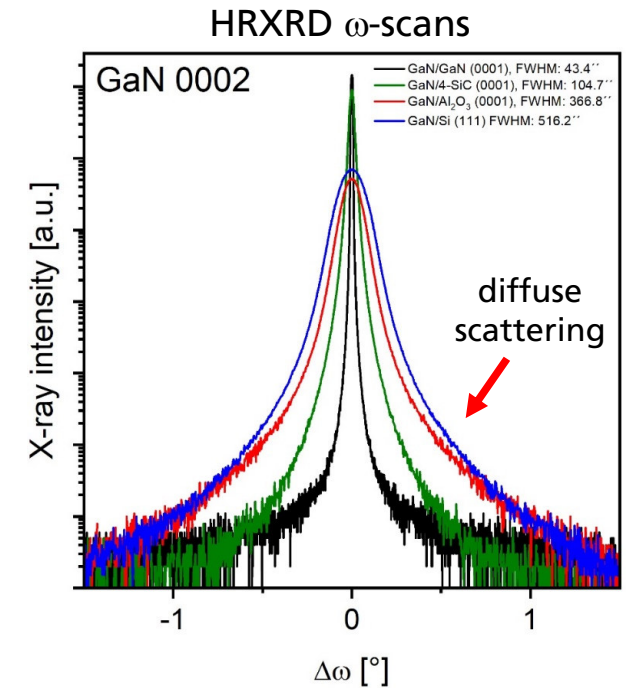


Unipress PAS, Warsaw, Poland

Lattice and thermal mismatch for GaN (0001) growth on different substrates:

	Al_2O_3	4H-SiC	Si	GaN
lattice mismatch (20°C) [%]	-13.9	-3.4	+20.4	0
rel. thermal mismatch (20°C) [%]	+43.2	-1.4	-66.4	0

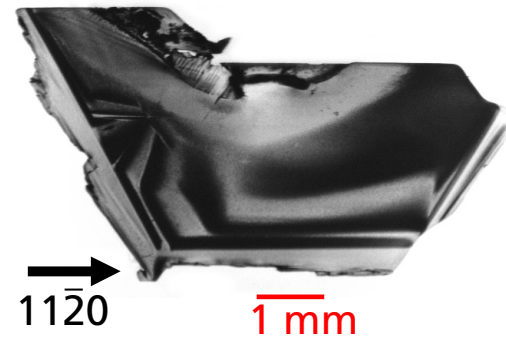
Comparison of the GaN layers' quality grown on different substrates



→ best quality for homoepitaxial layer growth on GaN substrates

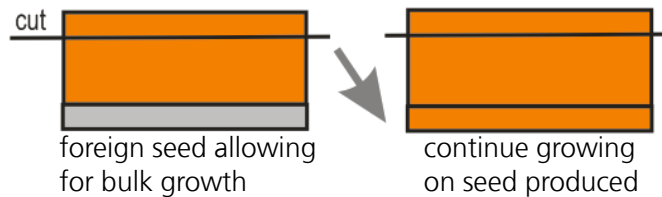
Motivation: growth techniques and strategies for freestanding GaN substrate material

- High nitrogen-pressure solution growth (HNPS)
 - Hydride vapor phase epitaxy (HVPE)
 - Ammonothermal method
 - Sodium flux method
 - (...)
- } commercially available substrates



HNPS GaN, Institute of High Pressure Physics PAS, Warsaw

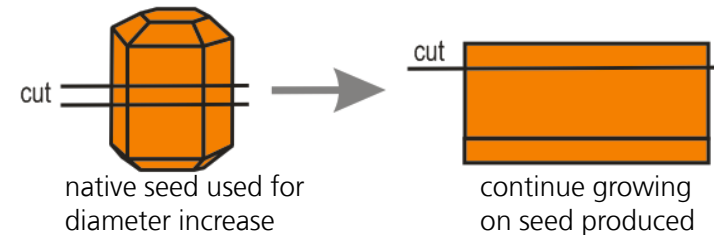
"Quasi bulk" growth using foreign seeds



- high defect density due to lattice and thermal mismatch between foreign seed and bulk material
- large crystal diameter possible due to availability of large foreign seeds

Quasi bulk growth of GaN: Hydride vapor phase epitaxy (HVPE) on GaN/Al₂O₃, GaN/Si, GaN/GaAs, ...

"True bulk" growth using native seeds



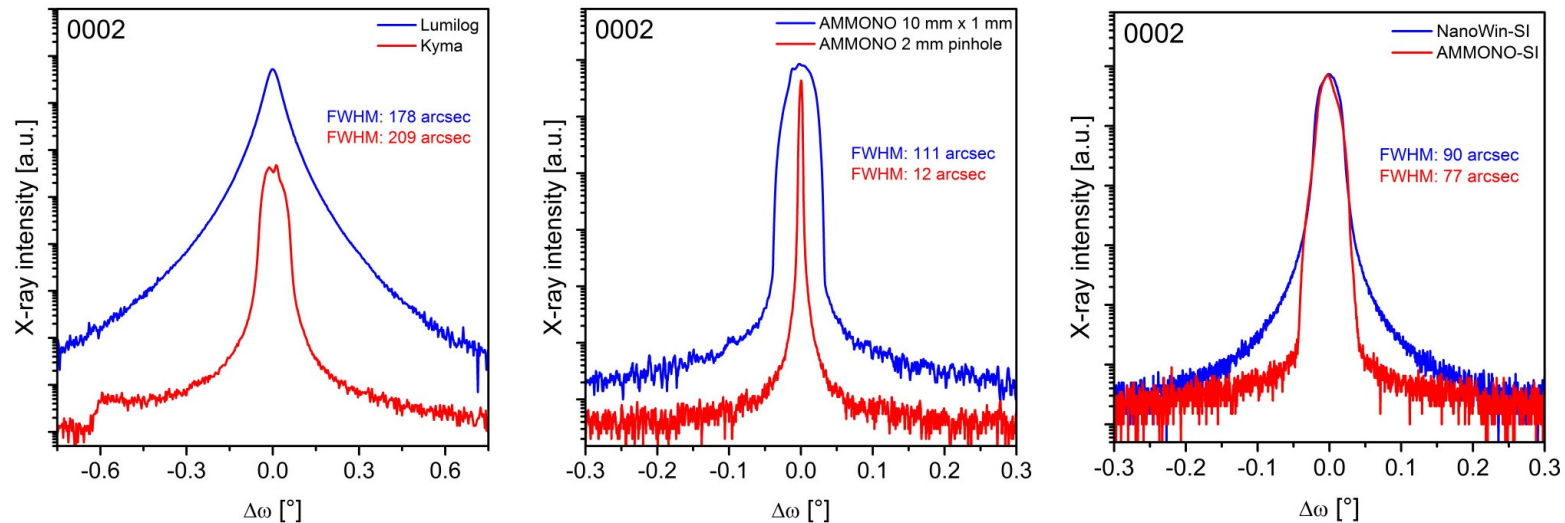
- low defect density
- crystal enlargement is difficult

True bulk growth of GaN with GaN seed: Ammonothermal method, hydride vapor phase epitaxy (HVPE)

Motivation: finding the best structural analysis techniques and strategies for GaN substrates (1)

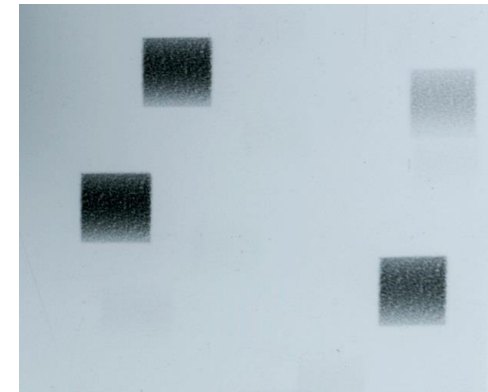
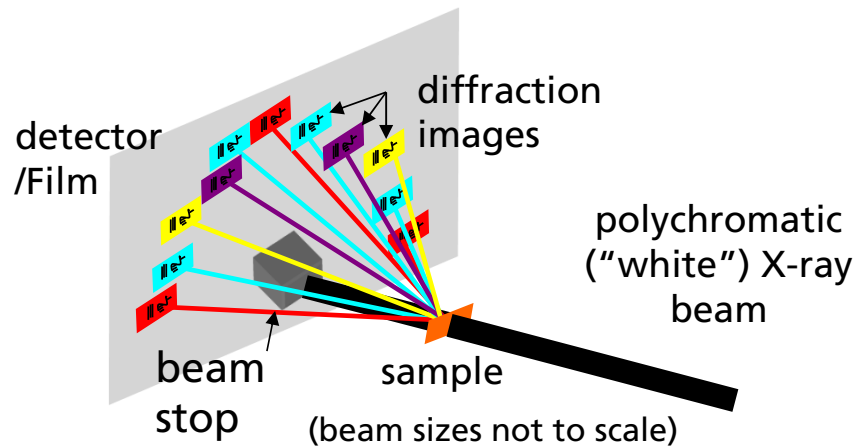
Often HRXRD rocking curves are used to analyze the defect structure of bulk GaN

... but how reliable are these measurements?



- large differences for the shape of the profiles
- interpretation of the sheer numbers of the FWHM are difficult
- defect structure difficult to identify
- Can X-ray topography provide better information about the exact defect structure?

Synchrotron Bragg diffraction imaging techniques: White Beam X-ray Topography (SWXRT)

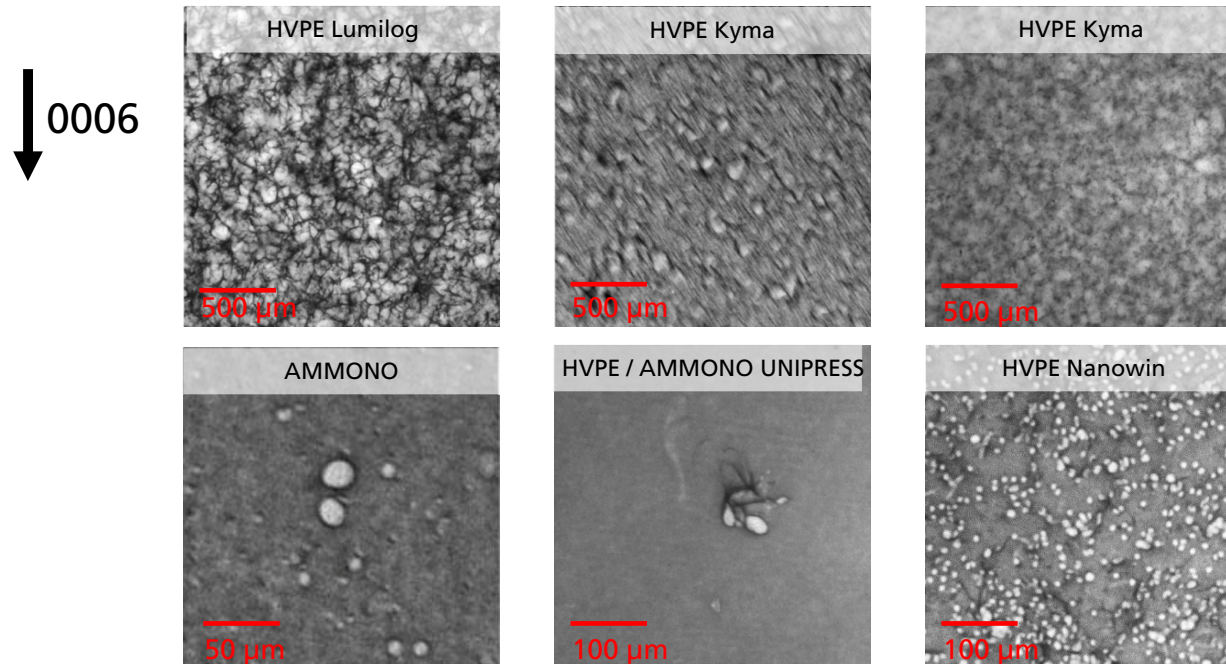


SWXRT topographies of HVPE GaN

- Diffraction imaging of defects and strain in single crystals, epitaxial layers, devices
- White beam (polychromatic) => Laue-pattern of topographies
- High intensity X-ray beam => short recording time (~1 second)
- High energy X-rays => easy to penetrate high absorbing samples
- X-ray beam emerging from source has low divergence => good spatial resolution
- Ability to cover large mm² areas at micron resolution
- Transmission and reflection geometry

Motivation: finding the best structural analysis techniques and strategies for GaN substrates (2)

Synchrotron White Beam Topography of Various GaN (0001) Substrates



Kirste et al., ECS Journal of Solid State Science and Technology, 4 (8) P324-P330 (2015)

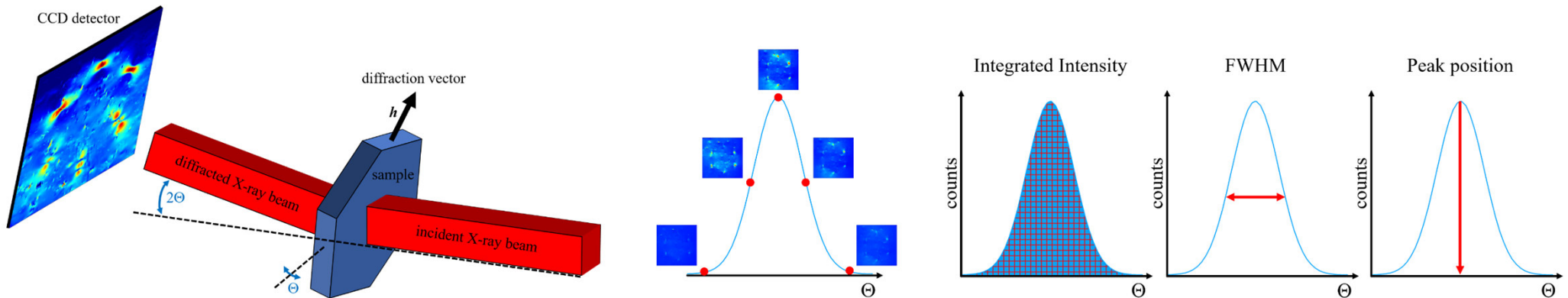
- SWXRT provides an overview of the defect structure and defect distribution
- for HVPE GaN on a foreign substrate (defect density $\sim 10^{-6}$ - 10^{-7} cm⁻³) → no single defects can be identified
- ammonothermal GaN → identification of individual defects possible

SWXRT: Qualitative (or semi-quantitative) approach → information about the defect structure with high spatial resolution

Need for a method that provides quantitative → **Rocking Curve Imaging (RCI)**

Synchrotron Bragg diffraction imaging techniques: Synchrotron Rocking Curve Imaging - Projection Mode

Step 1: Local RC measurement

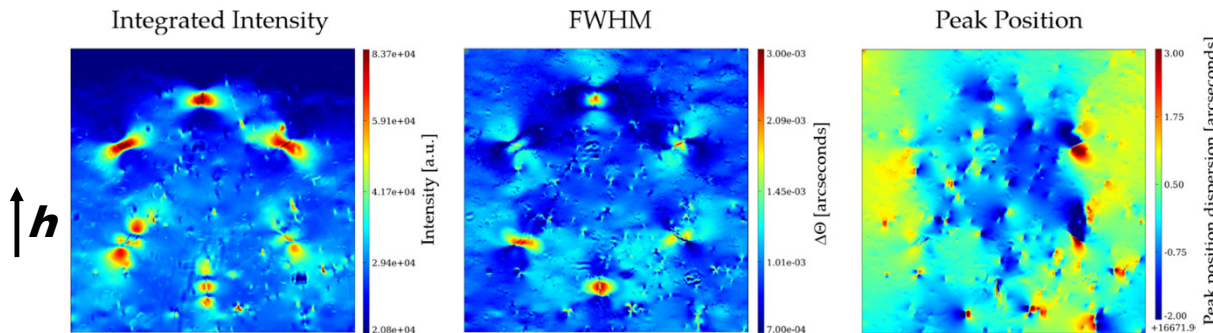


The crystal is rotated along the diffraction curve for a given set of lattice planes

Bragg diffracted beam is recorded on a two-dimensional pixel detector

→ each pixel records its own 'local' rocking curve

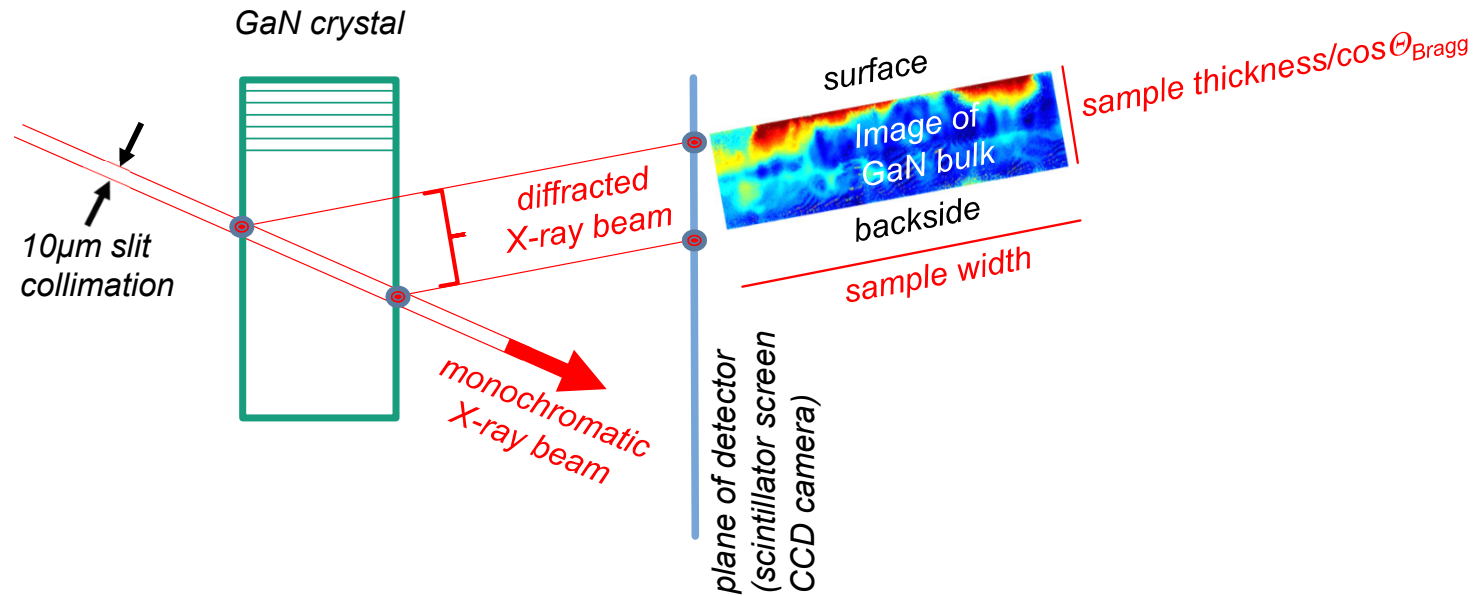
→ Step 2: Map reconstruction



→ Spatially resolved distributions of integrated intensity, full widths at half maximum and peak positions of local rocking curves

Pixel per pixel: quantitative measurement

Synchrotron Bragg diffraction imaging techniques: Synchrotron Rocking Curve Imaging - Section Transmission Mode



Observation of a “virtual slice”: $1.2 \times 0.01 \text{ mm}^2$

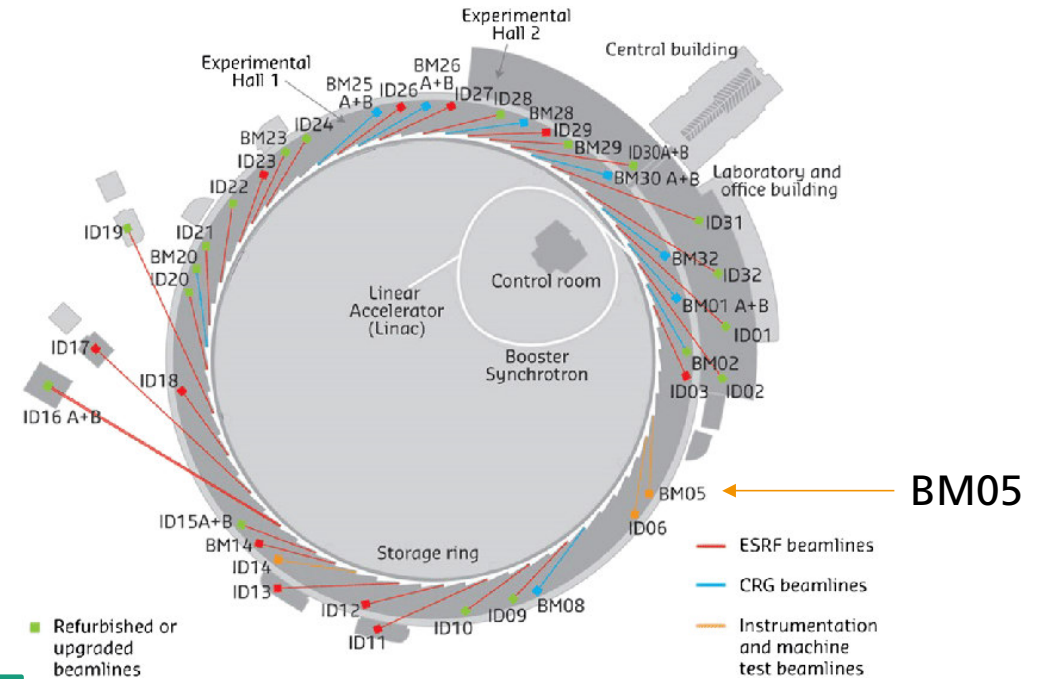
→ **Depth profiling**

For more details of the method: T.N. Tran Thi et al., J. Appl. Cryst. (2017). 50, 561–569

ESRF - European Synchrotron Radiation Facility and BM05 Beamline

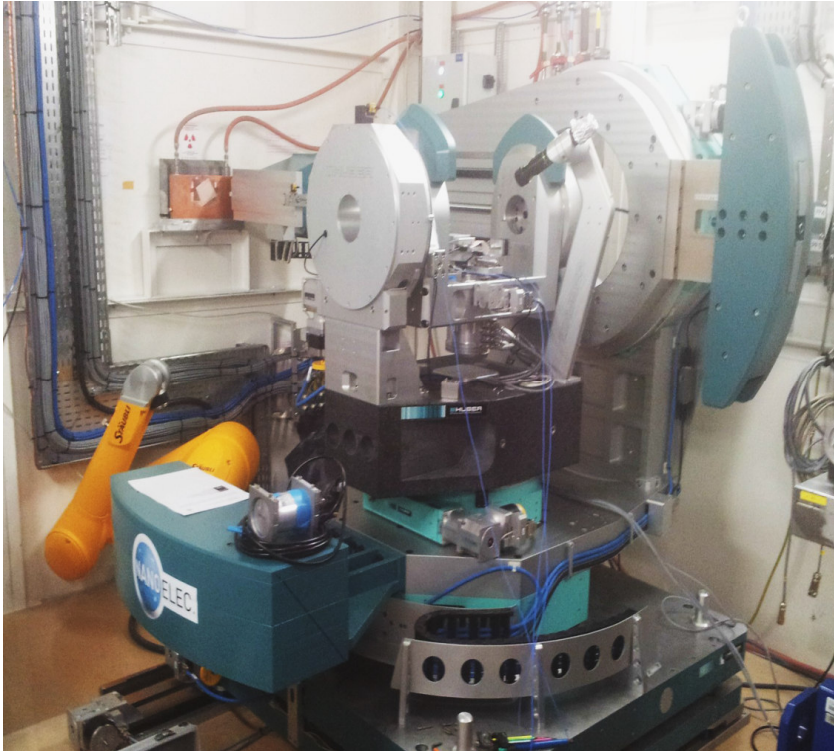


From 2020, ESRF-EBS, the first of a new generation of high-energy synchrotron sources, opens up new opportunities in X-ray science.



- BM05 beamline:**
- 60 m far from source
 - Parallel beam to cm size
 - Focused beam to μm size
 - White beam Energy: 3 to 160 keV
 - Monochromatic Energy: 4 to 60 keV

Synchrotron Bragg diffraction imaging techniques: Synchrotron Rocking Curve Imaging



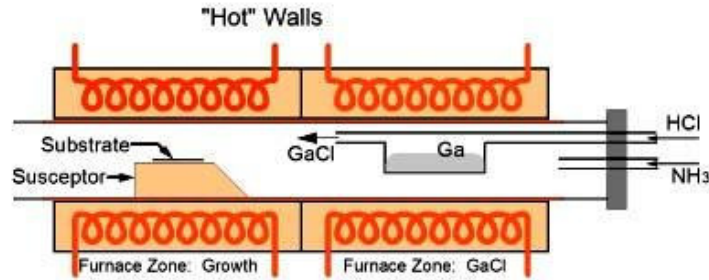
Diffractometer for RCI
at BM05-ESRF

Measurement conditions at ESRF for RCI:

- Field of view: $1.2 \times 1.2 \text{ mm}^2$ or $2.4 \times 2.4 \text{ mm}^2$
- CCD camera: 2048 x 2048 pixels, 16 bit
pixel size: $0.65 \text{ }\mu\text{m} \times 0.65 \text{ }\mu\text{m}$ or $1.3 \text{ }\mu\text{m} \times 1.3 \text{ }\mu\text{m}$
- Transmission geometry in projection and section mode
- μ_{GaN} for 30 keV = 1.9 – 2.8

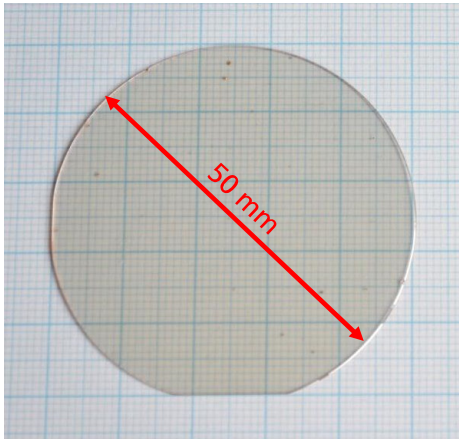
Hydride vapor phase epitaxy (HVPE) GaN on GaN/Al₂O₃ seed

Hydride vapor phase epitaxy (HVPE) of GaN on foreign seed



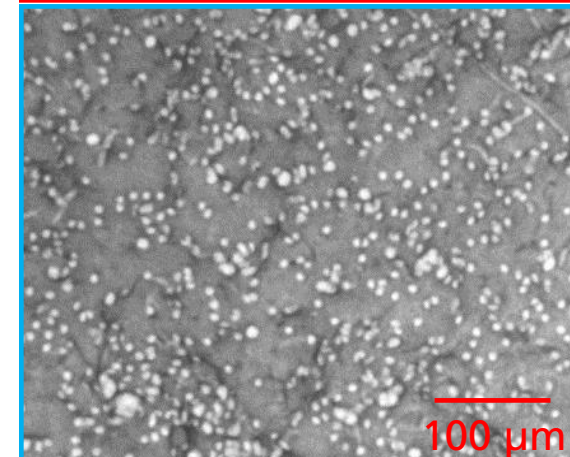
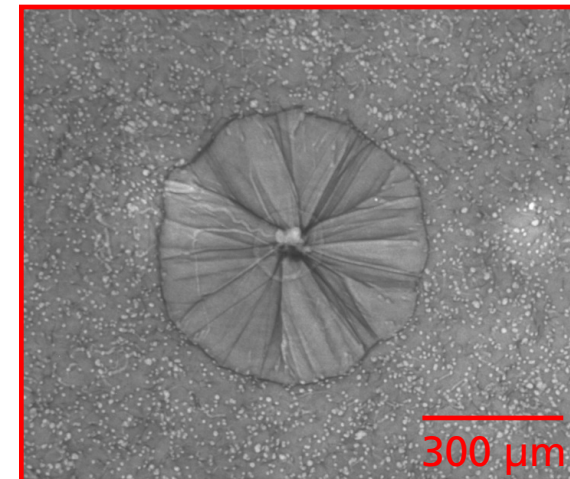
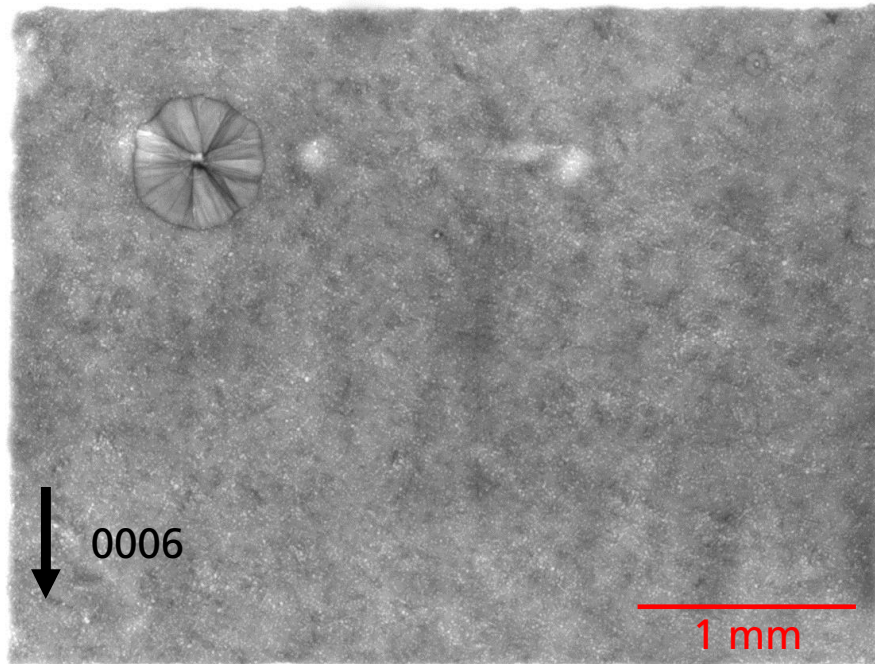
- quasi-bulk method
=> use of a template (e.g. MOCVD GaN/Al₂O₃)
- high growth rate (~100 μm/h)
- (often) single crystal process
- dislocation density of ~ 10⁶ - 10⁷ cm⁻²

Investigated GaN sample



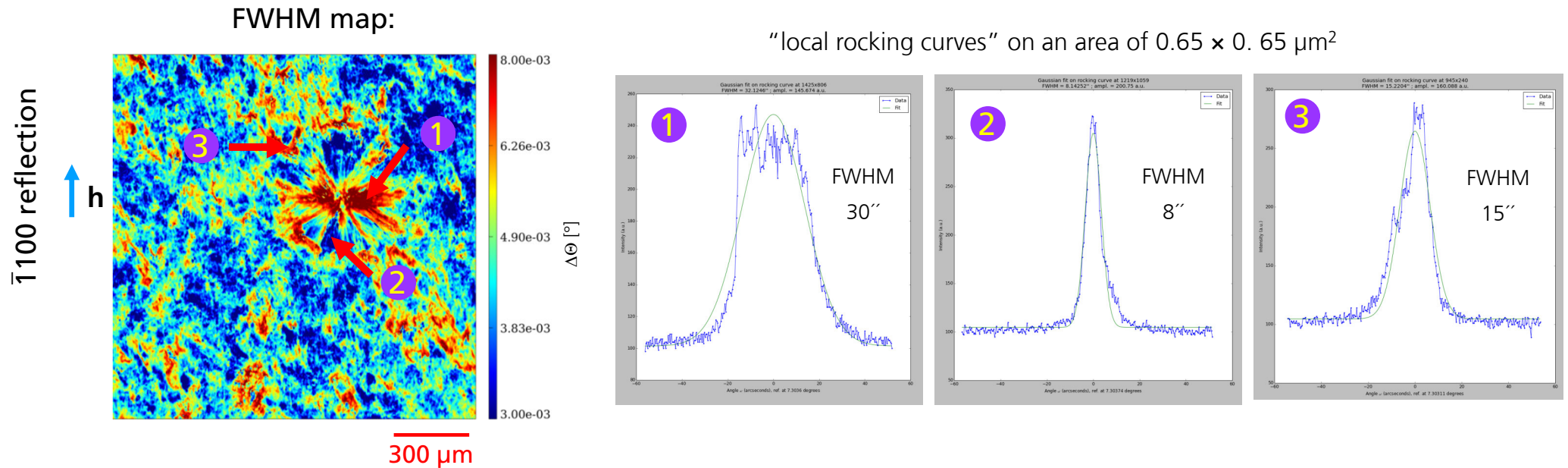
Vendor	Nanowin, China
Orientation	(0001)
Diameter	50 mm
Thickness	350 ± 25 μm
Polishing	< 0.2 nm
Bow	≤ 20 μm
Dislocation Density (nom.)	less than 5·10 ⁵ cm ⁻²

HVPE GaN: Synchrotron White Beam X-ray Topography



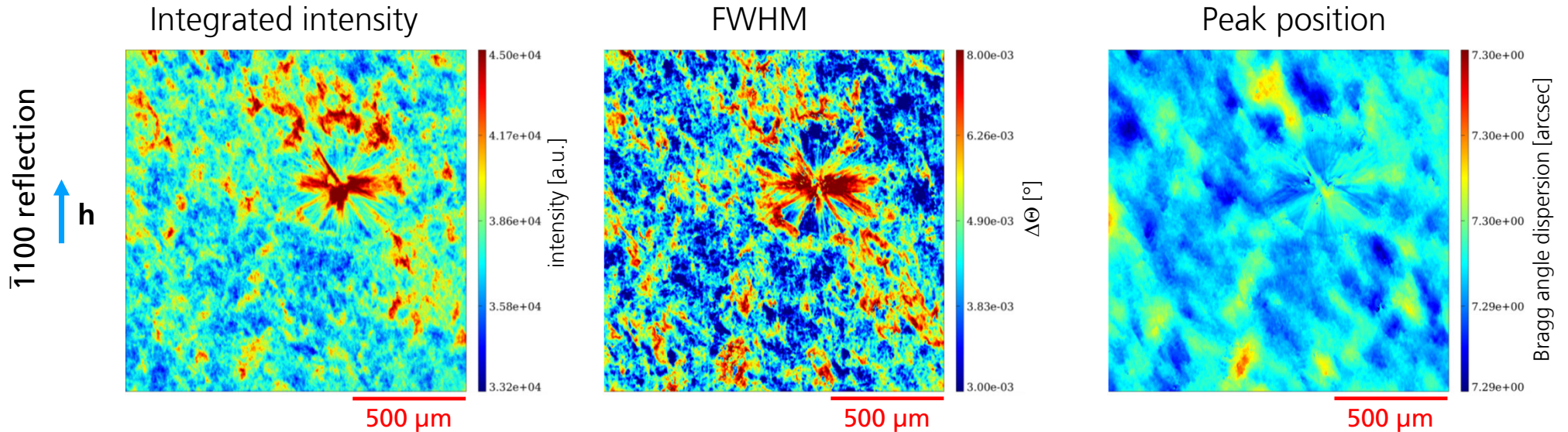
- ➔ “flower-like” defects ➔ pits
- ➔ white “dots”, surrounded by a darker region

HVPE GaN: Synchrotron Rocking Curve Imaging – projection (1)



- FWHM very often originates from the fit of a series of Bragg peaks, which partially overlap
- FWHM goes up to more than 30 arcsec in the neighborhood of the “flower-like defect”
- many (better!) regions exhibit FWHM of about ~6 arcsec

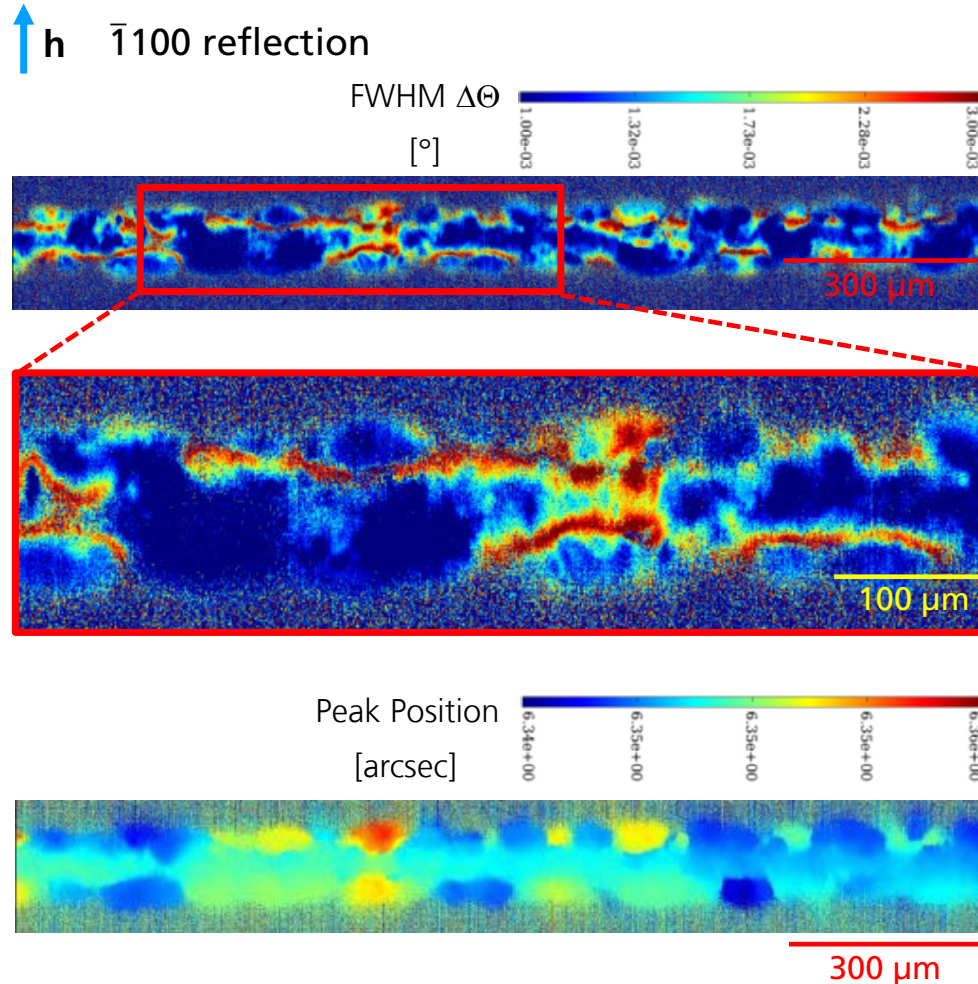
HVPE GaN: Synchrotron Rocking Curve Imaging – projection (2)



- The comparison of the INT and FWHM maps shows that, there is a partial correspondence between the regions of high INT and high FWHM
- sample is composed by a series of slightly misoriented regions (global misorientation 15-30 arcsec)
- lateral sizes of domains / grains in the 10 - 100 μm range
- estimating local defect density D from FWHM using Hirsch's formula $\Rightarrow 3.3 \cdot 10^6 \text{ cm}^{-2} - 8.3 \cdot 10^7 \text{ cm}^{-2}$

$$D = \frac{FWHM^2}{9b^2} \quad b = \text{Burger's vector}$$

HVPE GaN: Synchrotron Rocking Curve Imaging – section

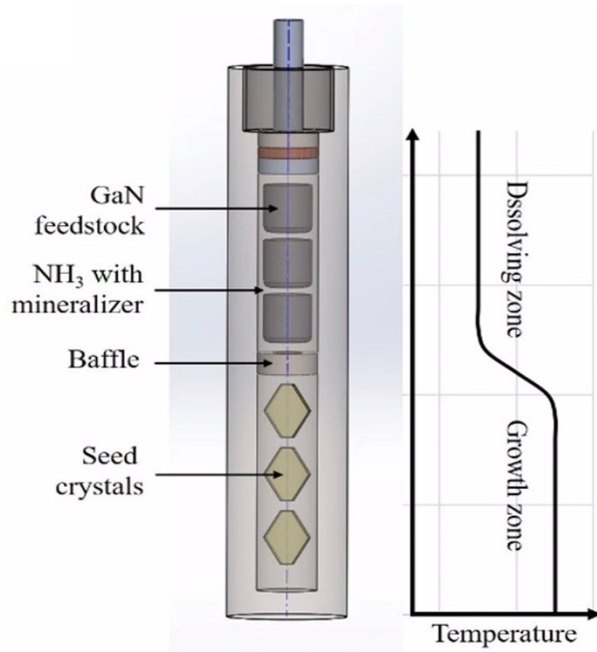


Formation of a cellular subgrain structure

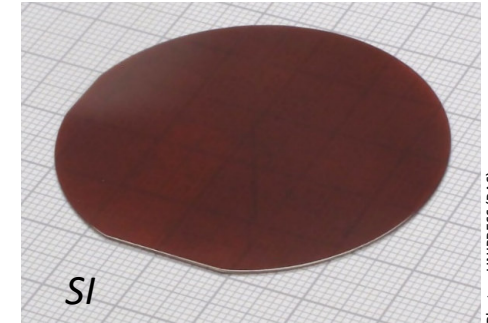
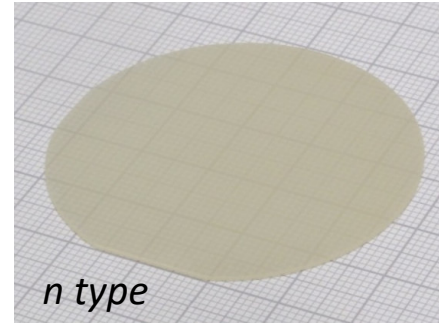
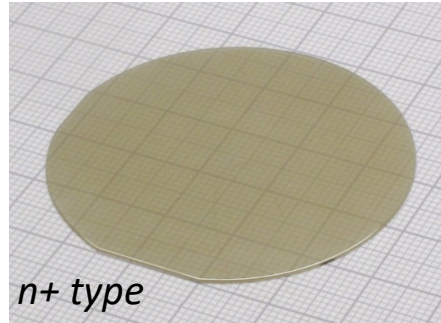
- the regions with high FWHM correspond to the **subgrain boundaries**, these **subgrains** being very clearly observed on the Peak Position map.
- the dislocations therefore tend to be concentrated in and around cellular walls with central regions tending to have less dislocation density.

Ammonothermal GaN

Basic ammonothermal GaN growth



$p = 0.1-0.4 \text{ GPa}$
 $T = 400 - 600^\circ\text{C}$

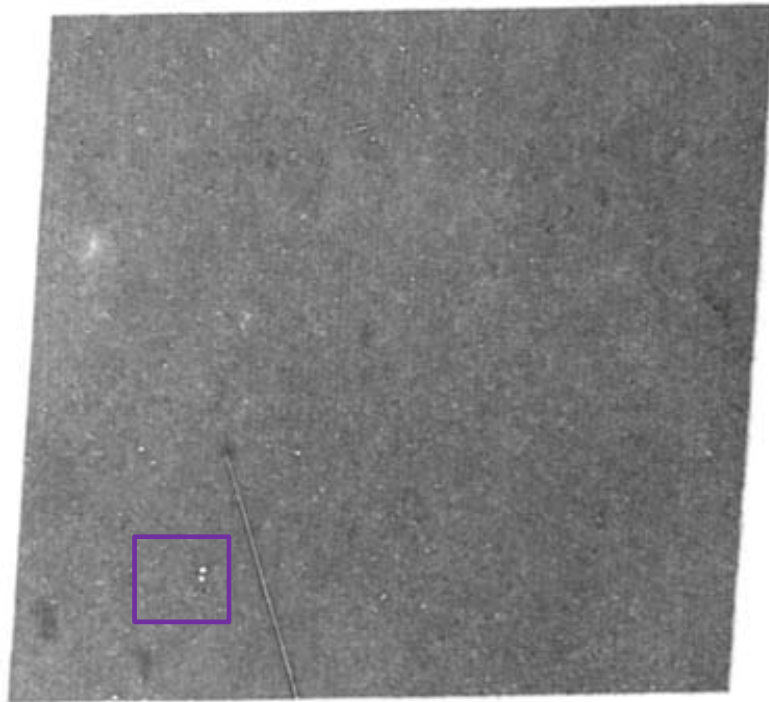


Photos: UNIPRESS (PAS)

- ➔ bulk method
 => use of native seeds
- ➔ low growth rate ($\sim 4 \mu\text{m/h}$ in $[000\bar{1}]$)
- ➔ multi crystal process
- ➔ dislocation density of $\sim 10^2 - 10^4 \text{ cm}^{-2}$

Vendor	UNIPRESS PAS, Poland
Orientation	(0001)
Diameter	50 mm
Thickness	300 - 400 μm
Polishing	< 0.5 nm
Bow	0 (± 10) μm
Etch Pit Density (EPD)	< $5 \cdot 10^4 \text{ cm}^{-2}$

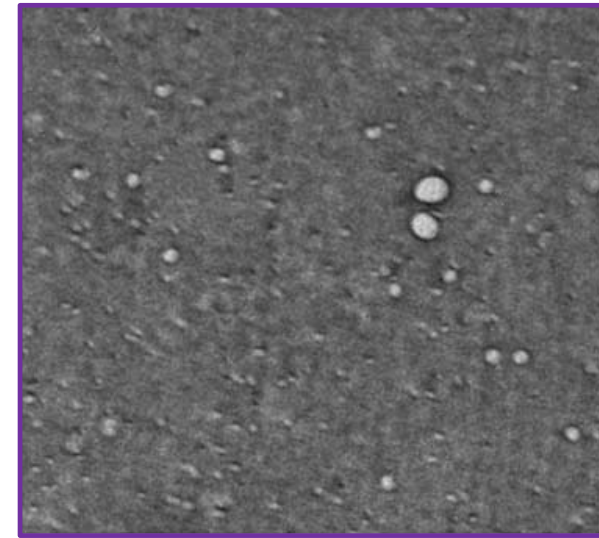
Ammonothermal GaN: Synchrotron White Beam X-ray Topography



01 $\bar{1}$ 5

500 μm

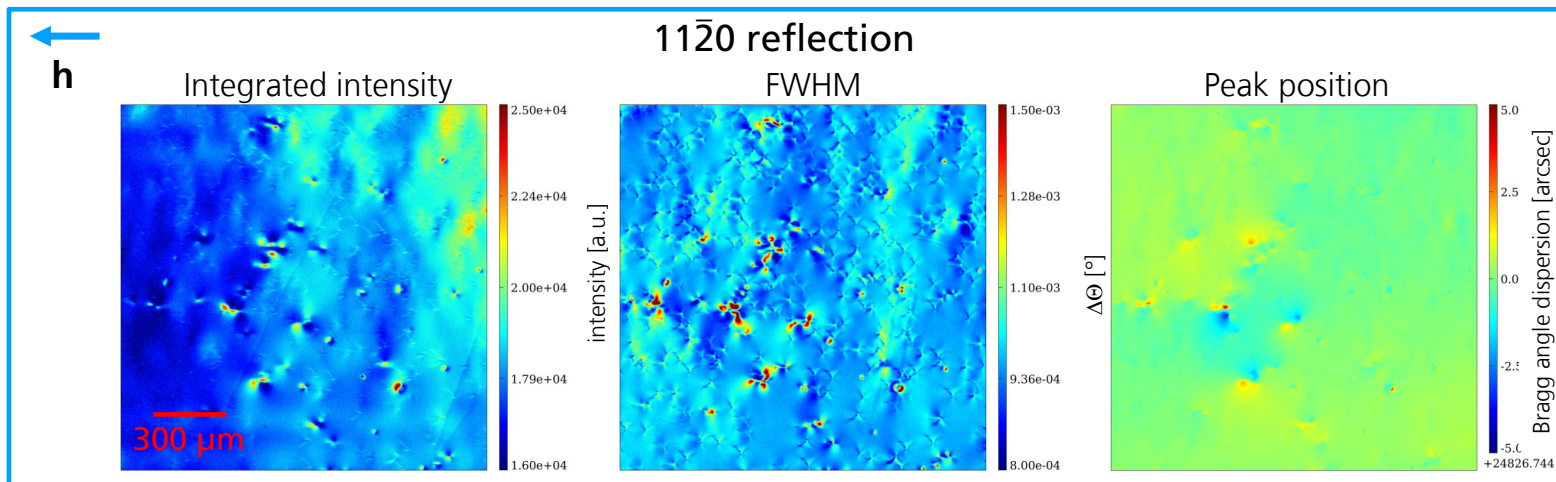
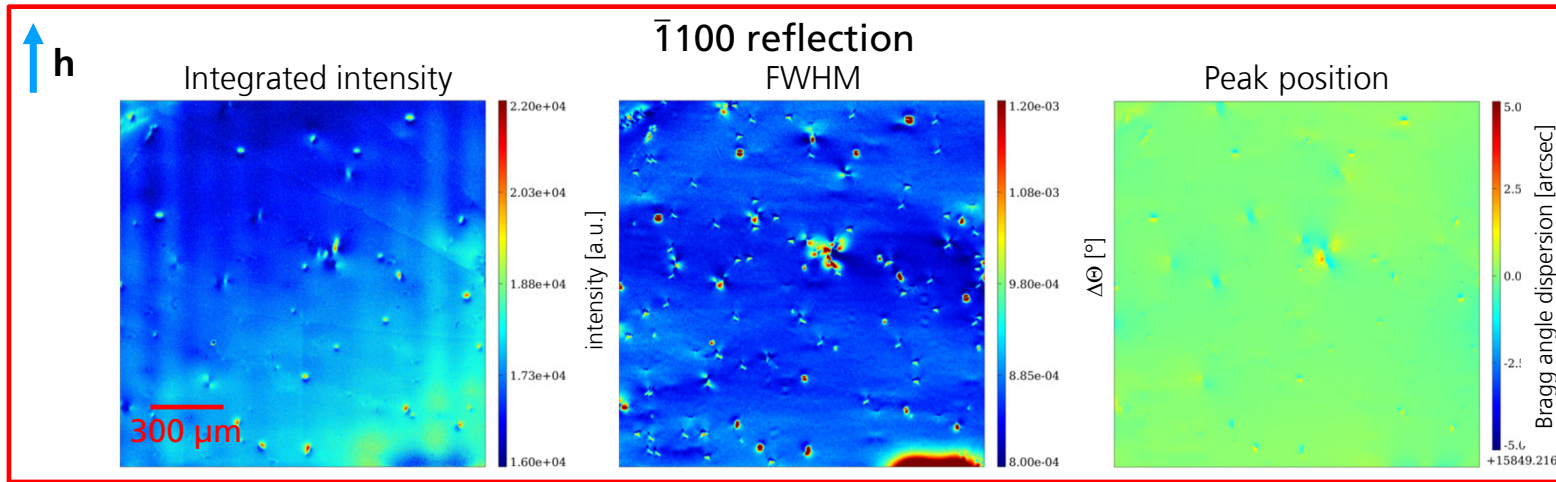
→ Uniform gray contrast indicating low defect density



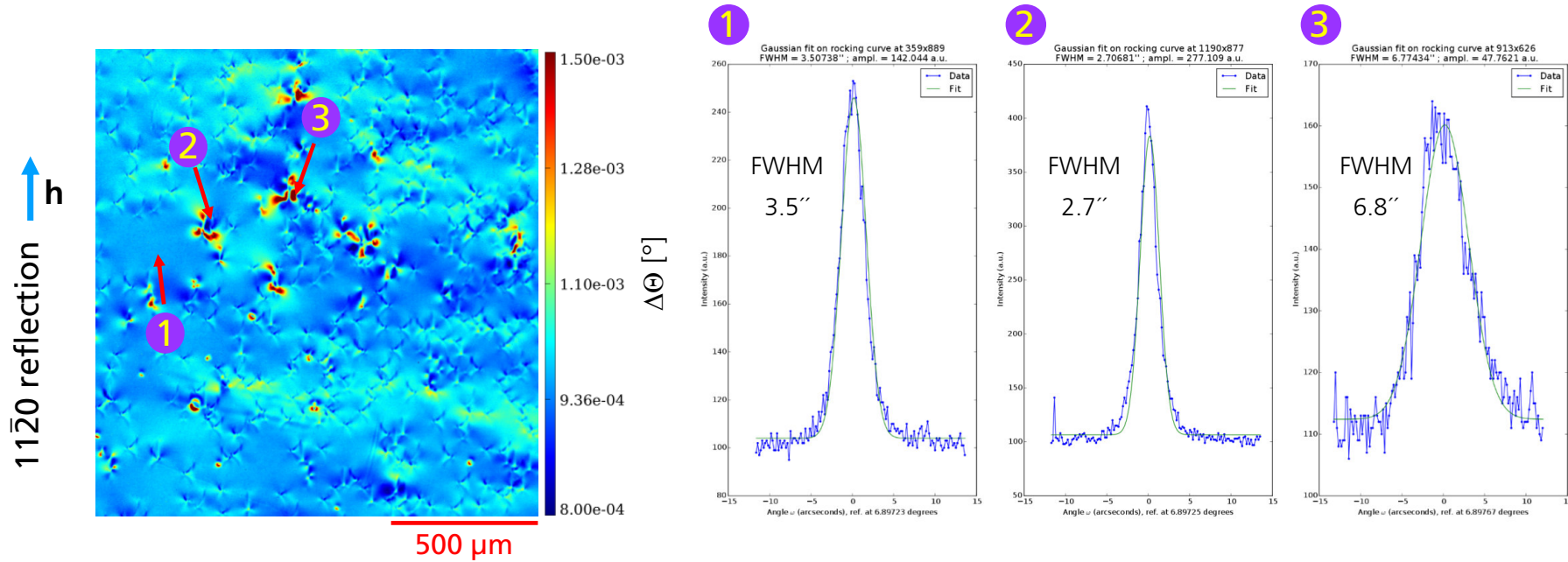
100 μm

- Threading dislocations show up as white circular contrasts
- Diameter: up to 20 μm
- Density: $\sim 8 \times 10^3 \text{ cm}^{-2}$

Ammonothermal GaN: Synchrotron Rocking Curve Imaging – projection (1)

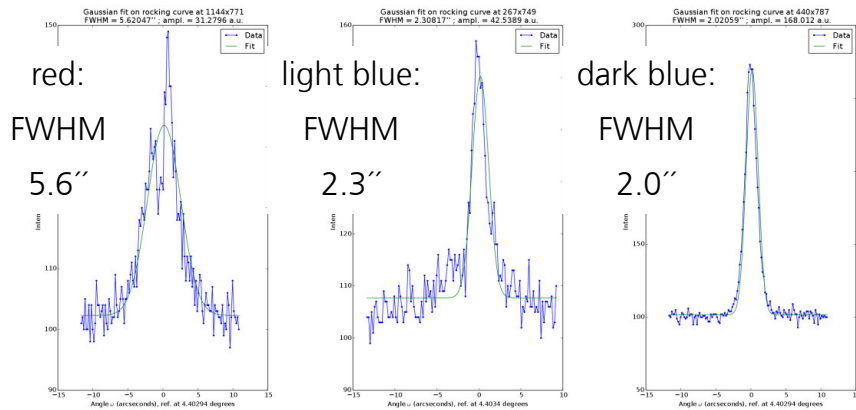
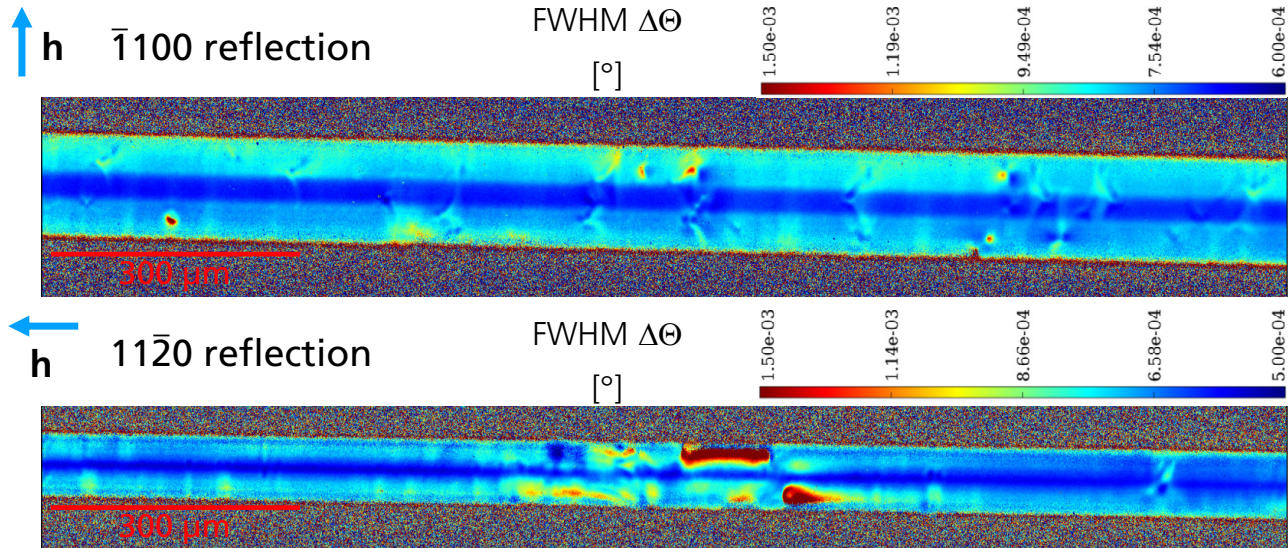


Ammonothermal GaN: Synchrotron Rocking Curve Imaging – projection (2)



- RCI FWHM 2-7 arcsec → low defect density
- Bragg angle dispersion is very low → low mosaic tilt
- contrast of individual dislocations
- threading dislocations density: $1.7 \cdot 10^{-4} \text{ cm}^{-2}$

Ammonothermal GaN: Synchrotron Rocking Curve Imaging – section

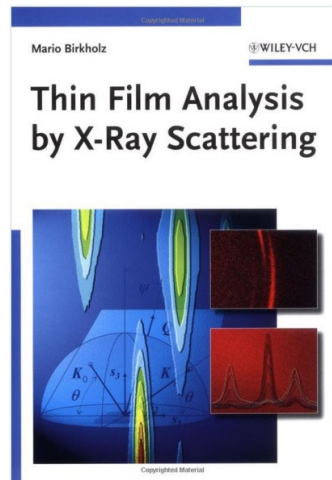


- one area with stronger lattice distortion, apart from this few individual defects that run through the volume
- observation of distorted Kato fringes (dynamical diffraction effect only visible in high perfection crystals)

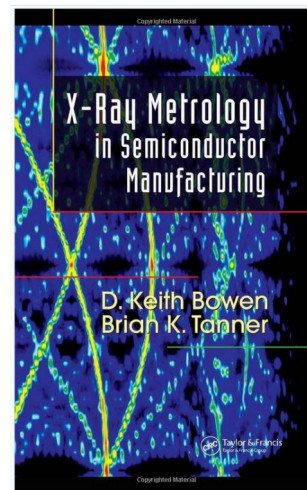
Outline

- Motivation
- Basics of X-ray Diffraction Method
- Instrumentation for High Resolution X-ray Diffraction
- Scanning in Reciprocal Space
- Stress and Strain in Epitaxial Thin Films
 - Fully strained Films
 - Partially Strained Films
 - Composition of Alloy Films
- Measurement of the Layer's Thickness
 - Single Layers and Layer Stacks
 - Superlattices
- Analysis of the Orientation of a Thin Film
- Mosaicity in Thin Films
- Synchrotron Bragg Diffraction Imaging for Substrate Analysis
- **Recommended Readings**

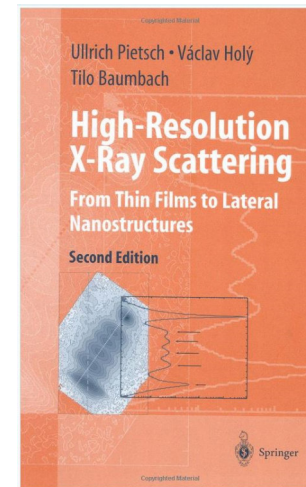
Recommended Readings



Thin Film Analysis by X-Ray Scattering
M. Birkholz
Wiley-VCH Verlag GmbH & Co. KGaA,
2005
ISBN-13: 978-3527310524



X-Ray Metrology in
Semiconductor Manufacturing
D.K. Bowen & B.K. Tanner
Taylor & Francis Group, 2006
ISBN-13: 978-0849339288



High-Resolution X-Ray Scattering:
From Thin Films to Lateral
Nanostructures
U. Pietsch, V. Holy und T.
Baumbach
Springer, 2004
ISBN-13: 978-0387400921

Lecturer

Lutz Kirste

Dr. rer. nat., Diplom Mineraloge

Group Leader „Structural and Chemical Characterization“

Deputy head of department Epitaxy

Fraunhofer Institute for Applied Solid State Physics (IAF)

Tullastraße 72,

79108 Freiburg



Phone: 0761/5159-330

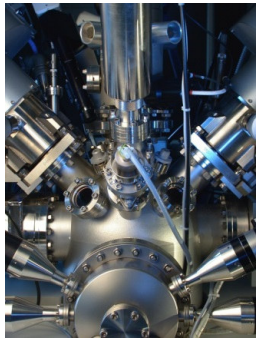
FAX: 0761/5159-71-330

Email: lutz.kirste@iaf.fraunhofer.de

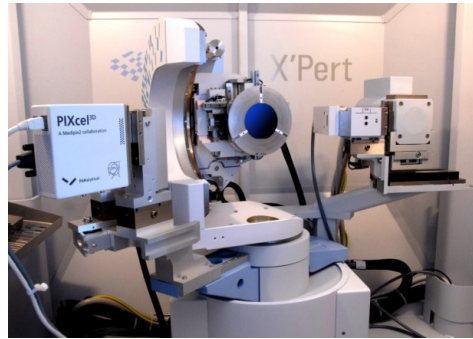
Education:

Graduate	Technical University Aachen, Germany	Diploma in Mineralogy	1998
PhD	University Freiburg, Germany	Dr. rer. nat.	2003

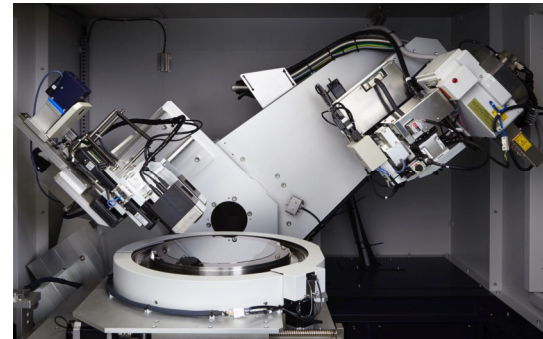
Structure Analysis Group at Fraunhofer IAF



Secondary Ion Mass Spectrometry



X-ray Diffraction



X-ray Topography



X-ray μ -Tomography (X-ray Microscopy)

The structural analysis team



N. Brückner Dr. P. Stranak M. Grimm E. Kelemen M. Prescher Dr. L. Kirste

**We are open for cooperation
... get in touch with us**

